Spontaneous and hepatic differentiation of human embryonic stem cells in 3D perfusion culture bioreactors

vorgelegt von
Diplom-Ingenieur
Harald Stachelscheid
aus Köln

Von der Fakultät III - Prozesswissenschaften
der Technischen Universität Berlin
zur Erlangung des akademischen Grades
Doktor der Naturwissenschaften
Dr. rer. nat.

genehmigte Dissertation

Promotionsausschuss:
Vorsitzender: Prof. Dr. Neubauer
Berichter: Prof. Dr. Roland Lauster
Berichter: Prof. Dr. med. PhD Jörg Gerlach

Tag der wissenschaftlichen Aussprache: 2.Juli 2009

Berlin 2009
D 83

Contents

1 Introduction

1.1 Embryonic Stem Cells (ESC)

Embryonic stem (ES) cells are pluripotent cells capable of unlimited self-renewal and differentiation into cells representative of all three embryonic germ layers. ES cells are derived from the inner cell mass of the blastocyst stage embryo. The blastocyst embryo develops from the morula, a cluster of undifferentiated cells formed by division of the fertilized oocyte. The outer layer of the morula differentiates and forms the trophectoderm. The cells inside the blastocyst (the inner cell mass) give rise to all cells of the adult body and some extraembryonic tissues, while the trophectoderm gives rise to the outer layer of the placenta.

ES cells were first derived from mice (Evans et al. 1981; Martin 1981) and later on from nonhuman primates and humans (Thomson et al. 1995; Thomson et al. 1998). A key characteristic of mouse ES cells (mESC) is the capability of germline transmission, which means that when the cells are injected into a pre-implantation embryo they contribute to the formation of tissues and organs including the germline (Bradley et al. 1984). In principle, human ES cells (hESC) should be able to produce the same results; however, because of obvious ethical reasons, this cannot be verified with hESC.

When transplanted into animals, ES cells generate tumors consisting of different types of tissue that are called teratomas (Przyborski 2005; Blum et al. 2008). In these tumors the presence of cells derived from all three germ layers demonstrates their pluripotency.

Human ES cells are karyotypically normal and, even after clonal derivation and/or prolonged undifferentiated proliferation, they maintain their differentiation potential (Amit et al. 2000). Pluripotent ES cells always express a characteristic set of markers, which are down-regulated upon differentiation. Mouse and human ES cells differ in the expression of these markers (Ginis et al. 2004; Rao 2004). ES cells from both species express OCT3/4, Nanog, and REX-1 and show high alkaline phosphatase and telomerase activity (Ben-Shushan et al. 1998; Rao 2004; Adewumi et al. 2007; Buitrago et al. 2007; Pan et al. 2007). hESC express exclusively the cell surface markers tumor-related antigen-1-60 (TRA-1-60) and tumor-related antigen-1-81 (TRA-1-81) as well as the stage specific embryonic antigens 3 (SSEA-3) and SSEA-4 whereas mESC express only SSEA-1 (Thomson et al. 1998; Koestenbauer et al. 2006). The functional significance of these antigens is unknown.

Because of their unique characteristics hESC hold great potential as a cell source for applications in basic science, pharmacological drug screening, toxicity testing and cell based therapies in regenerative medicine. It has been demonstrated that under certain growth conditions, hESC are able to differentiate into a wide variety of somatic and extraembryonic tissues *in vitro* (Pera et al. 2004). Accordingly, hESC make it possible to investigate the molecular pathways and control mechanisms that control the fate of cells during early embryonic development, which was not possible before due to the inaccessibility of human embryos to research (Dvash et al. 2006).

Possible clinical applications of hESC can be seen in the provision of stem cell-derived cell preparations for cell-based therapies in patients with organ defects like hepatic insufficiency (Asahina et al. 2006), spinal cord injuries (Kim et al. 2007) or myocardial defects (Zhang et al. 2008).

The areas of possible utilization of hESC derived differentiated cells in drug discovery can be seen in pre-clinical activities like target identification and validation, screening of compound efficacy and safety assessment studies (Sartipy et al. 2007). Regarding embryotoxicity testing, undifferentiated hESC also provide a novel tool for the development of better test systems (Pellizzer et al. 2005).

However, significant cell numbers are required to fulfill the potential applications of hESC.

1.2 Culture methods for human embryonic stem cells (hESC)

The first hESC lines were derived using culture conditions known for mouse ES cells that use mouse embryonic fibroblast (MEF) feeder layers and serum containing medium (Thomson et al. 1998). Mouse ES cells can be cultured without MEF using serum containing medium supplemented with leukemia inhibition factor (LIF) or in serum-free medium containing LIF in combination with bone morphogenetic protein (BMP) (Ying et al. 2003). These specific factors used to keep mESC undifferentiated fail to support hESC (Thomson et al. 1998; Daheron et al. 2004; Humphrey et al. 2004). In contrast to mESC self renewal of hESC is influenced by basic fibroblast growth factor (bFGF) and dependent on TGF-ß/ Activin/ Nodal signaling. Serum can be replaced by bFGF together with serum replacement in hESC co-cultures (Amit et al. 2000).

For a prospective clinical application of hESC derived cells the use of mouse feeders and animal derived substances contained in the culture media is not acceptable

because of the inherent risk of the transmission of animal-borne viruses and potential immune rejection of transplanted cells because of contamination with xeno-proteins (Martin et al. 2005). Therefore culture protocols that avoid animal derived feeders and defined culture media are being developed. To replace MEF various human cell types like cells from fetal skin, fetal muscle, adult marrow cells, foreskin fibroblasts and autogeneic feeders (hESC derived) have been used (Amit et al. 2003; Cheng et al. 2003; Richards et al. 2003; Choo et al. 2008).

It is also possible to culture hESC without direct contact to feeder cells by using feeder conditioned medium and coating of the growth surface with a complex extra-cellular matrix like Matrigel (Braam et al. 2008). Feeder independent growth of hESC is also possible for example by using very high concentrations of bFGF (Xu et al. 2005; Xu et al. 2005). Finally some feeder independent protocols have been described that use xeno-free fully defined medium (Genbacev et al. 2005; Vallier et al. 2005; Ludwig et al. 2006).

1.3 Teratoma formation/ Tumorigenicity of hESC

Teratomas and teratocarcinomas are spontaneously occurring germ cell tumors that contain somatic tissues derived from each of the three embryonic germ layers. Teratomas are always benign tumors whereas teratocarcinomas contain a population of undifferentiated highly malign cells, the so called embryonic carcinoma (EC) cells (Blum et al. 2008).

EC cells share the expression of specific pluripotency markers like OCT4 and SSEA4 with hESC but often have karyotypic abnormalities. When isolated, EC cells can be cultured *in vitro* where they exhibit multilineage differentiation potential and form teratomas or teratocarcinomas when transplanted back.

Teratomas formed by hESC that have been transplanted into immunodeficient mice are often composed of less differentiated tissue compared to spontaneously occurring teratomas in humans and contain sometimes a pool of undifferentiated, OCT4 positive cells (Adewumi et al. 2007). Whether these undifferentiated cells represent remaining undifferentiated hESC or EC cells evolved by transformation of hESC is unclear. In human stem cell research teratoma formation is used as an important *in vivo* pluripotency assay combined with analysis of pluripotency marker expression and *in vitro* differentiation assays. It is the best testing method for the developmental potential

of isolated and cultured hESC because germ line transmission as it can be tested for mouse ES cells is not feasible with hESC due to ethical reasons (Heins et al. 2004; Valbuena et al. 2006; Adewumi et al. 2007).

In science teratomas represent an alternative development model because developmental processes can not be investigated in intact mammalian embryos. They exhibit a highly organized structure consisting of ordered arrangements of different tissue types that in many ways recapitulate organogenesis within the embryo (Przyborski 2005). Studying teratomas could result in a better understanding of the stepwise developmental processes and their molecular base and might provide information for the development of tissue engineering technologies (Aleckovic et al. 2008).

1.4 *In vitro* Differentiation of hESC: Focus on hepatic differentiation

1.4.1 Induction of hESC differentiation

When removed from feeder layers and/or transferred to suspension culture, hESC spontaneously begin to differentiate into various cells of the different germ layers.

In 2D cultures cells with different morphologies, including rhythmically contracting cardiomyocytes, pigmented and non-pigmented epithelial cells, neural cells with axons and dendrites and cells with mesenchymal characteristics can be observed (Odorico et al. 2001). In suspension, hESC form multicellular aggregates of differentiated and undifferentiated cells, that can be cavitated and cystic. These so called embryoid bodies (EBs) resemble early postimplantation embryos and frequently progress through a series of differentiation stages (Itskovitz-Eldor et al. 2000).

To direct the differentiation of embryonic stem cells towards a desired cell type two principal approaches exist: directed differentiation and lineage selection. Lineage selection is based on the selection of the desired cell type from a mixture of different cell types generated by spontaneous differentiation. Spontaneous differentiation is achieved by EB formation followed by cell dissociation and sorting or transferring of the EBs to adherent culture conditions where the EBs attach and form cell monolayers by outgrowth. While generation of EBs is relatively simple the need to use selection or other enrichment techniques is limiting the homogeneity and yield because for many cell types no specific markers exist that can be used for example in cell sorting techniques.

Directed differentiation is induced in monolayer culture by cues provided directly by growth factors and extracellular matrix components or indirectly by feeder cells with the

aim to direct differentiation of the entire cell population towards a specific cell type (Schuldiner et al. 2000). In this approach the specific temporal sequence and concentrations are the key factors for differentiation control. In addition specific culture conditions can additionally promote the selective enrichment of a desired cell type.

1.4.2 Development of the mammalian liver

The liver is one of the first organs to develop in the embryo and it rapidly becomes one of the largest organs in the fetus. The liver develops from the definitive endodermal epithelium of the embryonic foregut. Initially suppression of Wnt and fibroblast growth factor signaling (FGF4) in the foregut is necessary for induction of liver development (McLin et al. 2007). Then FGFs from the cardiac mesoderm and bone morphogenic proteins (BMPs) from the septum transversum mesenchyme induce spatial restricted cell proliferation which leads to thickening of the endodermal layer (Lemaigre et al. 2004). The cells then emerge from the epithelium and begin to migrate into the septum transversum. The mass of cells emerging from the endoderm and concentrating in the septum transversum is referred to the liver bud. Interactions with endothelial cells in this stage of organogenesis are crucial for this early budding phase (Matsumoto et al. 2001). The hepatic endoderm cells are quite immature in terms of function and morphology during this time and are now referred to as hepatoblasts (Zhang et al. 2008). Cords of hepatoblasts from the liver bud penetrate the mesoderm, intermingling with the vitelline and umbilical veins, which anastomose near the liver bud to form a capillary bed. These transitions establish the liver's sinusoidal architecture, which is critical for organ function and sets the stage for the liver to support fetal hematopoiesis. The hematopoietic stem cells that migrate into the liver bud secrete oncostatin M (OsM) that induces further hepatic maturation together with glucocorticoids (Kinoshita et al. 2002; Lemaigre et al. 2004). Other cell types that contribute to the embryonic liver mass are endothelial cells that surround the hepatic sinusoids, the Kupffer cells, and hepatic stellate cells (Arias et al. 2001). The hepatocyte growth factor (HGF) produced by these cells is important for the full functional hepatic maturation (Kamiya et al. 2001). In these later stages of liver differentiation Wnt signaling no longer inhibits but promotes growth and differentiation (Zaret et al. 2008).

1.4.3 Hepatic Differentiation of hESC *in vitro*

Studies on strategies for direction of hepatic differentiation of hESC *in vitro* led to the identification of several cytokines, growth factors and non-protein compounds that have an effect on hepatic differentiation (reviewed in Heng et al. 2005; Snykers et al. 2008). The growth factors include activin A, BMP2 and -4, epidermal growth factor (EGF), FGF1, -2 and -4, HGF, insulin and OsM. The non-protein factors include dexamethasone (DEX), dimetylsulfoxide (DMSO), nicotinamide and sodium butyrate. The key to the effect of each differentiation factor is the timing, concentration and combination with other factors.

To characterize the hESC derived hepatocyte like cells various markers and functional test have been utilized (reviewed by Snykers et al. 2008). The markers examined by immunocytochemistry, polymerase chain reaction (PCR) or enzyme-linked immunosorbent assays (ELISA) included secretion of plasma proteins like alpha fetoprotein (AFP), albumin (ALB) and urea, cytokeratines (CK8, CK18, CK7, CK19) and various hepatocyte specific enzymes like alpha-1-antitrypsin (α1AT), dipeptidyl peptidase IV (DPPIV) and cytochrome P450 isoenzymes. The expression of hepatocyte specific functions has been examined for example by detection of the storage of glycogen and metabolism of various test substrates specific for cytochrome P450 isozymes.

The first published protocols describing hepatic differentiation of hESC applied as a first step the induction of EBs followed by adherent culture using various growth factors to enrich for hepatic cells (Lavon et al. 2004; Shirahashi et al. 2004; Schwartz et al. 2005; Baharvand et al. 2006). In these studies only very low yields and purity of the final cell populations have been reported. The most successful differentiation protocols described so far try to mimic organ development of the liver starting with induction of definitive endoderm (DE) differentiation of the hESC (Cai et al. 2007; Agarwal et al. 2008; Basma et al. 2008; Shiraki et al. 2008). Basically, high concentrations of activin A together with low serum/ insulin conditions, to provide reduced insulin/ insulin-like growth factor (IGF) signaling, are applied for DE differentiation with yields of up to 80% DE cells (Kubo et al. 2004; D'Amour et al. 2005; McLean et al. 2007). This is followed by sequential treatment with FGFs, BMPs, HGF, OsM/ DEX. With this approach, described yields of hepatocyte like cells were about 50%. Other protocols include the treatment of the hESC with sodium butyrate (NaB) that inhibits histone deacetylase activity (Davie 2003). Application of this epigenetic differentiation agent in the first step of a

differentiation protocol yielded 10% hepatic cells from hESC and a purity of up to 70% of the final cell populations (Rambhatla et al. 2003). Combination of NaB treatment with DE induction by activin A showed promising results, attaining a yield of hepatic cells of up to 70% (Hay et al. 2008). (Table 6 in the appendix lists the details of published differentiation protocols and used characterization methods)

In summary the yield, purity and maturational degree of hESC derived hepatic cells derived by the current approaches are still suboptimal and therefore novel methods are needed.

1.4.4 Application of hESC derived hepatocytes

A future clinical use of hESC derived hepatocytes can be seen in their application for cell transplantation in patients with hepatic insufficiency, e.g. in the case of certain genetic defects or acute or chronic liver failure (Ito et al. 2009). Transplantation of stem cell derived hepatocytes could replace whole-organ transplantation in some clinical indications, and - when using immunocompatible cells - make dispensable the need of immunosuppressive therapy. A further therapeutic option can be seen in the provision of a reliable human cell source for extracorporeal liver support, to bridge the liver function until transplantation or until regeneration of the patient's organ, which would also solve the existing problem of cell availability for extracorporeal liver devices. Moreover, extracorporeal systems could also provide an interesting therapeutic option to bridge the liver function after cell transplantation until the applied cells show sufficient liver-specific metabolic performances.

Potential applications in pharmaceutical research are the use of hESC derived hepatocytes for the development of novel hepatic assays needed for drug discovery. This could overcome the poor predictive power of existing *in vitro* tools and lead to new human cell based test systems that will allow more reliable and relevant testing in the preclinical phase and hinder weak lead candidates to enter clinical phases (Jensen et al. 2009).

1.5 Culture of hESC in Bioreactors

For the development and implementation of stem cell-based applications in regenerative medicine and applied research, like drug screening or toxicology testing, large numbers of cells with well defined characteristics are needed. Therefore culture

systems are required that allow the expansion of undifferentiated human embryonic stem cells and a directed reproducible differentiation into mature cell types with a high yield and purity.

The most commonly used culture and differentiation methods typically utilize 2D culture systems in the form of plastic dishes, which represent static open systems with discontinuous medium exchange, which leads to periodical changes of the culture environment in form of accumulation of metabolites and reduction of nutrients in the culture medium between medium changes. Furthermore these 2D cultures are labor intensive because they require extensive manual intervention and therefore make handling of larger cell numbers impractical.

In general hESC cultures represent fragile systems that are highly susceptible to variations of culture parameters like medium composition, extracellular matrix, feeder cell quality, osmolarity, pH and temperature as well as to interindividual variations. Even factors that appear to be trivial like variations of the temperature and pH due to routine microscopic control of the cultures, during passaging or even by opening the incubator (Lo et al. 1994; Veraitch et al. 2008) can influence the culture quality in terms of growth and differentiation.

One approach to standardize ES cell culture is the automation of certain culture steps like quality control of cultures (Narkilahti et al. 2007) and mechanical passaging (Joannides et al. 2006) or application of automated culture platforms that allow automated cell plating, media change, growth factor addition and cell harvesting of ES cells cultures in 2D co-cultures (Terstegge et al. 2007). However, certain manual cell culture tasks still have to be performed outside such systems and the number of plates that can be handled in such systems, and therefore the number of cells that can be produced, is limited.

The use of bioreactors could provide a promising alternative compared to static culture vessels, handled manually or used in automated systems, because they provide a more homogeneous environment, the ability to monitor and control culture parameters and allow an easier scale up. In bioreactors the reduction of metabolite accumulation, fluctuation of nutrients and control of parameters such as oxygen partial pressure (pO2) and pH all resulting in the maintenance of favorable growth conditions can be easily addressed.

The types of bioreactors used for mouse and human embryonic stem cell culture and differentiation that have been described in literature are stirred bioreactors (e.g. Spinner

flasks), rotary systems like slow-turning lateral vessels (STLV) (Come et al. 2008; Hwang et al. 2009) or fibrous bed bioreactors (Li et al. 2003; Ouyang et al. 2008).

Because embryonic stem cells grow adherent in colonies and are dependent on tight cell-cell contacts they do not grow as single cells in suspension. To culture the cells in stirred tank bioreactors, it is necessary to culture the cells either as aggregates or adhered to microcarriers.

Undifferentiated expansion of mouse ES cells has been shown using microcarriers yielding up to 70-fold expansion (Abranches et al. 2007; Fernandes et al. 2007) as well as in carrier-free suspension (zur Nieden et al. 2007). However frequent subculturing (about every 3 to 4 days) and cell aggregate dissociation was necessary.

For the cultivation of lager cell or tissue masses perfusion is the only option to facilitate continuous nutrient and oxygen supply. This has been shown in a study by Ouyang et al. who demonstrated an 193-fold expansion of mouse ES cells in a perfused fibrous bed bioreactor where the cells were immobilized in a non-woven PET matrix (Ouyang et al. 2008). It was also shown that perfusion is beneficial in 2D cultures of undifferentiated hESC and increased the resulting hESC cell numbers by 70% compared to static conditions (Fong et al. 2005).

Expansion of undifferentiated hESC is more difficult because they are more fragile and sensitive than mouse ES cells. The use of microcarriers reduces the shear stress on the cells and first studies showing that hESC can be grown and expanded on microcarriers using feeder cell conditioned medium have been reported recently (Phillips et al. 2008; Nie et al. 2009). However only low cell expansions and seeding efficiencies could be achieved.

In general culture of mESC and hESC as aggregates in suspension is limited by the size of the cell clusters because if clusters become too large in size, mass transport of e.g. oxygen and nutrients into their center is reduced leading to cell necrosis. The use of microcarriers is limited by their surface requiring frequent cell dissociation and passaging, which leads to cell loss due to low seeding efficiencies and the fragility of the cells. To solve these problems novel culture techniques are needed.

1.6 Differentiation of hESC in bioreactors

The classical approach of embryonic stem cell differentiation is the induction of EB formation followed by cell dissociation and lineage selection (see above). Mouse EBs

can be formed directly from enzymatically dissociated mESCs in stirred reactors (Schroeder et al. 2005), by encapsulating cell aggregates in agarose beads (Dang et al. 2004) or by removing LIF from mESC aggregates produced in the same vessels (Fok et al. 2005). After formation, the EBs grow in size in these cultures and can be further differentiated e.g. towards cardiomyocytes (Niebruegge et al. 2008), bone tissue (Hwang et al. 2009) or hepatic cells (Yin et al. 2007).

Human EBs have been grown in a rotating bioreactor (Gerecht-Nir et al. 2004) or slow-turning lateral vessels (Come et al. 2008).

In general EBs cultured in stirred vessels exhibited greater cell expansion, more uniform morphology and size distribution compared with EBs cultured in T flasks. But some problems still remain to be addressed: Conventional stirred bioreactors and turning vessels have the disadvantage of generating shear forces that cause cell damage and formation of large cell aggregates (Dang et al. 2002).

To reduce the shear forces bioreactors with low and interrupted stirring and slow-turning lateral vessels (STLV) have been used. However sedimentation in such setups leads to agglomeration of EBs and formation of aggregates that are too large for optimal growth and differentiation due to limited nutrient and oxygen supply into the center of the aggregates, which leads to cell death. Therefore encapsulation of EBs has to be performed in these bioreactors to prevent aggregation.

The results from studies using stirred bioreactors are promising; however, it has been difficult to control cell proliferation and differentiation into higher-order structures of more mature cells. Several studies have shown that differentiation of embryonic stem cells into mature tissue can be achieved by using three dimensional matrixes (Levenberg et al. 2003; Baharvand et al. 2006; Lees et al. 2007; Inanc et al. 2008; Xie et al. 2009). For example mouse ES cells have been differentiated in a perfused three dimensional fibrous matrix towards hematopoietic cells (Li et al. 2003) and in perfused polyurethane/spheroid cultures towards a hepatic fate (Matsumoto et al. 2008).

Regarding hepatic differentiation of hESC studies by Soto-Gutierrez et al. indicate that a more complex environment, using complex matrix structures or co-culture with nonparenchymal cells supports hepatic differentiation of hESC (Soto-Gutierrez et al. 2006). Levenberg et al. showed that in biodegradable scaffolds of PLGA-poly(lactic-co-glycolic acid) and PLLA-poly(L-lactic acid) seeded with ES cells or EBs induction of hepatic tissue-like structures was possible by treatment with activin A and IGF (Levenberg et al. 2003). Baharvand et al. reported enhanced hepatic differentiation of

hESC in 3D collagen scaffolds (Baharvand et al. 2006). Therefore use of perfused bioreactors providing a 3D culture environment could lead to more efficient and scalable methods for embryonic stem cell differentiation.

A novel approach is the usage of hollow fiber bioreactors for embryonic stem cell expansion and differentiation. Hollow fiber capillary membrane bioreactor technologies enable dynamic perfusion culture conditions and allow increasing the cell density as stem cells find it in the natural tissue. In addition scale-up for larger cell masses is possible. However, the typical two-compartment bioreactor devices (e.g. FiberCell Duet, FiberCell systems, Inc., www.fibercellsystems.com), with a cell compartment around a bundle of surrounding capillaries, nutrition mainly via diffusion and external oxygenation, are limited by non-uniform mass exchange with substrate gradient distances along decimeters of capillary length.

In the 3D multicompartment technology developed by Gerlach et al. (Gerlach et al. 1994; Gerlach et al. 1995; Zeilinger et al. 2002), another medium- and an additional oxygenation membrane compartment were added to the typical two-compartment devices (see Figure 1 in methods chapter). Interweaving the four compartments to form repetitive units enables scalability of the bioreactors, provides decentralized medium perfusion and -substitution, while mass exchange is enhanced and gradient distances are reduced. The concept is based on culturing cells in a closed and thus good manufacturing practice (GMP) suitable culture environment, which facilitates biotechnological applications, as well as potential clinical translation of the results. Initial clinical studies using primary porcine or human liver cells cultured in bioreactors demonstrated the feasibility of clinical extracorporeal liver support with the system (Sauer et al. 2003). In addition it was shown that primary cells can create their own typical microenvironment in such *in vitro* culture models, including formation of liver-like tissues with neo-sinusoids and biliary structures. Adult stem cells could benefit from parenchymal/nonparenchymal cell co-culture in such systems for the creation of an organotypical microenvironment (Gerlach et al. 2003; Schmelzer et al. 2009).

1.7 Aims of this Study

The aim of the study was to evaluate the above described multicompartment bioreactor system for its suitability as a novel *in vitro* system that supports growth and differentiation of hESC. Emphasis was on spontaneous and hepatic differentiation. This

aim was based on the hypothesis that the 3D environment of the bioreactor constitutes a more *in vivo*–like environment than standard 2D culture systems and therefore enables improved growth and differentiation of hESC compared to these systems.

A long term aim of this project is the application of the bioreactor containing hESC derived differentiated cells as an extracorporeal device in medical therapies and the development of methods using the multicompartment bioreactor technology as an alternative to animal testing in applications like for example pluripotency testing by teratoma formation and drug metabolism studies. Another long term aim of this project is the establishment of the bioreactor as a scalable system for the production of large numbers of undifferentiated or differentiated hESC needed for basic research, pharmacological drug screening and cell based clinical applications. For these applications, methods leading to cell preparations highly enriched for specific cell types are key prerequisites.

In one part of this study the capacity of the bioreactor system to support spontaneous multilineage differentiation and tissue formation of hESC was analyzed and compared to teratoma formation of hESC in NOD/SCID mice. Furthermore the influence of serum in the used culture medium and the presence of feeder cells on hESC differentiation in the bioreactor were examined. The differentiation of the cells was examined by the analysis of metabolic parameters in the culture medium, RNA expression profiling using microarrays, expression of differentiation markers, histology and the ultrastructure of the cells. To better understand the role of feeder cells on hESC growth and differentiation in the bioreactor experiments on the behavior of feeder cells were carried out in the bioreactor and in 2D cultures.

Based on the results of the previous experiments on the spontaneous differentiation behavior of the hESC in the bioreactor system the directed differentiation of hESC towards the hepatic lineage was investigated. For this purpose a method of directed hepatic differentiation that was developed for 2D cultures of hESC was translated to the 3D system and two pilot experiments were carried out.

2 Materials and Methods

2.1 Cell culture

2.2 Culture of human foreskin fibroblasts (HFF)

HFF were purchased from the Type Culture Collection (CRL-2429; Manassas, VA, USA) and expanded in Iscove's Modified Dulbecco's Medium (IMDM) containing GlutaMax-1 (Invitrogen), 10% fetal calf serum and 10,000 U/ 10,000 µg/ml penicillin/streptomycin (all Biochrom, Berlin, Germany) for not more than 44 population doublings. The cells were inactivated by gamma irradiation with 3000 rad and plated on 0.1% gelatin (Sigma-Aldrich)-coated culture dishes at a density of 30,000-70,000 HFFs per cm^2 in VitroHES medium (Vitrolife AB, Göteborg, Sweden) supplemented with 10 ng/ml human recombinant basic fibroblast growth factor (hrbFGF) (PeproTec) or Knockout DMEM containing 20% Knockout SerumReplacer, 2 mM GlutaMax–I (all Invitrogen), 0,1 mM nonessential amino acids (NEAA), 50 µg/ml Gentamycin (all Biochrom), 0.1 mM ß-mercaptoethanol (Sigma), 10 ng/ml hrbFGF (PeproTec, London, UK). Irradiated cell that were not directly used were frozen down in aliquots in fetal calf serum (Biochrom) containing 10% dimethyl sulfoxide (DMSO) (Sigma-Aldrich) and stored at -152°C for later use.

2.3 Culture of mouse embryonic fibroblasts (MEF)

MEFs were expanded in Dulbecco's modified Eagle's medium (DMEM) containing 10% fetal calf serum, 2 mM L-glutamine, 0.1 mM NEAA and 10,000 U/ 10,000 µg/ml penicillin/streptomycin (all Biochrom) for 2 to a maximum of 4 passages. Inactivated by gamma irradiation with 3000 rad and seeded to 0.1% gelatin (Sigma-Aldrich) coated “In Vitro Fertilization” (IVF) dishes (Falcon, Becton Dickinson) at a density of 65,000 cell/cm^2 in VitroHES medium (Vitrolife AB) or frozen down in aliquots in fetal calf serum (Biochrom) containing 10% DMSO (Sigma-Aldrich) and stored at -152°C for later use.

2.4 hESC maintenance culture

The human embryonic stem cell line SA002 (Heins et al. 2004) was provided by Cellartis (Gothenburg, Sweden). The cells were grown on irradiated MEF in IVF dishes (Falcon, Becton Dickinson) in VitroHES medium (Vitrolife AB) supplemented with 4 ng/ml human recombinant basic fibroblast growth factor (PeproTec) and routinely

passaged every 4–5 days. For passaging the hESC colonies were mechanically cut into pieces, 200 x 200 µm, by mechanical dissection using Stem Cell Cutting Tool™ (Vitrolife AB), removed from the culture dish and transferred to a new culture dish with fresh MEF cells and VitroHES supplemented with 4 ng/ml hrbFGF.

2.5 hESC expansion

Larger scale cell expansion for bioreactor inoculation was performed using the single-cell enzymatic dissociation (SCED) culture system (Ellerstrom et al. 2007). Briefly, to transfer manually passaged hESC to the SCED culture system, the cells were enzymatical detached from the culture dish using TrypLE Select (Invitrogen) and dissociated to a single-cell suspension with a pipet. After centrifugation (400g for 5 minutes), the supernatant was discarded, the hESC pellet was resuspended in VitroHES (Vitrolife) medium supplemented with 10 ng/ml hrbFGF (PeproTec) or Knockout DMEM containing 20% Knockout SerumReplacer, 2 mM GlutaMax–I (all Invitrogen), 0.1 mM NEAA, 50 µg/ml Gentamycin (all Biochrom), 0.1 mM ß-mercaptoethanol (Sigma), 10 ng/ml hrbFGF (PeproTech) and the single cell suspension was plated onto culture dishes containing a high-density HFF layer (30,000-70,000 HFFs per cm^2). For this initial passage, split ratios of 1:2 to 1:8 were used. Upon 80-90% confluence, the hESC cells were enzymatic dissociated using TrypLE Select (Invitrogen) and seeded onto fresh HFFs at split ratios between 1:4 and 1:10. Culture medium was replaced with fresh medium every 1–3 days and the cells were passaged every 6–12 days.

2.6 hESC karyotyping

hES cells designated for karyotyping were cultured in VitroHES containing 4 ng/ml hrbFGF and supplemented with 0.05 µg/ml colcemid (Invitrogen) for 1 hour. hESC colonies were detached using 200U/ml collagenase IV dissolved in VitroHES and separated from remaining MEF by sedimentation. To get a single cell suspension colonies were incubated with 0.05% trypsin/EDTA (Biochrom) for five minutes. Preparation of chromosomes, high resolution GTG-banding and comparative genomic hybridization (CGH) were performed by the Institute of Medical Genetics Charité – Universitätsmedizin Berlin using standard protocols.

2.7 Immunocytochemistry of cultured hESC

The cultured cells were fixed and stained directly in the culture dishes. Prior to fixation the culture medium was removed and the cells were rinsed once with PBS. The cells were fixed with 4% paraformaldehyde solution for 10 min at room temperature, then rinsed once with PBS and permeabilized with 80% methanol for 20 min at -20°C. The following steps were performed at room temperature. After rinsing with PBS, the cells were incubated in blocking buffer (PBS with 3% BSA, 0.2% fish gelatine, 2% FCS) for 60 min. Subsequently the cells were incubated for 60 min with primary antibodies that were monoclonal mouse IgG anti-SSEA4 (MC-813-70) (Developmental Studies Hybridoma Bank (DSHB), University of Iowa, IA, USA), monoclonal mouse IgM anti TRA-1-60, monoclonal mouse IgM anti TRA-1-81 and polyclonal rabbit IgG anti-OCT4 (Santa Cruz Biotechnology, Santa Cruz, USA) followed by incubation with fluorochrome coupled goat-anti-mouse, mouse-anti-goat or goat-anti-rabbit IgG antibodies (1:1000, Dianova, Hamburg, Germany). Between each step of incubation, cells were washed three times with PBS. For non-specific staining of the nuclei, cells were incubated with 4',6-diamidino-2-phenylindole (DAPI, Molecular Probes) at a dilution of 1:20,000 in PBS for 5-10 min and washed once with PBS. Subsequently the cells were mounted with Aqua Polymount solution (Polysciences Inc.), covered with a glass lid, and stored in a dark place at 4°C until fluorescence microscopic analysis.

2.8 Flow cytometry analysis

Cells were washed three times with staining buffer (PBS w/o CaMg, 3% normal goat serum). To fix and permeabilize the cells they were incubated at 4°C for 20 min in Fix/Perm solution and washed with Perm/Wash solution (both solutions Becton Dickinson). Subsequently cells were incubated for 30 minutes at room temperature with the primary antibodies monoclonal mouse IgG anti-human SSEA4 (MC-813-70) (Developmental Studies Hybridoma Bank [DSHB], University of Iowa, IA, USA) and polyclonal rabbit IgG anti-human OCT4 (Santa Cruz Biotechnology, Santa Cruz, USA). Samples were then washed once with Perm/Wash and incubated with secondary antibodies (Cy2-conjugated goat-anti-mouse IgG-1/2a, Cy3-conjugated goat anti-rabbit IgG; Dianova) for 30 minutes. After washing with Perm/Wash and Staining buffer cell pellets were resuspended in 400µl staining buffer and 100µl of counting beads were added (Caltec/Invitrogen, Karlsruhe Germany). Cells were sorted using FACS Calibur

(Becton Dickinson, Heidelberg). Data were analyzed using CELLQuest software (Becton Dickinson) or FlowJo (Treestar, Ashland, OR, USA).

2.9 2D Control cultures

2.9.1 Spontaneous differentiation of hESC in 2D cultures

For comparison of the cell growth and differentiation with standard 2D culture conditions control cultures treated in similar to the bioreactors were analyzed. Spontaneous differentiation was examined by measurement of soluble factors produced by hESC cultured on MEF in IVF dishes in VitroHES containing 10 ng/ml hrbFGF. The hESC were not passaged during the observation period of 30 days and half of the total medium volume was replaced every other day with fresh medium.

2.9.2 Influence of bFGF and used culture medium on HFF in 2D cultures

For analysis of the influence of basic fibroblast growth factor (bFGF) and the culture medium 5.5 x 10^4/ cm^2 active and inactivated HFF were seeded in Iscove's Modified Dulbecco's Medium (IMDM) containing GlutaMax-1 (Invitrogen), 10% fetal calf serum and 10,000 U/ 10,000 µg/ml penicillin/streptomycin (all Biochrom) into 6-well culture plates. On the next day culture medium was changed to VitroHES containing 0, 4 or 10 ng/ml hrbFGF or IMDM supplemented with GlutaMax-1, 10% fetal calf serum and 10,000 U/ 10,000 µg/ml penicillin/streptomycin containing 0, 4 or 10 ng/ml hrbFGF. Cells were cultured in the respective media for four days and media were changed every day. The collected supernatants were analyzed for activin A, AFP and ß-hCG.

2.10 The investigated bioreactor

The multi-compartment bioreactors used for the studies are composed of three independent, yet interwoven hollow fiber capillary membrane systems (compartments II to IV, see Figure 1A) that are integrated into a two-component polyurethane housing (PUR, Morton, Bremen, Germany). Two hydrophilic capillary systems for medium perfusion are made of microporous polyethersulfone capillary membranes with a molecular weight cut-off of approximately MW 500,000 (mPES, Membrana, Wuppertal, Germany). The third one is made of hydrophobic multilaminate hollow fiber membrane capillaries (MHF, Mitsubishi, Tokyo, Japan) to enable gas exchange. The cells located within the extra-capillary space (cell compartment, Figure 1A, I) are thus exposed to

decentralized medium supply with high mass exchange rates and direct membrane oxygenation via diffusion. For cell injection, a flow head and open ending silicone rubber capillaries (Silastic, Dow Corning, New York, USA) are used. The bioreactor is integrated into a processor controlled perfusion device with pressure- and flow regulation for modular pumps with exchangeable multichannel flowheads and gears for medium recirculation and substitution (Figure 2A). A heating unit provides a constant temperature within the perfusion circuit. Flow rates of air and CO_2 were either manually controlled using integrated rotameters or by using an external automated CO_2-regulated pH control system (Figure 2A+B). The control device continuously measures the pH value of the culture medium via an optical pH sensor integrated into the bioreactor perfusion circuit and adjusts the air/CO_2 mixture to maintain a preset pH.

Perfusion tubings with bubble traps (shown in Figure 2C) were made from standard medical grade dialysis PVC (B.Braun, Melsungen, Germany). Sterilization was performed with ethylene oxide or formaldehyde gas followed by a degassing period of at least 7 days.

During the experiment perfusion devices were connected via an integrated USB port to a PC and the perfusion parameters (pressure, temperature, pump speeds) were continually recorded and graphically monitored using a stand alone measurement program created with LabVIEW (National Instruments, Munich, Germany). The program also provides a web server that enables remote monitoring via the internet (Figure 2B).

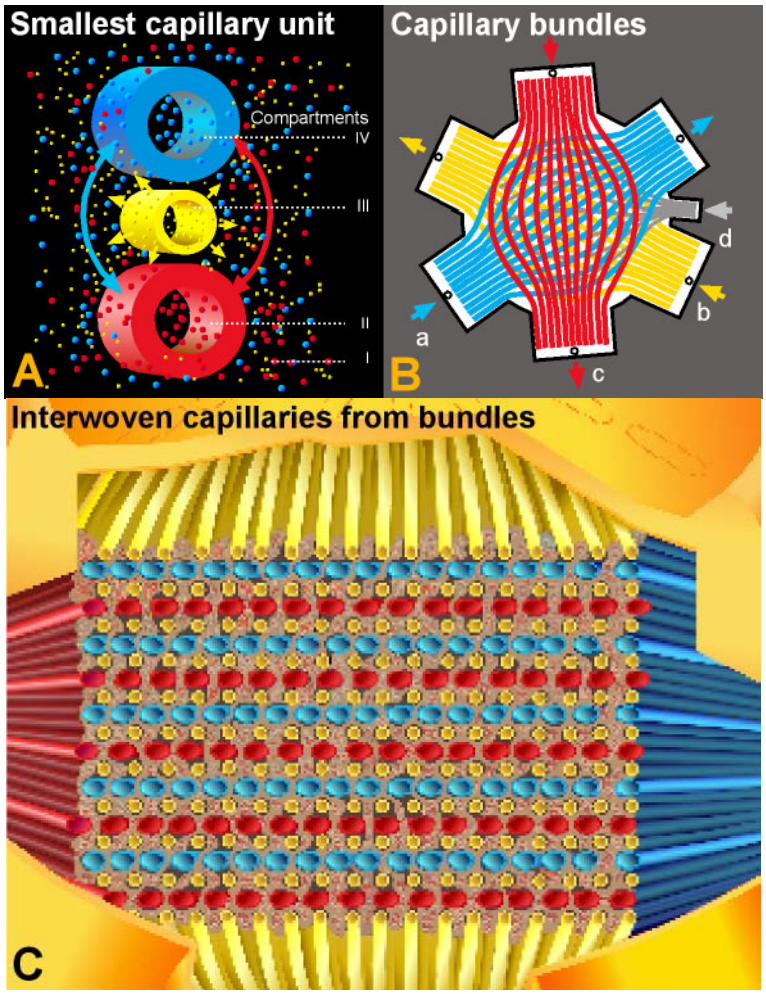

Figure 1: Bioreactor design. A) Smallest capillary membrane unit with independent compartments for medium perfusion (blue, II; red, IV), oxygenation (yellow, III) and cell accommodation (I); **B)** Capillary membrane bundles constituting these compartments; **C)** 3D arrangement of the capillaries/compartments within the cell compartment; The compartments can be perfused separately as shown in B, addressing the reduction of substance gradient distances between the capillary units and enhancing mass exchange. All membrane compartments are interwoven with each other within the cell compartment, forming a tight capillary network with intercapillary distances of averagely 500µm **(C)**. The capillaries of each compartment are bundled to in- and outflow heads, respectively, to be connected to tube systems for perfusion **(B)**. Cells are inoculated into the cell compartment via open ending tubes, which allows distribution of the injected cells within the cell compartment **(B, d;** shown in grey color).

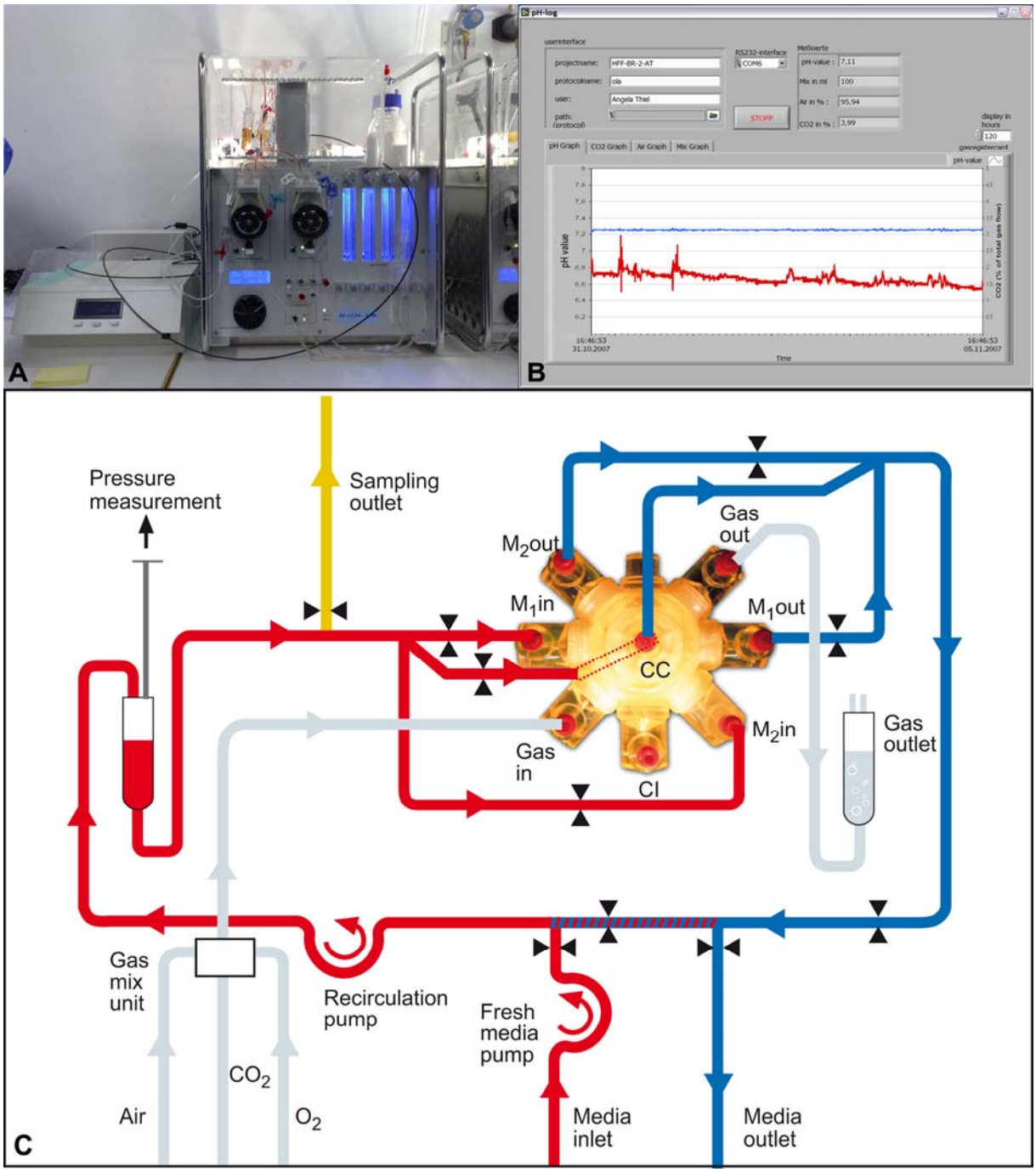

Figure 2: Perfusion system. **A)** Processor controlled perfusion device with pressure- and flow regulation for modular pumps with exchangeable multichannel flowheads and gears for medium recirculation and substitution and external automated CO2-regulated pH control system (on the left) **B)** Custom monitoring software that continually records and graphically monitors pressures, temperature, pump speeds, pH and gas flow. **C)** Schema of the tubing system used to perfuse the bioreactor with medium and gas.

2.11 Bioreactor Cultures

Before initial cell inoculation bioreactors underwent a conditioning phase of 24-72 hours with recirculation of medium. After cell inoculation cultures were perfused at a flow rate of 22-30 ml/minute. The bioreactors were kept at 37°C. The flow of the air/CO_2 mixture

in the gas compartment was maintained at 40 ml/minute. The pH, partial pressures of oxygen (pO_2) and carbon dioxide (pCO_2) and the acid/base status were periodically measured (ABL 5, Radio Meter Copenhagen, Copenhagen, Denmark). In case of manual gas control the air/CO_2 mixing ratio was adjusted to maintain a stable pH between 7.2 and 7.3. To allow online storage, access and analysis of the metabolic and perfusion data generated throughout the experiments a database was developed (Figure 3).

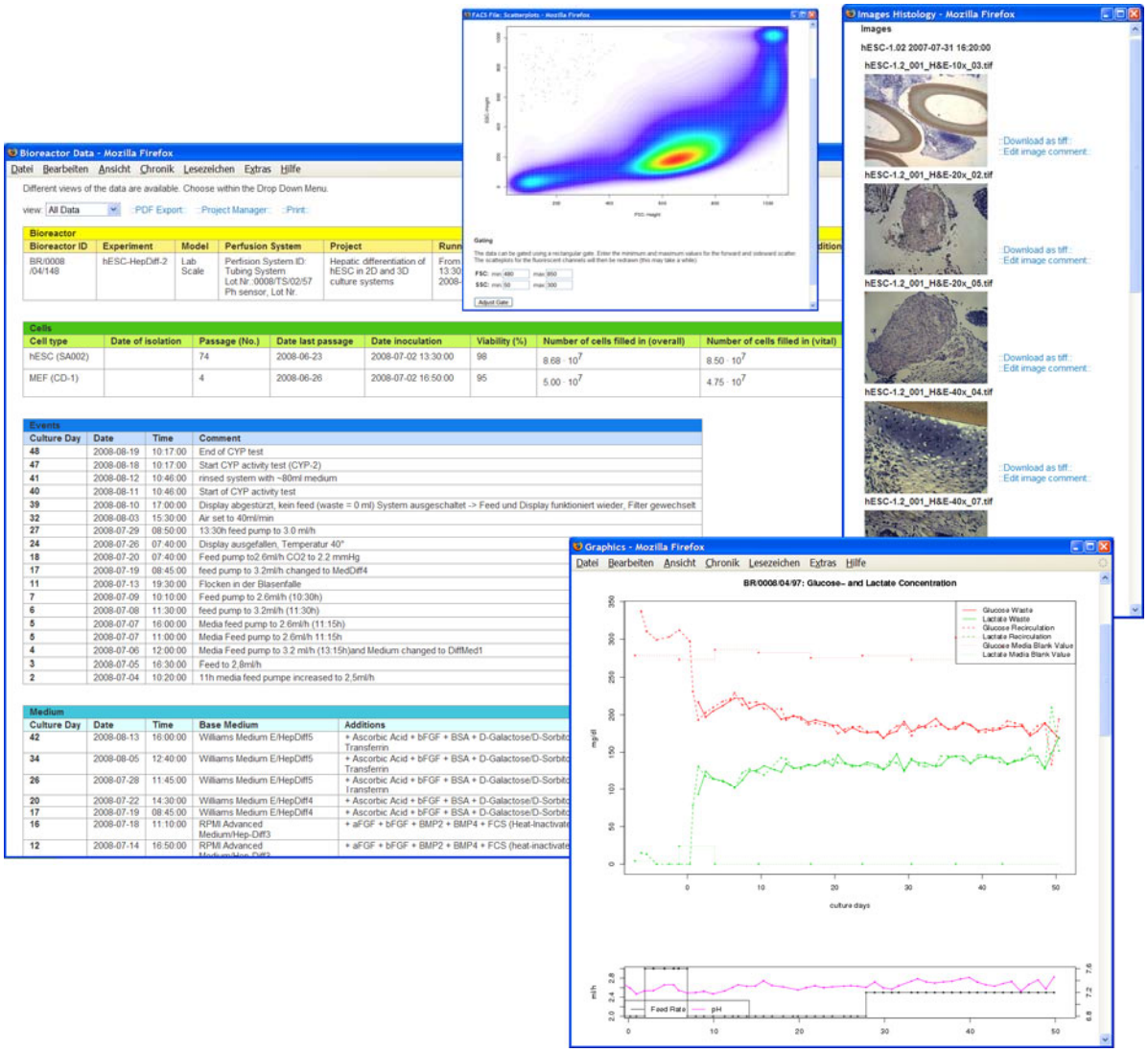

Figure 3: Screenshots of the database that was developed for online storage, access and analysis of the metabolic and perfusion data generated throughout the experiments. The database also provides an integrated sample management that stores information about sample storage and associates analysis results like pictures of histological stains and graphical display of flow cytometry data.

2.11.1 Spontaneous differentiation of hESC in the bioreactor

To examine spontaneous differentiation behavior of the hESC in the bioreactor, hESC were cultured with or without co-inoculation of inactivated HFF by using VitroHES medium (Vitrolife AB) supplemented with 10 ng/ml human recombinant basic fibroblast growth factor (hrbFGF; PeproTec) and 50 µg/ml gentamycin (Biochrom) or DMEM/F12 supplemented with 20% fetal calf serum, 1% non essential amino acids (NEAA), 50 µg/ml gentamycin (all Biochrom) and 1% Glutamax (Invitrogen) as culture medium. Table 1 lists the performed experiments and the experimental conditions. After cell inoculation fresh medium was continuously added to the perfusion circuit, initially at a flow rate of 2 ml/hour. The fresh medium feed was adjusted considering the parameters measured in the culture medium to maintain stable glucose levels, prevent accumulation of toxic metabolic cell products and maintain a stable medium osmolality.

Table 1: Overview of the performed bioreactor experiments

Experiment Name	Cell Types	Inoculated Cell Numbers	Medium	Length of the Bioreactor run
hESC-1	hESC HFF (irradiated)	$5.73x10^7$ $4.21x10^7$	VitroHES +10ng/ml bFGF	50 days
hESC-2	hESC HFF (irradiated)	$4.50x10^7$ $4.62x10^7$	VitroHES +10ng/ml bFGF	50 days
hESC-3	hESC HFF (irradiated)	$5.05x10^7$ $5.87x10^7$	VitroHES +10ng/ml bFGF	29 days
hESC-5	hESC	$15.9x10^7$	VitroHES +10ng/ml bFGF	50 days
hESC-4	hESC	$15.59x10^7$	DMEM/F12 +20% FCS +Glutamax +NEAA	50 days
hESC-HepDiff-1	hESC	$8.68x10^7$	Several	50 days
hESC-HepDiff-2	hESC MEF (irradiated)	$8.68x10^7$ $5.0x10^7$	Several	50 days
HFF-1	HFF (active)	$5.9x10^7$	IMDM +10% FCS > culture day 19 +4ng/ml bFGF > culture day 23 +10ng/ml bFGF	28 days
HFF-2	HFF (active)	$5.0x10^7$	VitroHES+10ng/ml bFGF > culture day 13: DMEM/F12 +20% SR +NEAA +ß-ME +10ng/ml bFGF	30 days

2.11.2 Bioreactor culture of HFF

To examine the behavior of active HFF cultured without hESC in the bioreactor, two additional bioreactor experiments were performed (see Table 1). The two bioreactor

experiments differed in the used medium: In one bioreactor (HFF-1) $5.6x10^7$ viable HFF were inoculated and cultured in IMDM containing GlutaMax-1 (Invitrogen), 10% fetal calf serum and 10,000 U/ 10,000 µg/ml penicillin/streptomycin (all Biochrom). Between culture day 19 and 23 4 ng/ml bFGF and from day 23 on 10 ng/ml bFGF were added to the medium.

In the other bioreactor (HFF-2) $4x10^7$ viable HFF were inoculated and cultured in VitroHES medium (Vitrolife AB) supplemented with 10 ng/ml human recombinant basic fibroblast growth factor (hrbFGF; PeproTec) and 50 µg/ml streptomycin (Biochrom) until culture day 13. Then the medium was changed to DMEM/F12 (Biochrom) containing 20% Knockout SerumReplacer, 2 mM GlutaMax–I (all Invitrogen), 0,1 mM nonessential amino acids, 10,000 U/10,000 µg/ml penicillin/streptomycin (all Biochrom), 0,1 mM ß-mercaptoethanol (Sigma) and 10 ng/ml hrbFGF (PeproTech). After cell inoculation fresh medium was continuously added to the perfusion circuit, initially at a flow rate of 2 ml/hour. The fresh medium feed was adjusted considering the parameters measured in the culture medium to maintain stable glucose levels, prevent accumulation of toxic metabolic cell products and maintain a stable medium osmolality.

2.11.3 Hepatic differentiation of hESC in the bioreactor

Two bioreactor runs were performed to examine directed hepatic differentiation. In one experiment the bioreactor was seeded with inactivated MEF two days before hESC inoculation while the other one was conducted without feeder cell addition (see Table 1 and Table 2). To induce hepatic differentiation of the hESC, bioreactors were perfused successively with five different media (HepDiff1-5) based on a differentiation protocol developed by Cellartis. An overview of the sequence, composition and fresh medium addition rates to the perfusion circuit of the media is shown in Table 2. For detailed medium compositions see Table 7 in the appendix.

Table 2: Overview of the sequence and composition of the media used to induce hepatic differentiation of hESC in the bioreactor (see Table 7 in the appendix for detailed medium compositions)

Culture Day		Medium Name	Medium Composition
Day -4- -3	Feed rate: 3 ml/ h	**hESC culture medium**	Knockout DMEM Medium +Knockout SR +Glutamax-I +ß-Mercaptoethanol +NEAA +bFGF
Day -2- -1	**Inoculation of MEF in one of the bioreactors** Feed rate: 2 ml/ h		
Day 0	**Inoculation of hESC in both bioreactors**		
Day 1-3	Feed rate: 2 ml/ h		
Day 4	rinse bioreactor initially with 300 ml medium Feed rate: 60 ml/ 24 h, 2,5 ml/ h	**DiffMed-1**	RPMI Advanced Medium +Glutamax-I +bFGF +Activin A
Day 5	Feed rate: 2,0 ml/ h		
Day 6	Feed rate: 60 ml/ 24 h, 2,5 ml/ h	**DiffMed-2**	RPMI Advanced +0.2% FCS +Glutamax-I +Activin A +bFGF
Day 7-8	Feed rate: 2,0 ml/ h		
Day 9	Feed rate: 60 ml/ 24 h, 2,5 ml/ h	**DiffMed-3**	RPMI Advanced Medium +0.2% FCS +Glutamax-I +aFGF +bFGF +BMP2 +BMP4
Day 10-16	60 ml/ 60 h equal to a complete medium exchange every 2-3 day, Feed rate: 1,0 ml/ h		
Day 17	Feed rate: 60 ml/ 24 h, 2,5 ml/ h	**DiffMed-4**	Williams Medium E +BSA +Ascorbic Acid +Glutamax-I +D-Galactose/D-Sorbitol +Hydrocortisone +Insulin +Transferrin +bFGF +EGF +HGF
Day 18-25	60 ml/ 60 h equal to a complete medium exchange every 2-3 day, Feed rate: 1,0 ml/ h		
Day 26	Feed rate: 60 ml/ 24 h, 2,5 ml/ h	**DiffMed-5**	Williams Medium E +BSA +D-Galactose/D-Sorbitol +Glutamax-I +Dexametasone +Ascorbic Acid +Hydrocortisone +Insulin +Transferrin +EGF +bFGF +HGF +Oncostatin M
Day 27-36	60 ml/ 60 h equal to a complete medium exchange every 2-3 day, Feed rate: 1,0 ml/ h		
Day 37	Testing of CYP450 activities Feed rate: 0 ml/ h		
Day 38-43	Feed rate: 1,0 ml/ h		
Day 44	Testing of CYP450 activities Feed rate: 0 ml/ h		
Day 45-49	Feed rate: 1,0 ml/ h		
Day 50	Shutdown of bioreactor		

(NEAA: non essential amino acids, bFGF: basic fibroblast growth factor, HGF: hepatocyte growth factor, EGF: epidermal growth factor, BSA: bovine serum albumin, BMP: bone morphogenic protein)

2.12 Metabolic parameters in the perfusion medium

The metabolic activity and differentiation of the cells inside the bioreactors were characterized on a daily basis by measuring soluble factors in the medium outflow and in the recirculating medium. The following parameters were measured using automated clinical chemistry analyzers (Roche Diagnostics, Heidelberg, Germany): α-fetoprotein (AFP), alkaline phosphatase (AP), alanine transaminase (ALT), aspartate transaminase (AST), beta-human chorionic gonadotropin (ß-hCG), c-peptide, carcinoembryonic

antigen (CEA), cytokeratin fragment 19 (Cyfra 21-1), erythropoetin, estradiol, follicle stimulating hormone (FSH), factors II-V-X-XIII, fibrinogen, gamma-glutamyltransferase (GGT), glucose, lactate, lactate dehydrogenase (LDH), luteinizing hormone, neuronspecific enolase (NSE), osmolality, osteocalcin, pseudocholinesterase (PCHE), prealbumin progesterone, prolactin, S-100, thyroid-stimulating hormone (TSH), tissue plasminogen activator (TPA), transferrin (for a detailed description of the measurement methods see Table 8 in appendix). Additionally glutamine, glutamate, glucose, lactate, ammonium, pH, sodium (Na^+), potassium (K^+) were measured with a BioProfile 100 Plus device (Nova Biomedical, Waltham, MA, USA).

Activin A, insulin and albumin were measured with enzyme-linked immunosorbent assays (ELISAs) following the manufacturer's recommendations (activin A using products DY338, DY999, DY994, DY995 from R&D Systems, Wiesbaden-Nordenstadt, Germany; insulin using an ELISA from Invitrogen; albumin using an ELISA from Albuwell, Exocell Inc., Philadelphia, PA, USA).

Urea was measured using a colorimetric determination kit (QuantiChrom, BioAssay Systems, Hayward, CA, USA). Galactose and sorbitol concentrations were measured by enzymatic assays (Roche Diagnostics).

The production or consumption rate of each substance was calculated per bioreactor per day by multiplying the actual waste volume of the day by the difference between the substance concentration in the feed medium and that in the waste medium.

2.13 CYP450 activity

Bioreactor cultures that were treated with the hepatic differentiation protocol were tested for their ability to metabolize phenacetin, diclophenac and midazolam via the phase I cytochrome (CYP) P450 enzymes CYP1A2, CYP2C9 and CYP3A4, respectively.

At days 40 and 47 after inoculation of the cells a CYP P450 activity test was performed. For this purpose, fresh medium inflow and medium outflow was closed and a cocktail of the test substances was injected into the recirculating medium to get the following concentrations at the beginning of the test: 3 µM Midazolam, 9 µM Diclophenac and 26 µM Phenacetin.

During the next 24 hours, the bioreactor was operated in recirculation mode (no fresh medium was added and only the medium recirculation pump recirculates the medium). Samples from the recirculation were taken before starting the experiment and after 1, 4,

8 and 24 hours and analyzed for the metabolites of the test substances (Figure 4) by liquid chromatography/ mass spectrometry (LC/MS). Analyses were performed at Astrazeneca AB, Gothenburg, Sweden. After the last sample was taken the bioreactor was flushed with fresh medium in single pass mode with two times the volume of the bioreactor and tubing system and then switched to the normal perfusion mode (recirculation with fresh medium inflow).

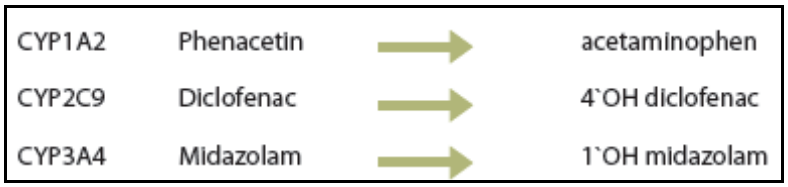

Figure 4: Used test substances for cytochrome P450 activity and their specificity.

2.14 Sample acquisition from the bioreactor

At the end of the scheduled culture period, bioreactors were shut down and the tubing was disconnected. The lower bioreactor lid was opened and samples of the cell mass including the capillary layers were cut out using sterile scalpels and forceps for further analysis. For histological analysis samples were directly fixed and embedded as described below.

For teratoma testing, FACS and RNA analysis, cells were separated from the capillaries and dissociated by washing with PBS w/o CaMg and incubation for 3 minutes in 0.05%-0.02% trypsin-EDTA solution (Biochrom). Trypsination was stopped by addition of DMEM containing 10% fetal calf serum (Biochrom). Separation of the capillaries from the cell solution was achieved by sieving using a 100µm cell strainer (Falcon, Becton Dickinson, Heidelberg)

2.15 In vivo teratoma formation

Studies on *in vivo* teratoma formation were performed in cooperation with the group Experimental Pharmacology at the Max Delbrück Center of Molecular Medicine (MDC) in Berlin. Into each recipient NOD/SCID mouse an aliquot of 1-3x10^6 cells from the cell suspension used for bioreactor inoculation or harvested from the bioreactor at the end of the experiment were injected subcutaneously within a Matrigel suspension (BD Biosciences). Body weights and tumor sizes were measured once per week. If cells were injected at the start of the bioreactor the run mice were sacrificed at the day of

experiment shut down or in one case after 49 days. Tumors were excised and used for RNA expression profiling and histological analysis.

2.16 Expression Profiling

2.16.1 Isolation of RNA

To isolate RNA from cells/ tissue cultured in the bioreactor excised capillaries were washed with PBS w/o CaMg and incubated for 3 min in 0.05%-0.02 trypsin-EDTA solution (Biochrom). Total RNA was isolated using the RNeasy Kit (Qiagen, Hilden, Germany) following the manufacturer's protocol. Teratomas were disrupted using a TissueLyser II followed by homogenization with a QIAshredder (both Quiagen). Single cells were lysed by direct addition of lysis buffer to the cell pellet. The concentration and quality of the isolated RNA was determined using a Nanodrop spectrophotometer (Thermo Fischer Scientific) and with a Bioanalyser (Agilent 2100 Bioanalyser) or by native agarose gel electrophoreses.

2.16.2 Array hybridisations

Biotin-labeled cRNA was generated using the Illumina® TotalPrep RNA Amplification Kit (Ambion, Austin, TX, USA) with 300 ng of quality-checked total RNA as input. Chip hybridizations, washing, Cy3-streptavidin (Amersham Biosciences) staining, and scanning were performed on an Bead Station 500 (Illumina, San Diego, USA) platform using reagents and following protocols supplied by the manufacturer. cRNA samples were hybridized on Illumina human-8v2 BeadChips, which harbor approximately 24,000 RefSeq transcripts (Kuhn et al. 2004).

2.16.3 Data analysis

Quantil normalized and non-normalized RAW data files for all samples were generated using the BeadStudio V3 software (Illumina).

Further data analysis was performed by importing the data generated with the BeadStudio software into the microarray data analysis tools MultiExperiment Viewer (MeV), a component of the TM4 suite of microarray analysis tools (http://www.tm4.org) (Saeed et al. 2003) or Chipster (http://chipster.sourceforge.net/), which is a graphical interface that uses Bioconductor (Gentleman et al. 2004) as its analysis backend. Functional enrichment analysis was performed using DAVID

(http://david.abcc.ncifcrf.gov) (Dennis et al. 2003). Venn diagrams of the expressed genes were generated after filtering the expression data for a detection p-value <0.01.

Table 3: Samples used for expression profiling

Sample Name	Origin of the RNA Sample
hESC-1 (BR90)	Isolated from the bioreactor at the end of the experiment
hESC-2 (BR91)	
hESC-3 (BR92)	
hESC-4 (BR97)	
hESC-5 (BR98)	
Teratom B2	Teratoma grown from cell suspension used to inoculate bioreactor hESC-3, grown for 69 days
Teratom MV8479-A2	Teratoma grown from cell suspension used to inoculate bioreactor hESC-4-5, grown for 50 days
Teratom MV8479-A3	
Teratom MV8479-A4	
SCED (SA002)	hESC/HFF co-culture (passage 36) cultured in VitroHES +10ng/ml bFGF
SCED (BR97-98)	hESC/HFF co-culture (passage 53) cultured in VitroHES +10ng/ml bFGF, inoculated in bioreactors hESC-4/5
SCED StdMed	SCED culture (passage 56) cultured in Standard Medium (DMEM/F12, 20% Knockout SerumReplacer, Non essential amino acids, GlutaMax, ß Mercaptoethanol, 10ng/ml bFGF)
hESC undiff (SA002)	undifferentiated hESC cut from a MEF co-culture (passage 35)
HFF	HFF inactivated by irradiation cultured a gelatin coated flask for two days in VitroHES +10ng/ml bFGF
HFF 2D StdMed+FCS	active HFF cultured in IMDM +10% FCS

2.17 Histology

2.17.1 Histochemistry

Paraffin embedded samples were fixed in 4% buffered formaldehyde solution, embedded in paraffin and cut into 5 µm sections. Sections were deparaffinized with xylene and rehydrated with decreasing alcohol series followed by hematoxylin and eosin (H&E) staining.

2.17.2 Immunohistology

Paraffin embedded samples were fixed in 4% buffered formaldehyde solution, embedded in paraffin and cut into 5 µm sections. Sections were deparaffinized with xylene and rehydrated with decreasing alcohol series. Antigens were retrieved by boiling sections for 25 min in a pressure cooker in citrate buffer (0.01 citric acid monohydrate, pH to 6.0; Merck, Darmstadt, Germany) followed by incubation for 20 min in 5% Triton/PBS. Sections were blocked with 5% skim milk; they were incubated with

primary antibodies for 30 min, washed with PBS and incubated with the secondary fluorescence conjugated antibodies.

The following primary antibodies were used: monoclonal mouse anti human smooth muscle actin IgG2a (ASMA), monoclonal mouse anti human desmin IgG1 (Dako, Glostrup, Denmark), monoclonal mouse anti neuron-specific ß-III-Tubulin IgG2a (R&D Systems), monoclonal mouse anti nestin IgG1 (Becton Dickinson), polyclonal goat anti HNF-3ß IgG, monoclonal mouse anti OCT-4 IgG2b and polyclonal rabbit anti vimentin IgG (Santa Cruz Biotechnology). As secondary antibodies the following polyclonal antibodies were used: goat anti mouse IgG-Cy2, goat anti rabbit IgG-Cy3 (Dianova), goat anti mouse IgG2a-TRICT, goat anti mouse IgG-FITC, goat anti mouse IgG-FITC, goat anti mouse IgG-Cy3, goat anti mouse IgG-FITC (Jackson Immunoresearch Laboratories, West Grove, PA) and donkey anti goat IgG-Cy3 (Santa Cruz Biotechnology). For non-specific staining of the nuclei, sections were incubated with 4',6-diamidino-2-phenylindole (DAPI, Molecular Probes, Leiden, Germany). Subsequently the sections were mounted with Aqua Polymount solution (Polysciences Inc., Warrington, PA, USA. Sections were analyzed using an inverse microscope (Axiovert 200M, Carl Zeiss, Göttingen, Germany) equipped with a CCD-camera (Retiga 2000R, QImaging, Burnaby, Canada). The pictures were acquired and processed using the digital imaging software “Image Pro Plus” (Media Cybernetics, Silver Spring, USA).

2.17.3 Transmission Electron Microscopy (TEM)

Transmission electron microscopy was performed in cooperation with the Department of Anatomy at the Charité (Prof. Dr. S. Bachmann). Material from the bioreactor cell compartment was fixed with 5% glutaraldehyde (Serva, Heidelberg, Germany). After immersion for 30 minutes in 60 mmol/l phosphate buffer, pH 7.3, the cellular aggregates were post-fixed in 2% OsO4 (Paesel+Lorei, Frankfurt, Germany) for 2 h, progressively dehydrated in ethanol and then embedded in araldite (Serva, Heidelberg, Germany). Ultra-thin sections were contrasted with uranyl acetate and Reynold´s lead citrate (Chroma, Münster, Germany) before electron microscopic examination.

3 Results

3.1 Preparatory work

The first part of this work was the establishment of culture and characterization methods of human embryonic stem cells in our laboratory. This was achieved in close cooperation with the company Cellartis in Gothenburg, Sweden, that also supplied the used hESC line SA002.

Basic procedures were established including cultivating, mechanical passaging, proliferation and cryopreservation of hESC. For bioreactor experiments large numbers of hESC are needed, which cannot be produced using manual mechanical passaging methods. Therefore a protocol using a co-culture system with human feeder cells and utilizing enzymatic passaging was established to enable production of large cell numbers.

In addition culture, mitotic inactivation and cryopreservation of the two feeder cell types (human foreskin fibroblasts (HFF) and mouse embryonic fibroblasts (MEF)) needed for hESC culture were established and optimized.

For quality control and analysis of the differentiation state of hESC a karyotyping method and immunostaining protocols for pluripotency markers were established as well as a protocol for FACS analysis to examine the composition of the cell suspensions that were inoculated into the bioreactors. This also included the adaptation of staining procedures, such as antigen retrieval, blocking of non specific binding, incubation times and antibody concentrations.

The existing protocols for the culture of liver cells in the bioreactor system were evaluated and adapted to the requirements of hESC culture.

This preparatory work resulted in standard operating protocols (SOPs) for the efficient cultivation and expansion of undifferentiated hESC in 2D and accomplishment of culture and differentiation experiments in the four compartment bioreactors.

3.2 Quality control of the inoculated cells

It is known that hESC are prone to genetic and epigenetic alterations due to culture conditions (Hanson et al. 2005; Maitra et al. 2005; Catalina et al. 2008). Therefore the quality of the hESC was regularly controlled by analyzing the morphology, immunofluorescence staining of pluripotency markers and karyotypisation.

3.2.1 hESC morphology and pluripotency markers

During every passage hESC morphology was microscopically assessed. Undifferentiated hESC that grow on MEF feeders form sharply bordered, homogenously patterned flat colonies of small cells with a low cytoplasm to nucleus ratio (Figure 5a). To yield enough cells needed for inoculation into a bioreactor, mass expansion of the hESC in 2D cultures was necessary. To achieve this hESC were grown in co-cultures with HFF because this culture system allows higher cell densities and is much more efficient in suppression of spontaneous hESC differentiation. In HFF co-cultures undifferentiated hESC form more compact, often multilayered, sharply bordered colonies compared to those in MEF co-cultures (Figure 5d).

To further asses the differentiation state of the cells immunofluorescence staining of the pluripotency markers OCT4, TAR-1-81, TRA-1-60 and SSEA4 was performed (Figure 5b, c, e, f). Undifferentiated hESC showed co-expression of these markers and it could be observed that OCT4 expression was the most sensitive pluripotency marker which disappeared first at the onset of differentiation.

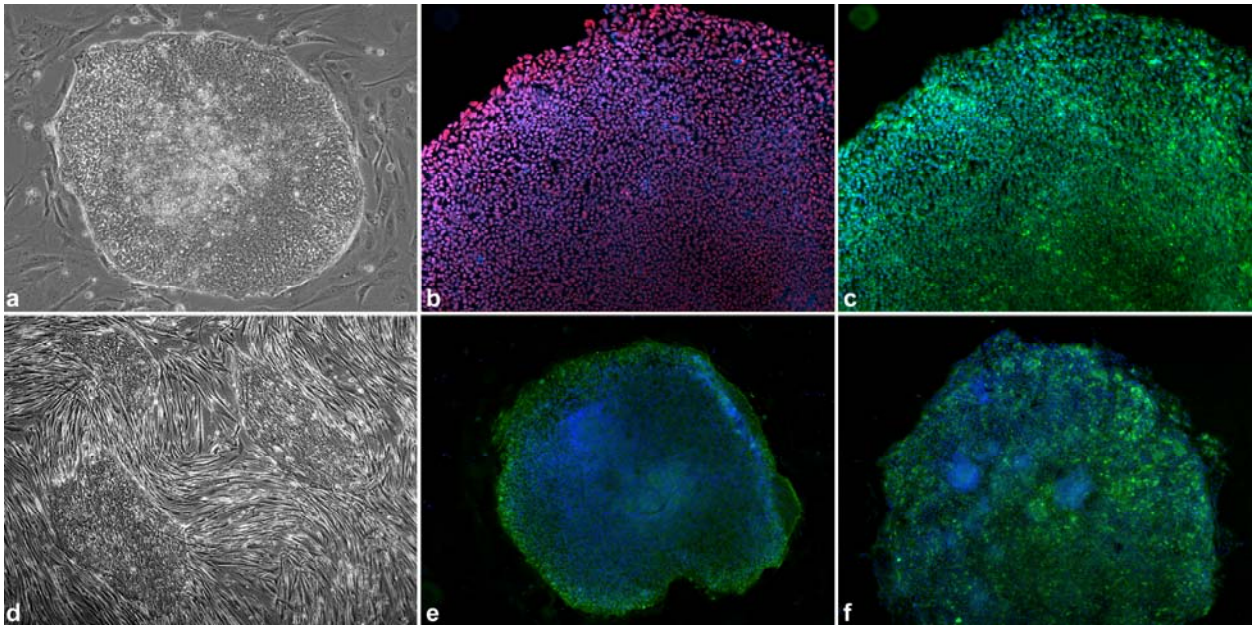

Figure 5: Pluripotency markers of the cultured hESC (SA002). For maintenance hESC were cultured in small scale on MEF feeders **(a)** and for expansion of the hESC for bioreactor inoculation cells were cultured on HFF feeders **(d)**. Cells were routinely examined for expression of the pluripotency markers OCT4 **(b**, red**)**, TRA-1-81 **(c**, green**)**, SSEA4 **(e**, green**)**, TRA-1-60 **(f**, green**)**. Nuclei were stained with DAPI (blue). (magn. a,d-e: 50x; b,c: 100x)

3.2.2 Karyotyping of the hESC

To exclude possible alterations of the original karyotype of the hESC line due to culture conditions, karyotyping by high resolution GTG-banding and comparative genomic hybridization (CGH) was performed after 47 passages in culture in our lab respectively after 66 passages after derivation of the hESC line (Figure 6). The results showed that the hESC had a female karyotype carrying a trisomy of chromosome 13 (47, XX, +13), which is the described original karyotype of the hESC line SA002 (Heins et al. 2004). Therefore karyotypic alterations could be excluded.

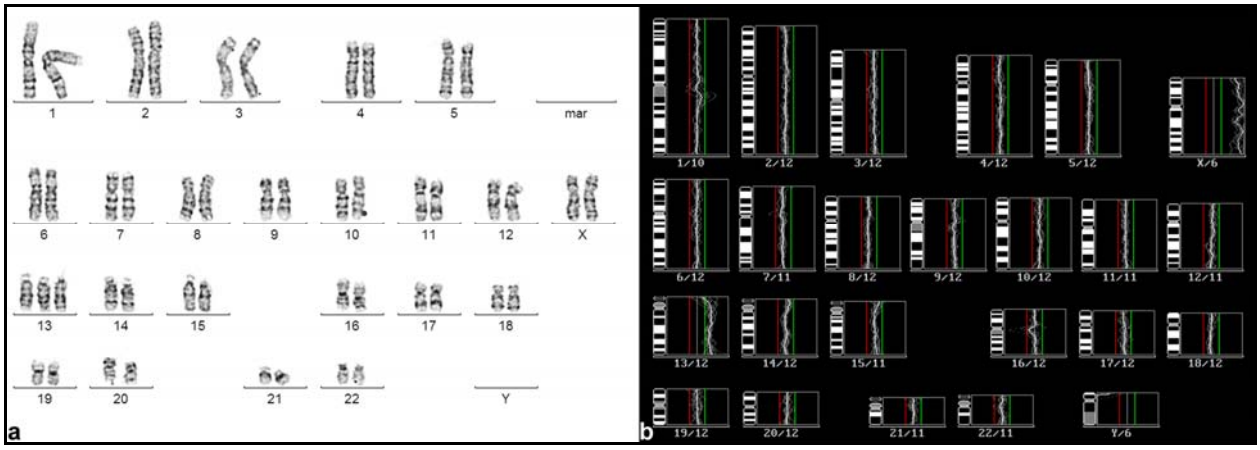

Figure 6: Karyotyping of the cultured hESC (SA002). (a) High resolution GTG-banding. **(b)** Comparative genomic hybridization (CGH). After 47 passages in culture in our lab (total passages of the hESC: 66) no alterations of the original karyotype (47, XX, +13) of the hESC cell line SA002 were detected.

3.2.3 Flow cytometry analysis

Cell compositions of the cell suspensions derived from the hESC/ HFF co-cultures that were inoculated into the bioreactors were assessed by flow cytometry regarding the cells forward (FSC) and sideward scatter (SSC) characteristics and their expression of the pluripotency markers OCT4 and SSEA4.

The FSC and SSC characteristics of the hESC and HFF were similar and therefore efficient gating of only hESC was not possible (Figure 7b). Cell suspensions contained 45±13% of cells that were double positive for OCT4/SSEA4 and therefore can be assumed to represent undifferentiated hESC (Figure 7a). In addition cell suspensions contained 21±5% of cells that were single positive for SSEA4. These cells are most probably hESC that already entered differentiation or undifferentiated hESC that transiently do not express OCT4. The cells that are negative for both pluripotency markers represent HFF or other cell types developed from the hESC by differentiation.

The influence of the cell harvesting procedure from the 2D co-cultures on the negative cell fraction in the cell suspension becomes visible by comparison of its size in the different suspensions. During cell harvesting for experiments hESC-1, -2, -3, -4 and -5 the HFF feeder layer was detached together with the hESC that were growing on top by enzymatic treatment followed by thoroughly pipetting to detach the hESC. This resulted in a fraction of 32±9% of OCT4/SSEA4 negative cells in these cell suspensions. In experiments hESC-HepDiff-1+2 the HFF feeder layer was not detached and hESC were washed off the layer by rinsing with enzyme solution. The resulting solutions contained considerably less OCT4/SSEA4 negative cells (11%), which indicates a reduction of HFF in this cell preparation.

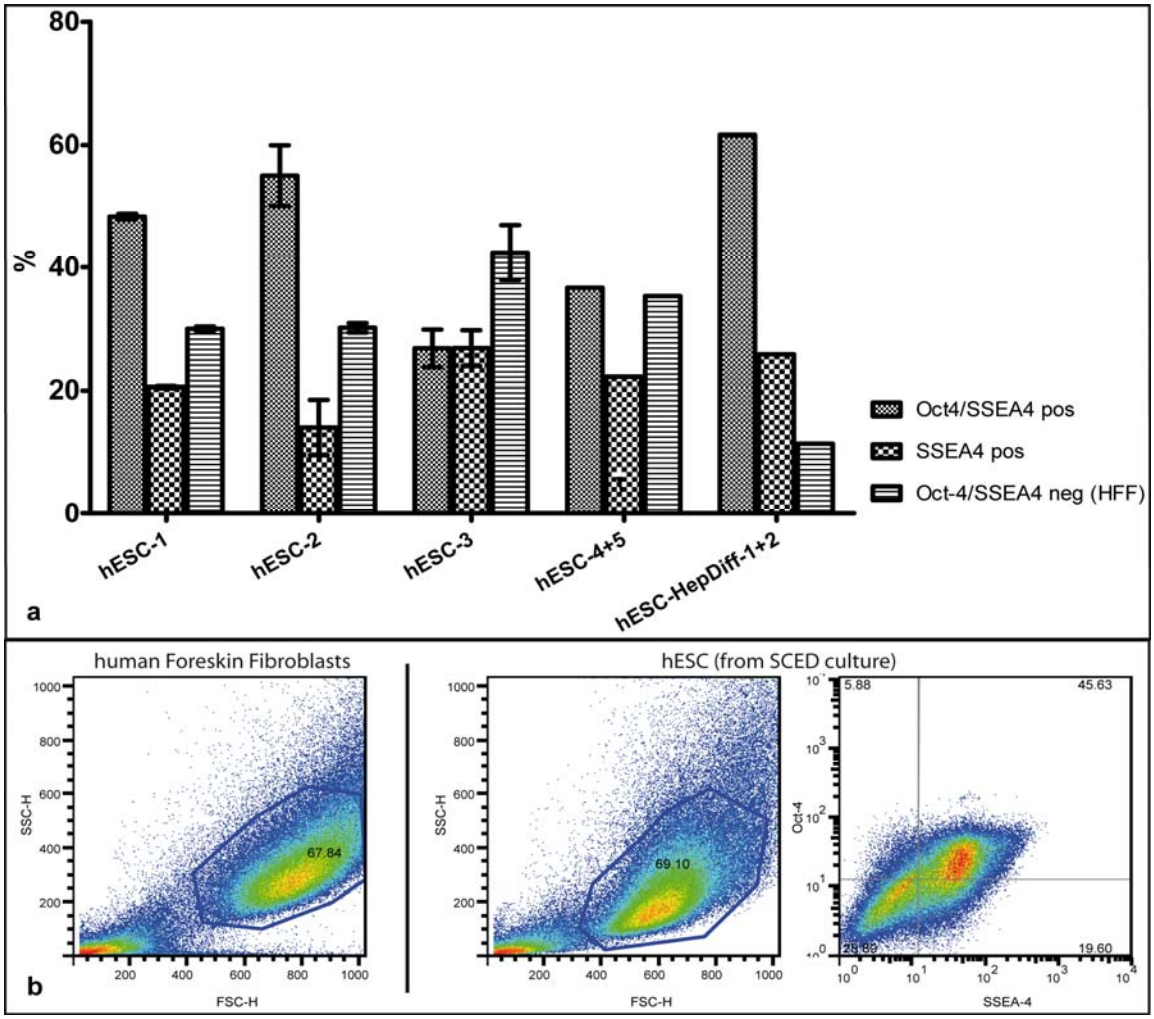

Figure 7: Flow cytometric analysis of the cell suspensions inoculated into the bioreactors. Compositions of the cell suspensions from hESC/ HFF co-cultures were analyzed by the expression of the pluripotency markers OCT4 and SSEA4. Exemplary scatter plots of the forward and sideward scatter characteristics of HFF alone and cells harvested from a SCED culture (hESC+ HFF) are shown in **(b).** In average 32±9% of the inoculated cells were OCT4/ SSEA4 double positive **(a).**

3.3 Spontaneous differentiation of hESC in the investigated bioreactor

To validate the bioreactor system for its suitability as an *in vitro* system that supports growth and differentiation of hESC, five bioreactor experiments were carried out (experiments hESC-1, -2, -3, -4 and -5; see Table 1 in the methods chapter).

In these experiments bioreactors were inoculated with hESC suspensions and the growth and spontaneous differentiation behavior was analyzed by monitoring soluble factors during the bioreactor runs as well as by analysis of samples taken from the cell compartment at the end of the experiments using histological and molecular biological methods.

As an *in vivo* reference a sample of the particular cell suspensions that were inoculated into the bioreactors was subcutaneously injected into NOD/SCID mice to induce teratoma formation. The mice were sacrificed at the day of bioreactor shut down and the excised teratomas were analyzed with the same methods as the bioreactor samples. As a control the spontaneous differentiation behavior of hESC was analyzed in 2D cultures over a period of 30 days.

3.3.1 Metabolic parameters in the perfusion medium

3.3.1.1 Bioreactor cultures with additional HFF inoculation and using medium containing serum replacement

In three bioreactors a number of 4.5±0.5 $x10^7$ irradiated HFF were inoculated two days before inoculation of the 5.4±0.5$x10^7$ hESC/HFF harvested from the 2D co-cultures. The used culture medium contained serum replacement and 10 ng/ml bFGF (experiments hESC-1, -2 and -3). During culture glucose consumption and lactate production were daily measured in the bioreactor circuits and medium outflow to oversee the general cell activity and LDH release to detect potential cell damage. In bioreactors hESC-1 and -2 glucose consumption and lactate production showed a slow but constant increase over the culture time, suggesting an increase in cell number. LDH showed decreasing levels after an initial peak due to cell damage after cell inoculation (Figure 8a+b). In bioreactor hESC-3 that was only cultured for a period of 29 days glucose, lactate and LDH showed decreasing levels (Figure 8c).

To screen for cell differentiation several differentiation markers were measured in the medium outflow (see Table 8 in the appendix). Among these factors activin A, alpha fetoprotein (AFP), and beta-human chorionic gonadotropin (ß-hCG) could be detected

and showed significant changes in their time courses. Yet again these factors showed a similar time course in bioreactors hESC-1 and -2 (Figure 9a+b). Activin A production showed initially high concentrations, subsequently decreased and reached a minimum between day 15 and 25. Afterwards activin A again slowly increased until the end of the bioreactor runs. AFP production started to rise at about days 15 to 20 and continued to increase during the entire observed period of 50 days. ß-hCG started to increase in the bioreactor at about day 20, peaked at around day 40 and decreased thereafter. The onset of production of AFP and ß-hCG suggests ongoing cell differentiation.

Differentiation markers measured in bioreactor hESC-3 showed a different profile. Activin A production stayed on a continuous high level and no production of AFP or ß-hCG could be detected (Figure 9c). On evaluation of the results from bioreactor hESC-3 it has to be considered that it experienced some temperature fluctuations due to technical malfunction that could be the reason for its differing behavior.

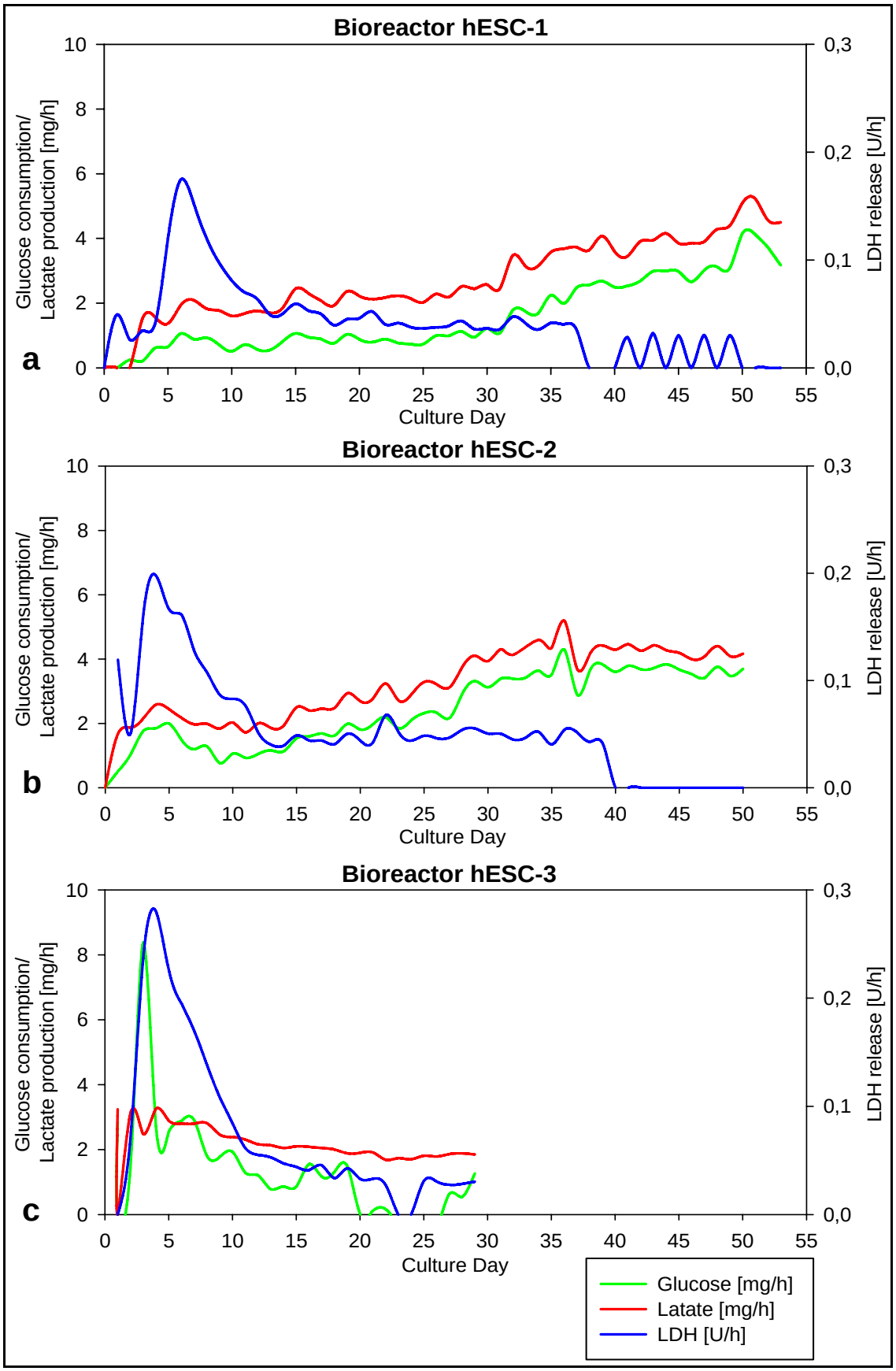

Figure 8: Time course of the metabolic parameters measured in the medium outflow of bioreactors hESC-1, -2 and -3. Glucose consumption (green), lactate production (red) and LHD release (blue) of the cells in bioreactors hESC-1 **(a),** hESC-2 **(b)** and hESC-3 **(c).**

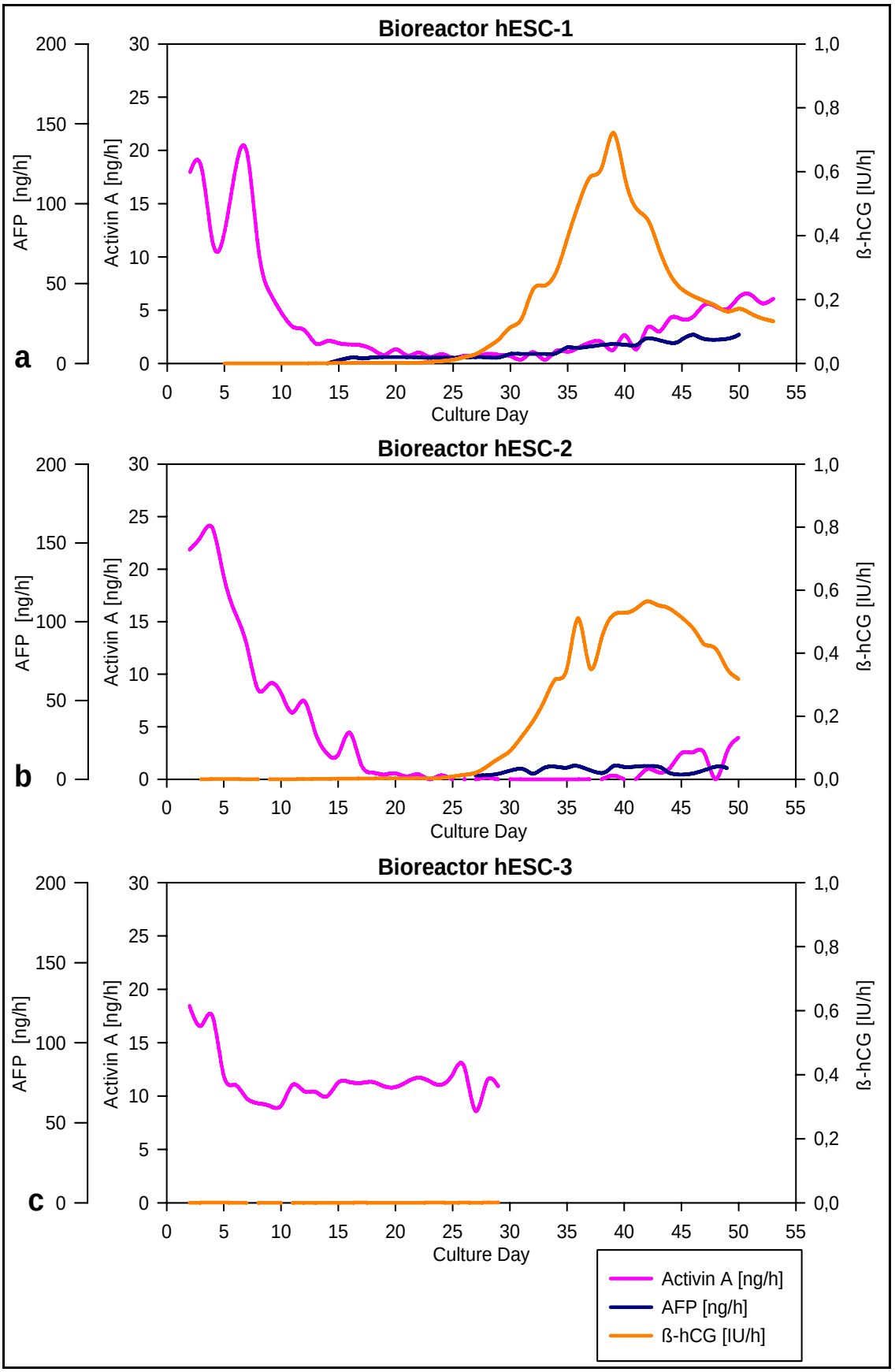

Figure 9: Time course of the differentiation markers measured in the medium outflow of bioreactors hESC-1, -2 and -3. Activin A production (pink), AFP production (dark blue) and ß-hCG production (yellow) of the cells in bioreactors hESC-1 **(a),** hESC-2 **(b)** and hESC-3 **(c).**

3.3.1.2 Influence of HFF and serum containing medium on hESC differentiation

To further analyze the influence of the HFF feeder cells and of the culture medium one bioreactor experiment was performed without additional HFF inoculation but using the same medium as before (hESC-5) and another experiment was also performed without HFF inoculation while using a nutrient rich culture medium containing FCS (hESC-4). The medium was chosen based on the hypothesis that such a medium better approximates to the *in vivo* environment the cells experience when they are transplanted in a mouse in a teratoma formation assay and therefore will enhance differentiation.

In bioreactor hESC-4 glucose, lactate and LDH showed constant levels after an initial peak in LDH release (Figure 10a). Activin A production decreased slowly and could not be detected after day 32. ß-hCG production could not be detected throughout the experiment duration of 50 days and only low levels of AFP starting day 41 were observed (Figure 11a).

Time courses of glucose, lactate and LDH in bioreactor hESC-5 (Figure 10b) were similar to bioreactors hESC-1 and -2 unlike the measured differentiation factors (Figure 11b). Specifically only a low rapidly decreasing activin A production could be detected from the beginning of the experiment until day 10 and ß-hCG production started to increase beginning on day 10 but stayed on a much lower level compared to bioreactors hESC-1 and -2. Most notable the level of AFP exhibited an exponential increase from day 10 onwards with a peak on day 25 of 350 ng/h followed by a slight decrease until day 37 and a stable level of about 250 ng/h until the end of the experiment.

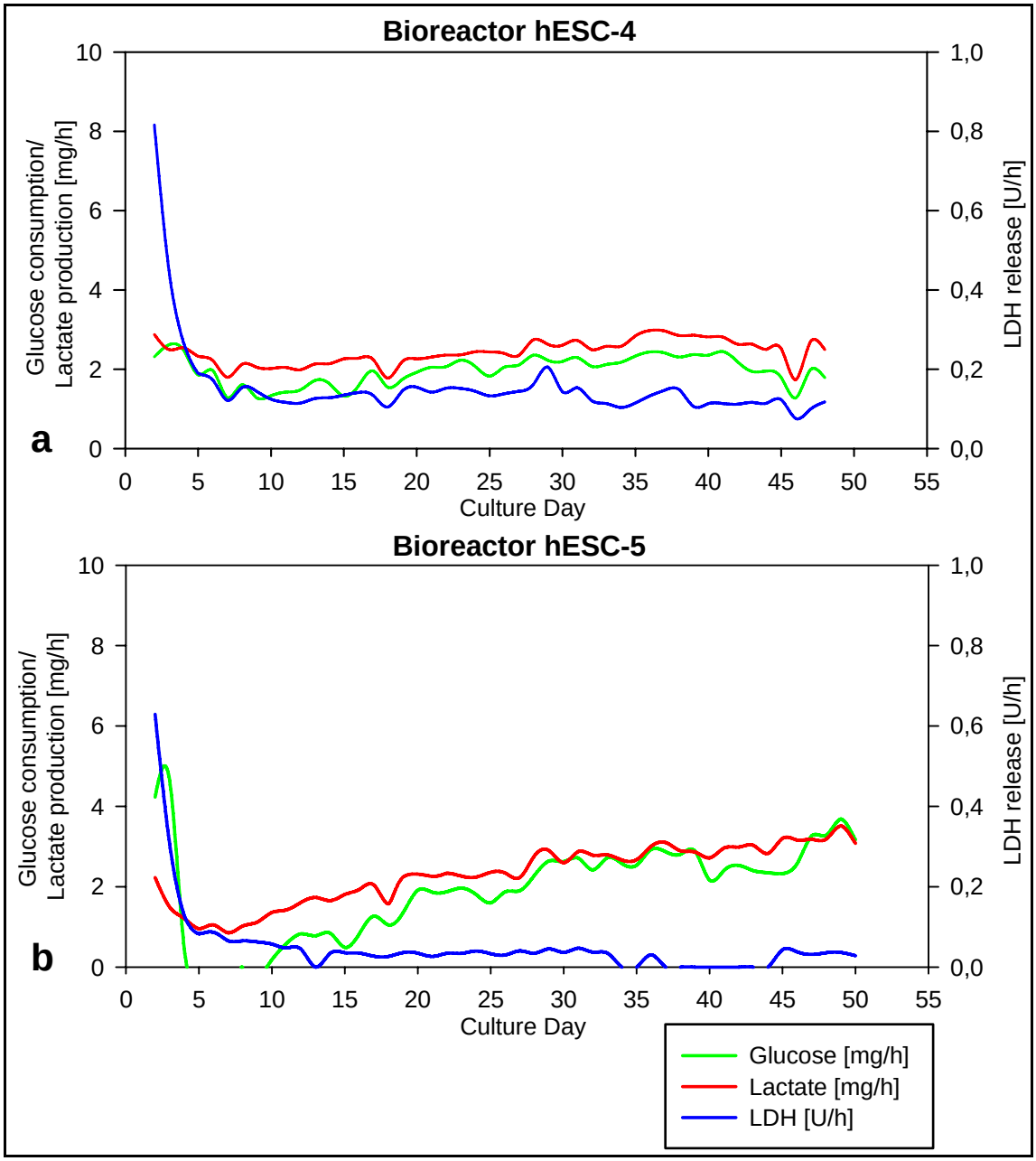

Figure 10: Time course of the metabolic parameters measured in the medium outflow of bioreactors hESC-4 and -5. Glucose consumption (green), lactate production (red) and LHD release (blue) of the cells in bioreactors hESC-4 **(a)** and hESC-5 **(b).**

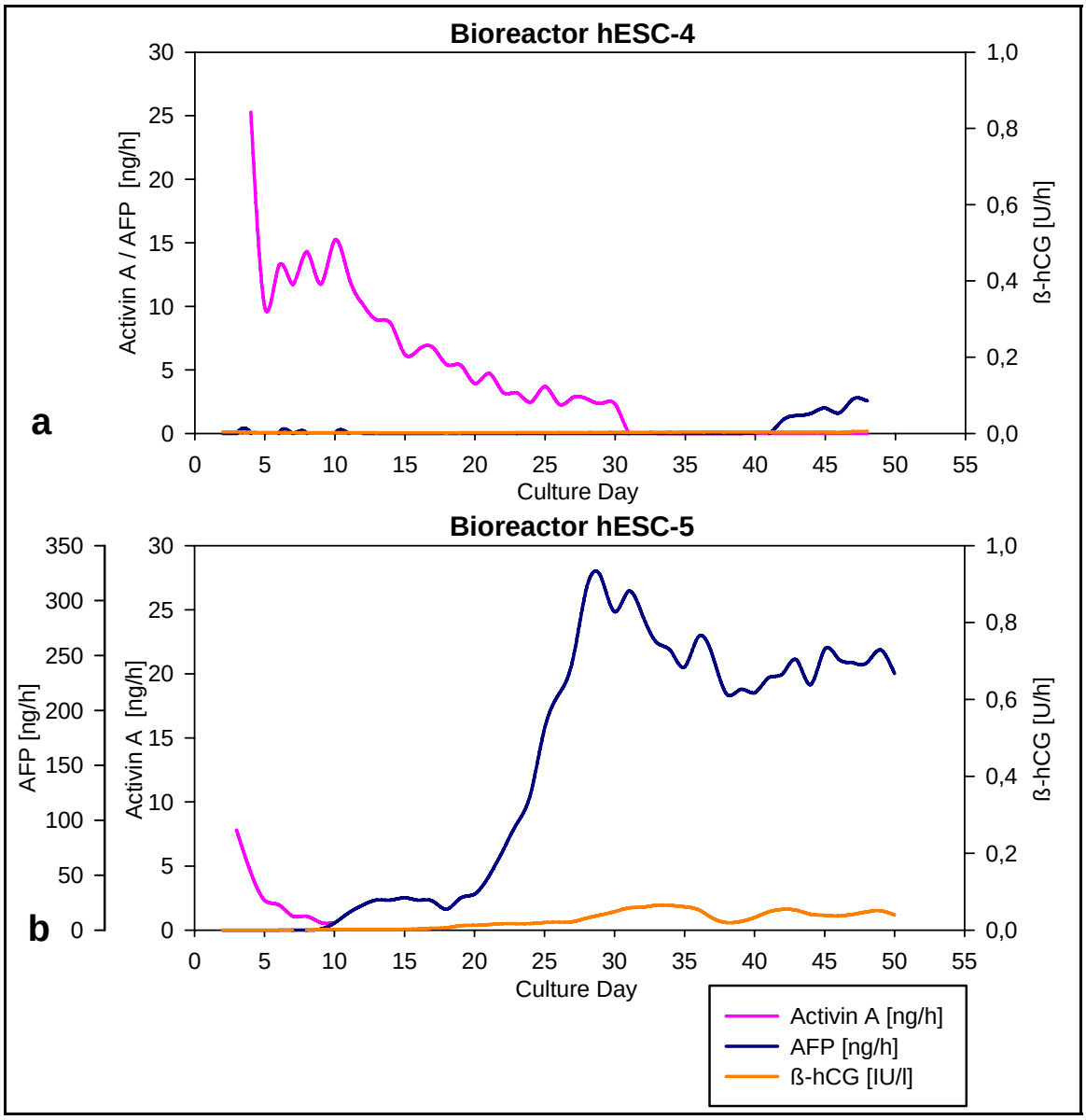

Figure 11: Time course of the differentiation markers measured in the medium outflow of bioreactors hESC-4 and -5. Activin A production (pink), AFP production (dark blue) and ß-hCG production (yellow) of the cells in bioreactors hESC-4 **(a)** and hESC-5 **(b).**

3.3.2 Expression Profiling

To compare the gene expression profiles of hESC cultured in the bioreactors with that of the teratomas that were grown in parallel, whole genome microarray profiling was performed. As controls active and inactivated HFF, samples from the hESC/HFF cell suspensions that were inoculated into the bioreactors (abbreviated with 'SCED') and undifferentiated hESC cut from colonies growing in co-culture with MEF were used. (see Table 3 in methods chapter for a detailed sample description)

3.3.2.1 Global gene expression analysis

Transcriptional similarities between the different samples were analyzed by hierarchical clustering and non-metric multidimensional scaling (NMDS), which allows finding possible non-parametric monotonic relationships between the dissimilarities in the item-item matrix and the Euclidean distance between items, and the location of each item in the low-dimensional space.

Results of both methods show that the transcriptomes of bioreactors hESC-1, -2 and -5 are very similar and therefore cluster together (Figure 12). This group of bioreactors is also closely related to the group of teratomas, which indicates a similar expression profile of these groups. Thus a similar cell differentiation in these bioreactors and in the teratomas can be assumed. In detail the expression profile of bioreactor hESC-5 is more related to the expression profiles of the teratomas than the expression profiles of hESC-1 and -2.

Bioreactors hESC-3 and 4 each fall into different clusters. Bioreactor hESC-3 clusters together with the samples of HFF, while bioreactor hESC-4, which contained no additional HFF and was cultured using FCS containing medium, exhibits a similar transcriptome to undifferentiated hESC grown in HFF and MEF co-cultures.

The correlation between the expression profiles was also assessed using a correlogram. Results from this analysis are in line with the clustering results (see Figure 33 in the appendix). In detail the comparison of the gene expression profiles of the bioreactors hESC-1, -2 and -5 shows that the correlation coefficients are in the range of 0.95 - 0.99 and for the teratomas the correlation coefficients are in the range of 0.93 - 0.99. When comparing the group of teratomas with the group of bioreactors hESC-1, -2 and -5 the correlation coefficients are between 0.89 and 0.95. These values also indicate a high degree of correlation between these two groups.

In summary bioreactors with a similar expression profiles exhibit also similar time courses of differentiation factors as described above. Specifically the reactors hESC-1, -2 and -5 showed similar time courses and bioreactors hESC-3 and -4 exhibited distinct time courses, which are reflected by the results of the analysis of their gene expression profiles.

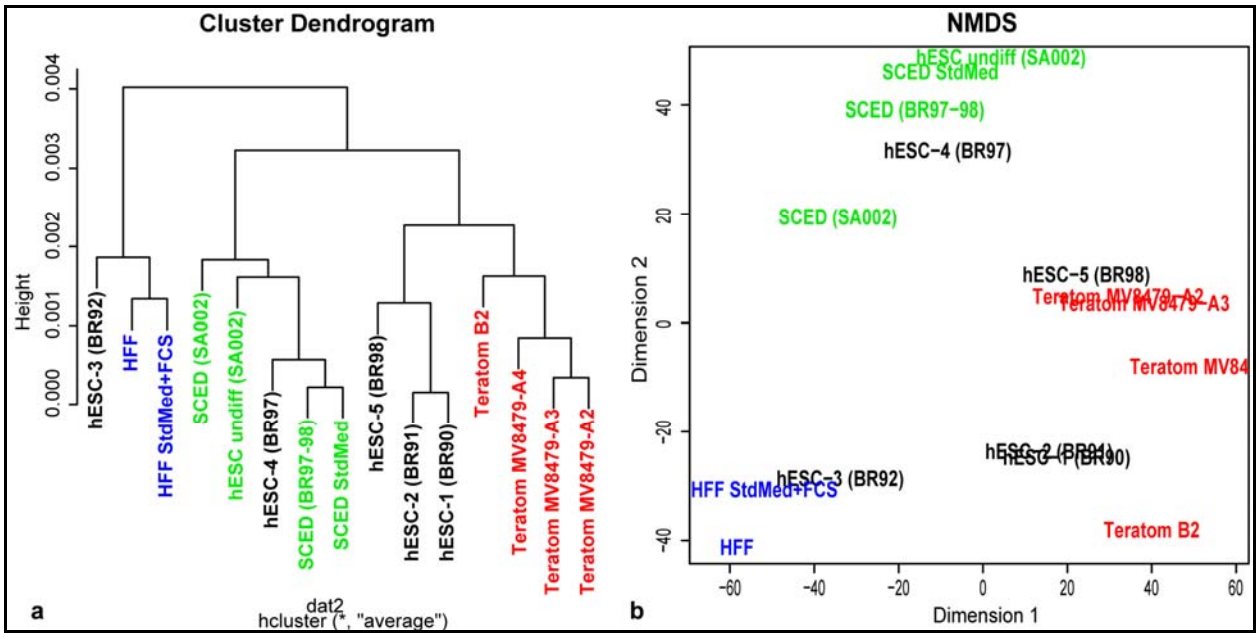

Figure 12: Hierarchical clustering and non-metric multidimensional scaling (NMDS). (a) Hierarchical clustering with average linkage clustering showing that bioreactors hESC-1, -2 and -5 form a cluster and exhibit a similar expression profile to the teratomas. **(b)** NMDS was also used to explore how similar the samples are and confirms the result of the hierarchical clustering.

The Venn diagram in Figure 13a shows the amount of common and exclusively expressed genes within bioreactors hESC-1, -2 and -5, the inoculated cell suspensions (SCED) and the teratomas. Overall the number of commonly expressed genes of bioreactors and teratomas that were not expressed in the cells of the inoculated cell suspensions was larger than the number expressed genes bioreactors or teratomas had in common with the cells in the inoculated cell suspensions. Specifically there are 943 genes that show a common expression in the bioreactors and teratomas while 551 genes are exclusive expressed in the bioreactors and 615 in the teratomas. These three gene sets were subsequently further analyzed by functional annotation analysis that was performed using DAVID (http://david.abcc.ncifcrf.gov). Results showed that in the gene sets of specifically expressed genes in the bioreactors and the genes shared between the bioreactors and the teratomas terms of neuronal differentiation are enriched whereas these are absent in the gene set specifically expressed in the teratomas (for functional annotation analysis results see Table 9, Table 10 and Table 11 in the appendix). The comparison between the bioreactors hESC-1, -2 and -5, hESC-3, hESC-4 is shown in the Venn diagram in Figure 13b. The diagram demonstrates that the overlap of specific genes shared between hESC-3 and hESC-4 was larger than that of the genes of shared between these reactors and bioreactors hESC-1-2-5.

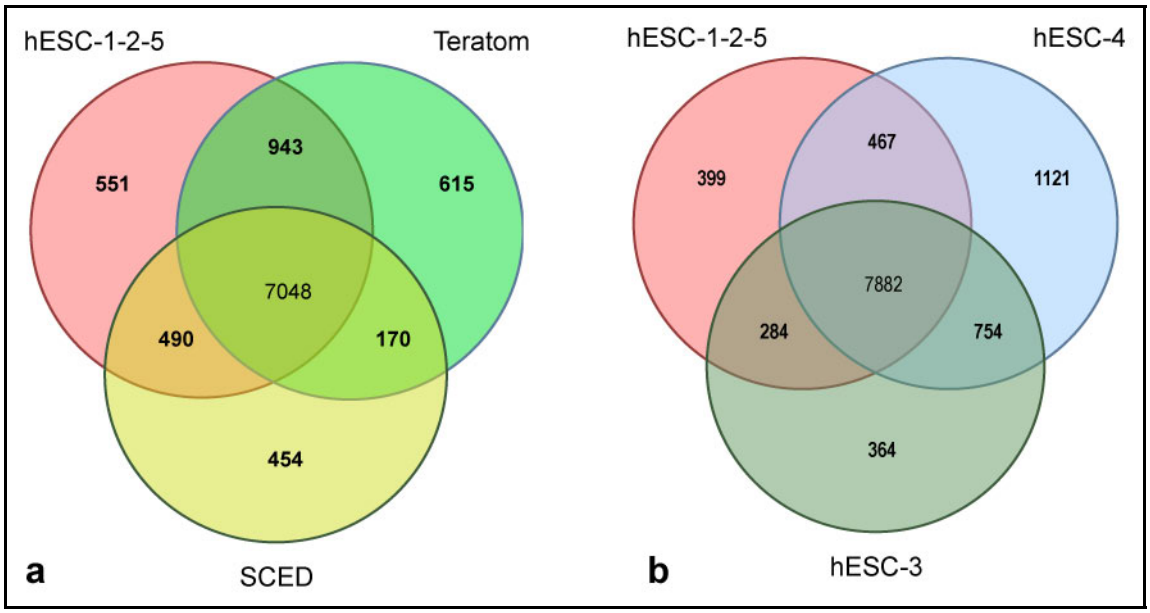

Figure 13: Venn Diagrams comparing the expressed genes in the different bioreactors, teratomas and inoculated cell suspensions (SCED). (a) Comparison of expressed genes in bioreactors hESC-1, -2 and -5, teratomas cells of the inoculated cell suspension (HFF+hESC). **(b)** Comparison of expressed genes in bioreactors hESC-3 and hESC-4 and the group of bioreactors hESC-1-, 2 and -5.

3.3.2.2 Differential expression of hESC bioreactors and teratomas

To further compare the expression profiles of the group of bioreactors that clustered together (hESC-1, -2 and -5) with the group of teratomas a differential expression analysis was performed between these groups.

Testing was performed with the significance analysis of microarrays (SAM) algorithm using the two-class unpaired option and a delta value set to 5.15 which resulted in a false discovery rate of 0% (Figure 14a). The analysis resulted that 12 genes were differentially expressed in the teratomas compared to 146 genes in the bioreactors respectively. In Figure 14b+c heatmaps of the resulting gene lists are shown that are additionally analyzed by hierarchical clustering of the samples and genes. The resulting gene lists are relatively short, which is a further indication that both groups are closely related.

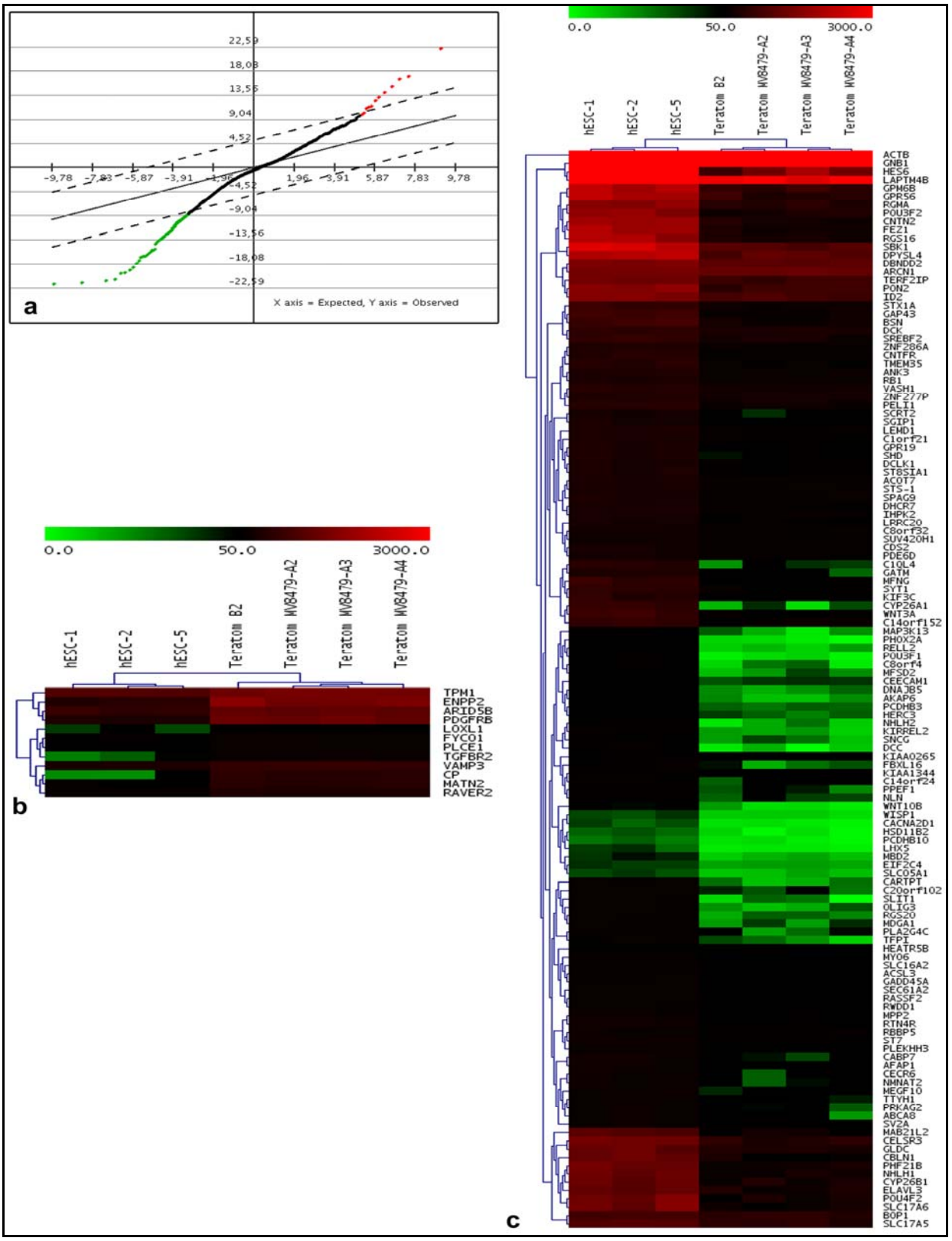

Figure 14: Differential gene expression. Testing of the differences in the expression profiles of hESC grown in bioreactors compared to teratomas was performed by significance analysis of microarrays (SAM) testing. The resulting graph of the observed vs. expected genes with a delta value set to 5.15, which resulted in a false discovery rate of 0% is shown in **(a).** The analysis resulted in 12 genes differentially expressed in the teratomas **(b)** compared to 146 genes in the bioreactors respectively **(c).** (b+c are represented as heatmaps clustered by hierarchical clustering of the samples and genes).

3.3.2.3 Functional annotation analysis

To further analyze the genes differentially expressed in the group of bioreactors hESC-1, -2 and 5 that were determined by SAM, a functional annotation analysis was performed using the online tool DAVID (http://david.abcc.ncifcrf.gov). The result of the functional annotation clustering performed is shown in Table 4. Most notable are the first and fourth functional groups that contain gene ontology (GO) terms describing developmental or morphogenic processes and the functional groups two and nine that contain terms describing neural differentiation.

Table 4: Result of functional annotation clustering using DAVID. The differentially expressed genes in the bioreactors compared to the teratomas were analyzed using the online tool DAVID. The results show that developmental processes and neurogenesis are pronounced in the bioreactors.

Category	Term	Count	PValue	Fold Enrichment
Functional Group 1				
GOTERM_BP_ALL	GO:0048731~system development	31	8,84E-07	2,6013986
GOTERM_BP_ALL	GO:0048856~anatomical structure development	34	2,29E-06	2,33234485
GOTERM_BP_ALL	GO:0007275~multicellular organismal development	35	5,51E-06	2,2006091
GOTERM_BP_ALL	GO:0032502~developmental process	40	8,24E-05	1,81106447
Functional Group 2				
GOTERM_BP_ALL	GO:0022008~neurogenesis	11	4,60E-05	5,20710059
GOTERM_BP_ALL	GO:0031175~neurite development	8	1,31E-04	7,07508061
GOTERM_BP_ALL	GO:0048699~generation of neurons	10	1,40E-04	5,11046047
GOTERM_BP_ALL	GO:0030182~neuron differentiation	9	2,76E-04	5,31692308
GOTERM_BP_ALL	GO:0048666~neuron development	8	3,18E-04	6,12196094
GOTERM_BP_ALL	GO:0007409~axonogenesis	7	3,43E-04	7,43774211
GOTERM_BP_ALL	GO:0048667~neuron morphogenesis during differentiation	7	4,63E-04	7,03296703
GOTERM_BP_ALL	GO:0048812~neurite morphogenesis	7	4,63E-04	7,03296703
GOTERM_BP_ALL	GO:0000904~cellular morphogenesis during differentiation	7	6,77E-04	6,54333009
GOTERM_BP_ALL	GO:0048858~cell projection morphogenesis	8	0,00102379	5,02782324
GOTERM_BP_ALL	GO:0030030~cell projection organization and biogenesis	8	0,00102379	5,02782324
GOTERM_BP_ALL	GO:0032990~cell part morphogenesis	8	0,00102379	5,02782324
Functional Group 3				
UP_SEQ_FEATURE	domain:Helix-loop-helix motif	6	3,70E-04	9,63837442
INTERPRO	IPR001092:Basic helix-loop-helix dimerisation region bHLH	6	7,90E-04	8,23868883
SMART	SM00353:HLH	6	0,00115959	7,44285714
UP_SEQ_FEATURE	DNA-binding region:Basic motif	5	0,01315427	5,42330184
Functional Group 4				
GOTERM_BP_ALL	GO:0000902~cell morphogenesis	12	5,13E-04	3,55171882
GOTERM_BP_ALL	GO:0032989~cellular structure morphogenesis	12	5,13E-04	3,55171882
GOTERM_BP_ALL	GO:0009653~anatomical structure morphogenesis	14	0,03942244	1,82497115
Functional Group 5				
UP_SEQ_FEATURE	domain:POU-specific	3	0,0051497	27,193985
INTERPRO	IPR013847:POU	3	0,00569122	26,0891813
INTERPRO	IPR000327:POU-specific	3	0,0063346	24,7160665
SMART	SM00352:POU	3	0,00758493	22,3285714
Functional Group 6				
GOTERM_MF_ALL	GO:0048503~GPI anchor binding	5	0,00582804	6,89756098

GOTERM_MF_ALL	GO:0035091~phosphoinositide binding	6	0,00659538	5,04
SP_PIR_KEYWORDS	gpi-anchor	5	0,00771304	6,37644928
Functional Group 7				
GOTERM_MF_ALL	GO:0005543~phospholipid binding	7	0,00449606	4,49909091
GOTERM_MF_ALL	GO:0035091~phosphoinositide binding	6	0,00659538	5,04
GOTERM_MF_ALL	GO:0008289~lipid binding	8	0,01966474	2,90051282
Functional Group 8				
INTERPRO	IPR012287:Homeodomain-related	6	0,01718235	3,97970562
UP_SEQ_FEATURE	DNA-binding region:Homeobox	5	0,02841874	4,28733997
INTERPRO	IPR001356:Homeobox	5	0,05338209	3,50975533
SP_PIR_KEYWORDS	Homeobox	5	0,06413052	3,29816342
SMART	SM00389:HOX	5	0,06979603	3,17072389
Functional Group 9				
GOTERM_BP_ALL	GO:0007416~synaptogenesis	3	0,01607041	15,2785146
GOTERM_BP_ALL	GO:0050808~synapse organization and biogenesis	3	0,03657165	9,84615385
GOTERM_BP_ALL	GO:0043062~extracellular structure organization and biogenesis	3	0,14257654	4,47552448

3.3.3 Histology

At the end of each bioreactor experiment the bioreactor was disconnected from the tubing system and the lower lid was cut open (Figure 15a). On the exposed capillaries cell clusters were macroscopically visible (Figure 15b). For further microscopic analysis and sample acquisition capillaries were excised from the bioreactor housing. Microscopy of fresh samples taken from the bioreactors showed both free floating and adherent cell clusters, whereas it could not be determined whether the floating clusters detached during sample acquisition or have already been in suspension during the bioreactor run (Figure 15c, d).

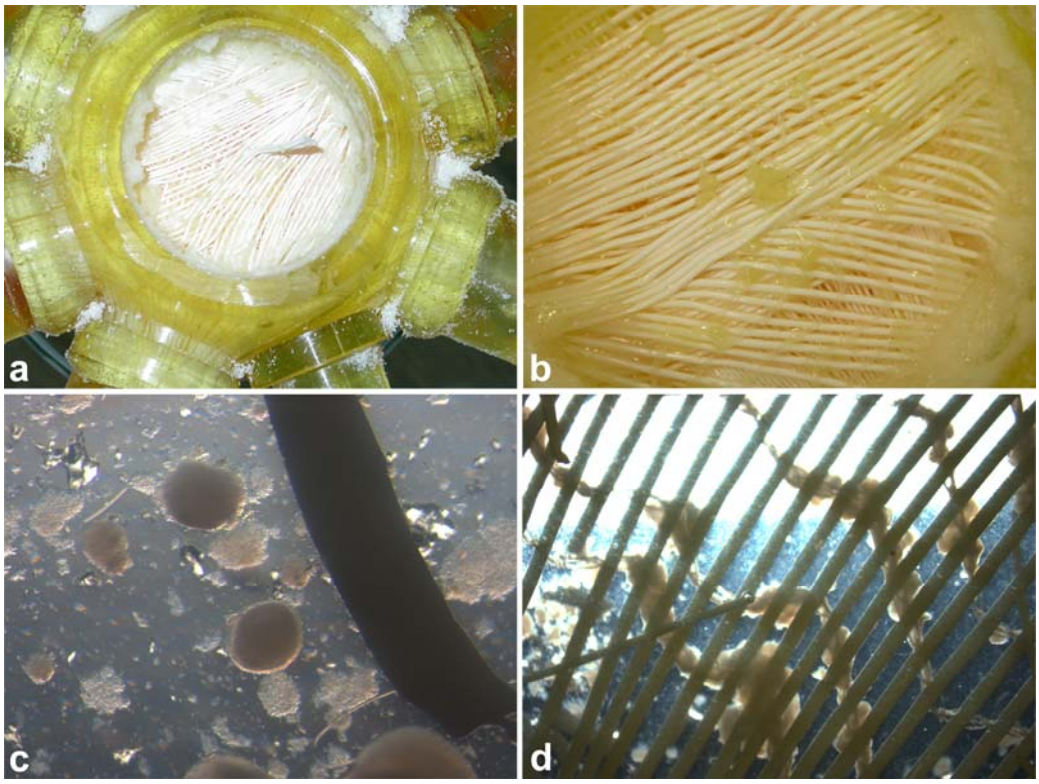

Figure 15: Opening of the bioreactor. At the end of the experiment the bioreactor was cut open **(a).** Cell aggregates on the capillaries in the opened bioreactor are shown in **(b).** The capillaries were excised from the bioreactor housing and placed in petri dishes containing PBS **(c + d).** Microscopic pictures of the capillaries showing free floating and adherent cell clusters.

3.3.3.1 Bioreactor histology

The morphology of the structures formed in the individual bioreactors was analyzed and compared by H&E staining. The histology of the bioreactors showed that the hESC proliferated, differentiated and formed tissue-like structures, although the degree of differentiation and the number of different tissue types differed between the individual reactors. Interestingly bioreactors that exhibited a similar gene expression profile also showed a similar histology.

The bioreactors hESC-1, -2 and -5 exhibited a comparable histology regarding to the number and types of different tissues that could be detected (Figure 16). The morphology of the structures observed in these reactors indicated differentiation into all three germ layers. Mesodermal tissues were present in the form of cartilage tissue showing different degrees of maturation (Figure 16a, e, i) and in form of connective tissue that was abundant in all examined histological sections (Figure 16c, f, h, i, l). Neuronal-like structures indicated ectodermal differentiation (Figure 16g) and different types of epithelia endodermal differentiation (Figure 16 b, c, j, k).

Comparison of the average maturational degree of the tissue types between the bioreactors hESC-1, -2 and -5 showed that bioreactors hESC-1 (Figure 16a-d) and hESC-2 (Figure 16e-h) exhibited a similar maturational degree. Structures observed in bioreactor hESC-5 (Figure 16i-l) showed a higher maturational degree compared to reactors hESC-1 and hESC-2. The result of this comparison is also in line with the result of the analysis of the gene expression profiles of the bioreactors (see Figure 12).

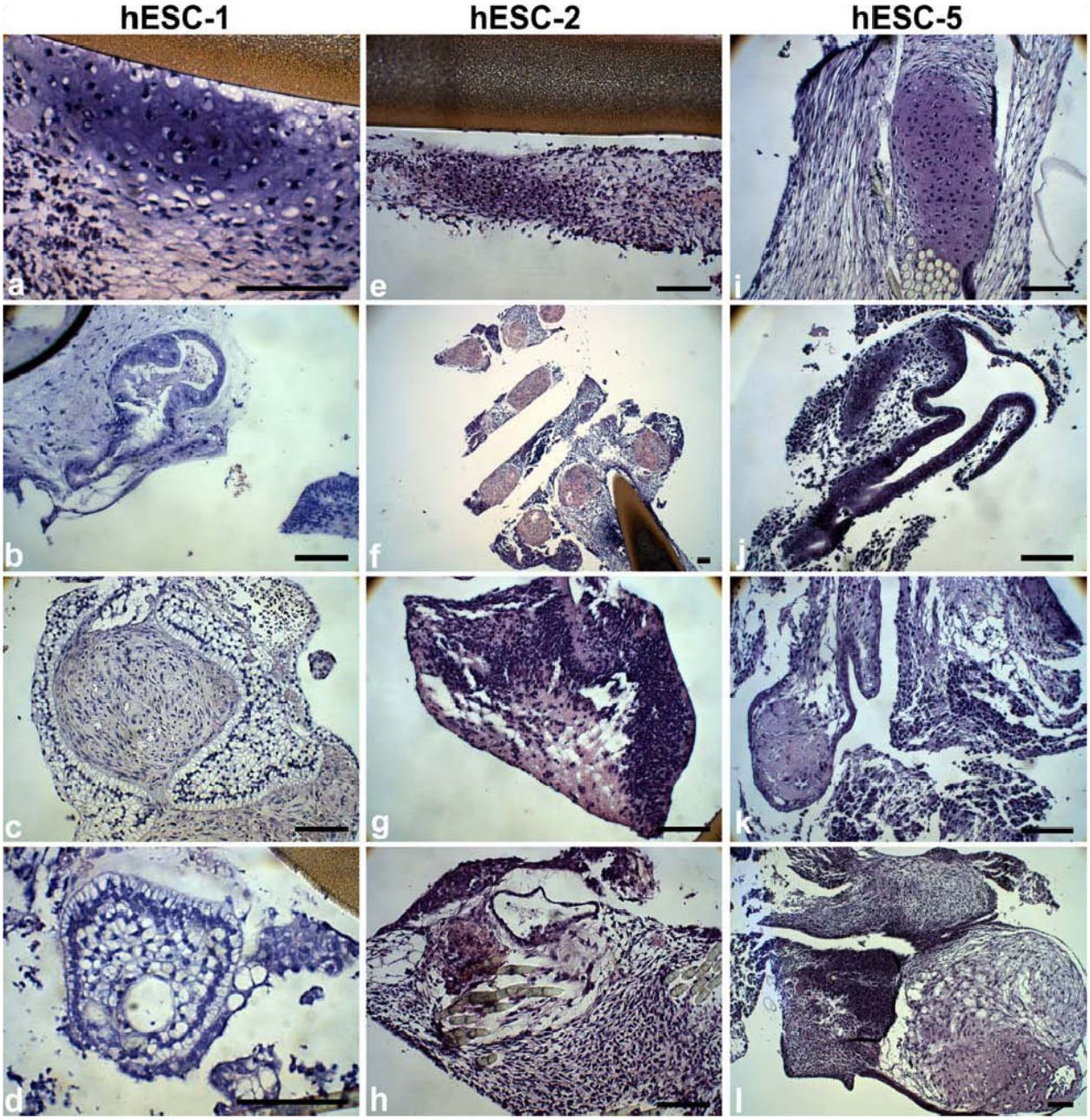

Figure 16: H&E staining of tissue samples taken from bioreactors hESC-1, -2 and -5. In samples from bioreactors hESC-1, -2 and -5 a similar morphology was observed, showing that the hESC differentiated and formed tissue-like structures. The morphology of these structures indicated differentiation into all three germ layers. Cartilage **(a, e, i)** and connective tissue **(h, l)** represented mesodermal, epithelial structures endodermal **(b, c, j, k)** and neuronal-like tissue **(g)** ectodermal differentiation. (Bar = 50 µm)

The histology of bioreactors hESC-3 and hESC-4 differed each from all other bioreactors. In bioreactor hESC-3 only connective tissue like structures and fibroblasts could be detected (Figure 17a-c). In reactor hESC-4 next to connective tissue like structures, some clusters of cells with a low cytoplasm to nucleus ratio but no structures displaying further maturation could be detected (Figure 17d-f).

Again the morphology of these reactors confirms the results of the gene expression analysis that indicated that bioreactor hESC-3 had a similar expression profile to HFF and the expression profile of bioreactor hESC-4 resembled the profile of the inoculated cell suspensions that were composed of undifferentiated hESC and HFF.

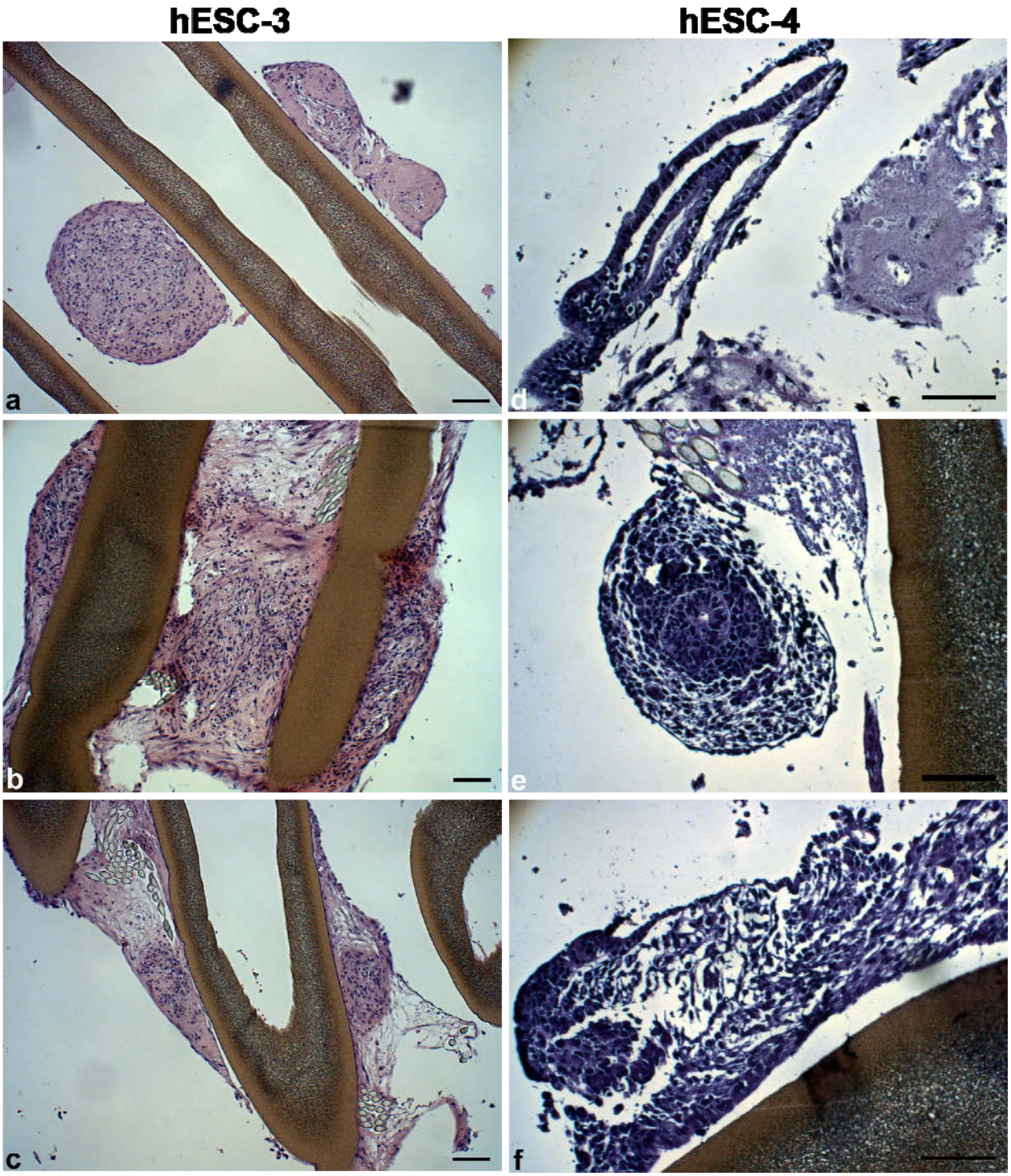

Figure 17: H&E staining of tissue samples taken from bioreactors hESC-3 and -4. In bioreactor hESC-3 only tissue structures formed by fibroblasts / connective tissue but no other differentiated structured could be observed **(a-c).** In bioreactor hESC-4 predominantly connective tissue and structures composed of small cells exhibiting a low cytoplasm to nucleus ratio but no structures displaying further maturation could be observed **(d-f).** (Bar = 50 µm)

3.3.3.2 Histology of the teratomas formed *in vivo*

To compare the differentiation behavior and potential of the hESC under *in vitro* conditions in the bioreactor to *in vivo* conditions, samples of the inoculated cells were

transplanted in NOD/SCID mice by subcutaneous injection. The hESC formed tumors at the site of injection, which were identified as teratomas by histological examination. These teratomas where grown in parallel to the bioreactor cultures for the same time period. At the end of each individual bioreactor run teratomas were excised and their histology was analyzed by using H&E staining or the RNA was isolated and used for microarray analysis (see above).

In H&E staining of histological sections of the teratomas in general no terminal differentiation into organoid structures as seen in mature teratomas could be observed. This is in accordance with the findings in the bioreactors and can be explained with the length of the culture time that was presumably too short for terminal differentiation.

In general predominantly mesodermal and endodermal structures but only few ectodermal structures could be detected. This is in contrast to the tissue types identified in the bioreactors where neural-like structures could be observed that have to be derived from ectodermal differentiation of the hESC. However this observation is in line with the gene expression analysis that showed that neural differentiation is more pronounced in the bioreactors hESC-1, -2 and -5 than in the teratomas.

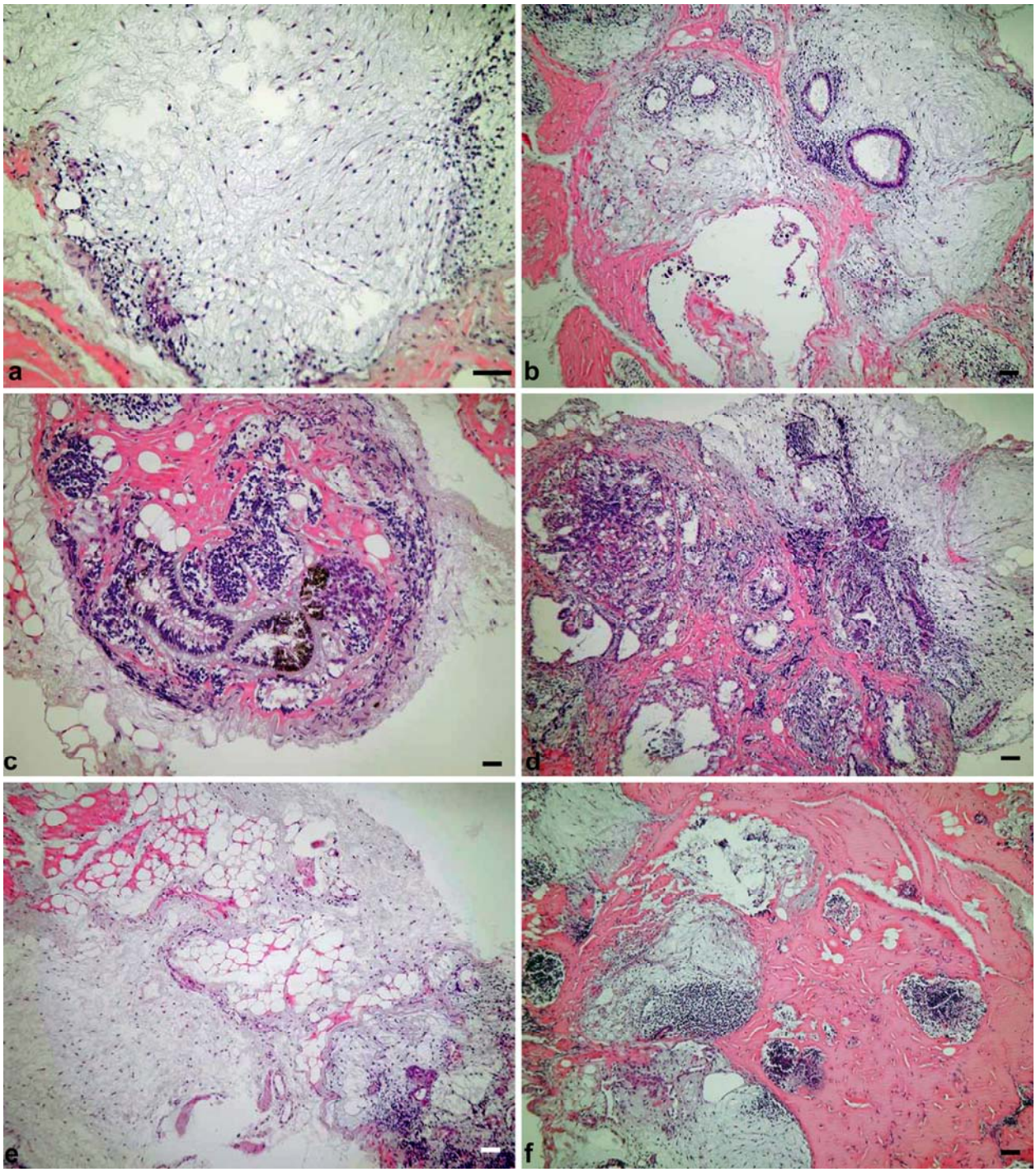

Figure 18: H&E staining of samples from the teratomas. In general no terminal differentiation into organoid structures was observed. In general predominantly mesodermal and endodermal structures but only few ectodermal structures could be detected. **(a, e)** connective tissue (mainly collagen rich) and many adipocytes, **(b)** collagen rich connective tissue, epithelial structures, adipose tissue, **(c, d)** pigmentary epithelial cells, epithelial structures forming some glandular structures, connective tissue interspersed with adipocytes, **(f)** connective tissue and glandular structures. (Bar = 50 µm)

3.3.3.3 Immunohistology

The tissue structures formed in the bioreactors and in the teratomas were further analyzed and compared by immunofluorescence staining using pluripotency and differentiation markers.

In general markers indicating differentiation in derivates of all three germ layers were detected in the examined samples of the bioreactors hESC-1, -2 and -5 as well as samples of the teratomas (Figure 19+Figure 20). Specifically the expression of nestin and ß-III-tubulin indicated ectodermal differentiation (Figure 19a, b, d, e). Mesodermal differentiation was identified by the expression of α-smooth muscle actin, desmin and vimentin (Figure 19c, f; Figure 20g, h, j, k) and the detection of HNF-3ß/FOXA2 indicated endodermal differentiation (Figure 20i, l).

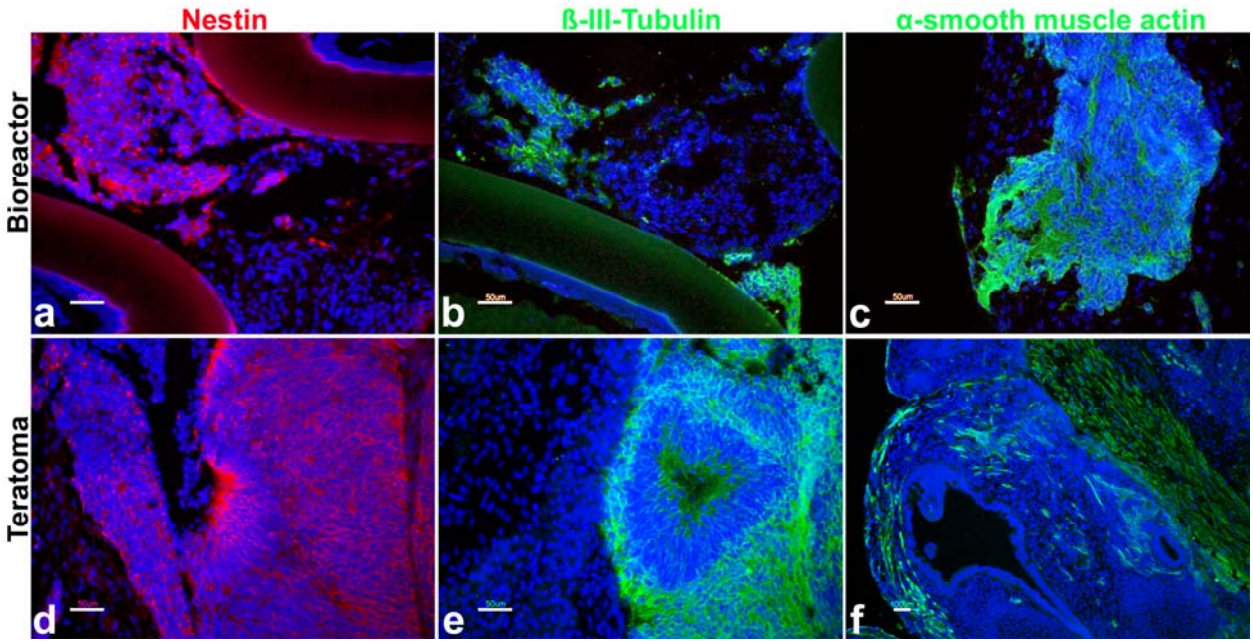

Figure 19: Immunofluorescence staining of tissue samples taken from the bioreactors hESC-1, -2, -5 and teratomas. (a-c) samples from bioreactors hESC-1,-2 and -5, **(d-f)** samples from teratomas. Ectodermal markers nestin **(a, d)** and ß-III-tubulin **(b, e)**, mesodermal marker α-smooth muscle actin **(c, f)**. All samples are co-stained with DAPI (blue). (Bar = 50 µm)

Qualitative comparison of the distribution and average percentage of tissue types in the examined sections showed that the samples from bioreactors hESC-1, -2 and -5 contained a high percentage of ectodermal derived tissues whereas in samples of the teratomas only a few ectodermal structures were detected. Mesodermal derived tissues were found in similar proportions in the bioreactors compared to the teratomas and

were frequently found in the examined samples. Endodermal derived tissues were only detected in a few samples from bioreactors and teratomas.

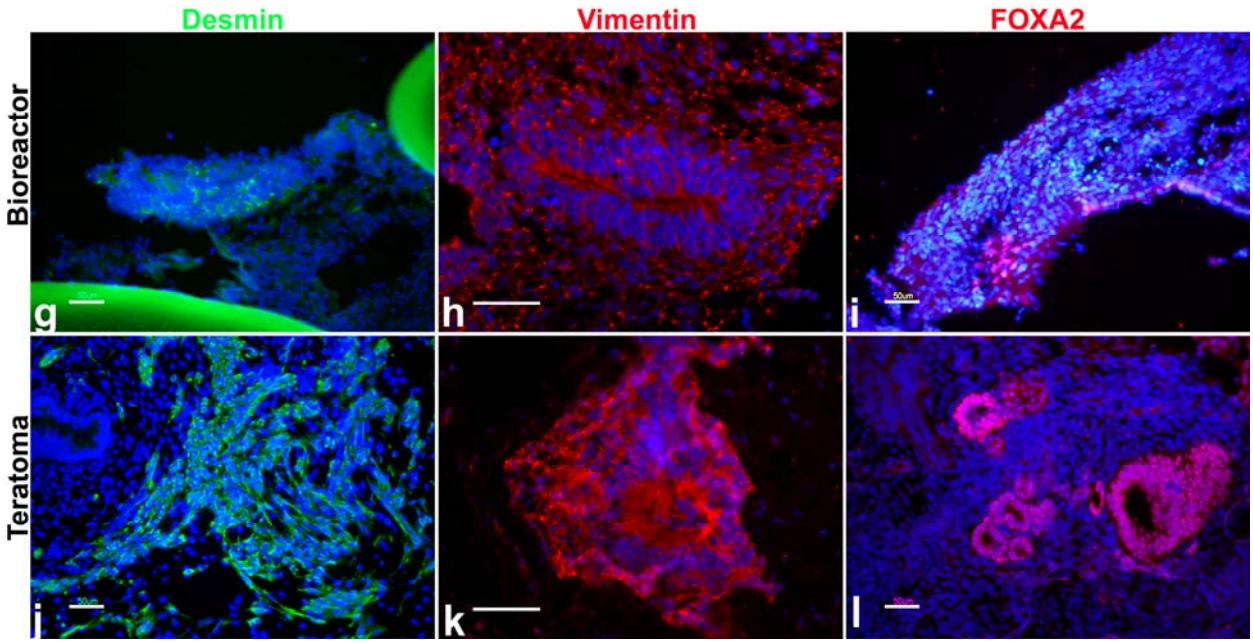

Figure 20: Immunofluorescence staining of tissue samples taken from the bioreactors hESC-1, -2 and -5 and teratomas. (g-k) samples from hESC-1, -2 and -5, **(j-l)** samples from teratomas. Mesodermal markers desmin **(g, j)** and vimentin **(h, k)**, endodermal marker HNF-3ß **(i, l)**. All samples are co-stained with DAPI (blue). (Bar = 50 µm)

The pluripotency marker OCT4 could only be detected in a few samples from the bioreactors hESC-1, -2 and -5 but not in the teratomas (Figure 21a).

In bioreactor hESC-4 many areas expressing the pluripotency markers OCT4 and TRA-1-81 could be observed (see exemplary pictures in Figure 21c, d), which is in line with the results of gene expression analysis that showed a similar expression profile of bioreactor hESC-4 and the inoculated cell suspensions that were composed of undifferentiated hESC and HFF.

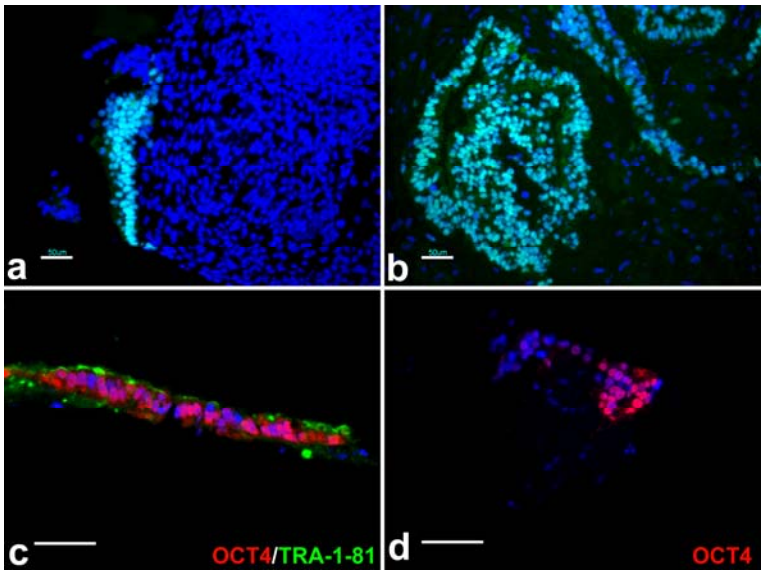

Figure 21: Immunofluorescence staining for pluripotency markers in tissue samples from bioreactors hESC-1, -2, -4 and -5. The pluripotency marker OCT4 could only be detected in a few samples from the bioreactors hESC-1, -2, and -5 **(a)**. Staining of pelleted undifferentiated hESC with OCT4 as a control **(b)**. In bioreactor hESC-4 many areas expressing the pluripotency markers OCT4 and TRA-1-81 could be observed **(c, d)**. All samples are co-stained with DAPI (blue). (Bar = 50 µm)

3.3.3.4 Transmission Electron Microscopy

To further analyze the type and the maturational degree of tissue structures that had been formed by differentiation of the hESC in the bioreactors hESC-1, -2 and -5, their ultrastructure was analyzed by transmission electron microscopy (TEM). Overall many areas were composed of connective tissue containing a collagen rich extracellular matrix (Figure 22a, b). Among the structures that could be identified were cartilage tissue and different epithelia.

The analysis of areas exhibiting cartilage morphology in immunhistochemical analysis showed hat these areas represent hyaline cartilage composed of mature chondrocytes surrounded by a collagen rich extracellular matrix (Figure 22d, e). The epithelial cells that could be observed differed in the expression of cellular processes. Some epithelial cells had pseudopodia on their surface (Figure 23a, b) and others had also kinocilia (Figure 23d, e). Kinocilia are typical for the respiratory epithelium present in nose, paranasal sinuses, larynx, trachea and bronchi.

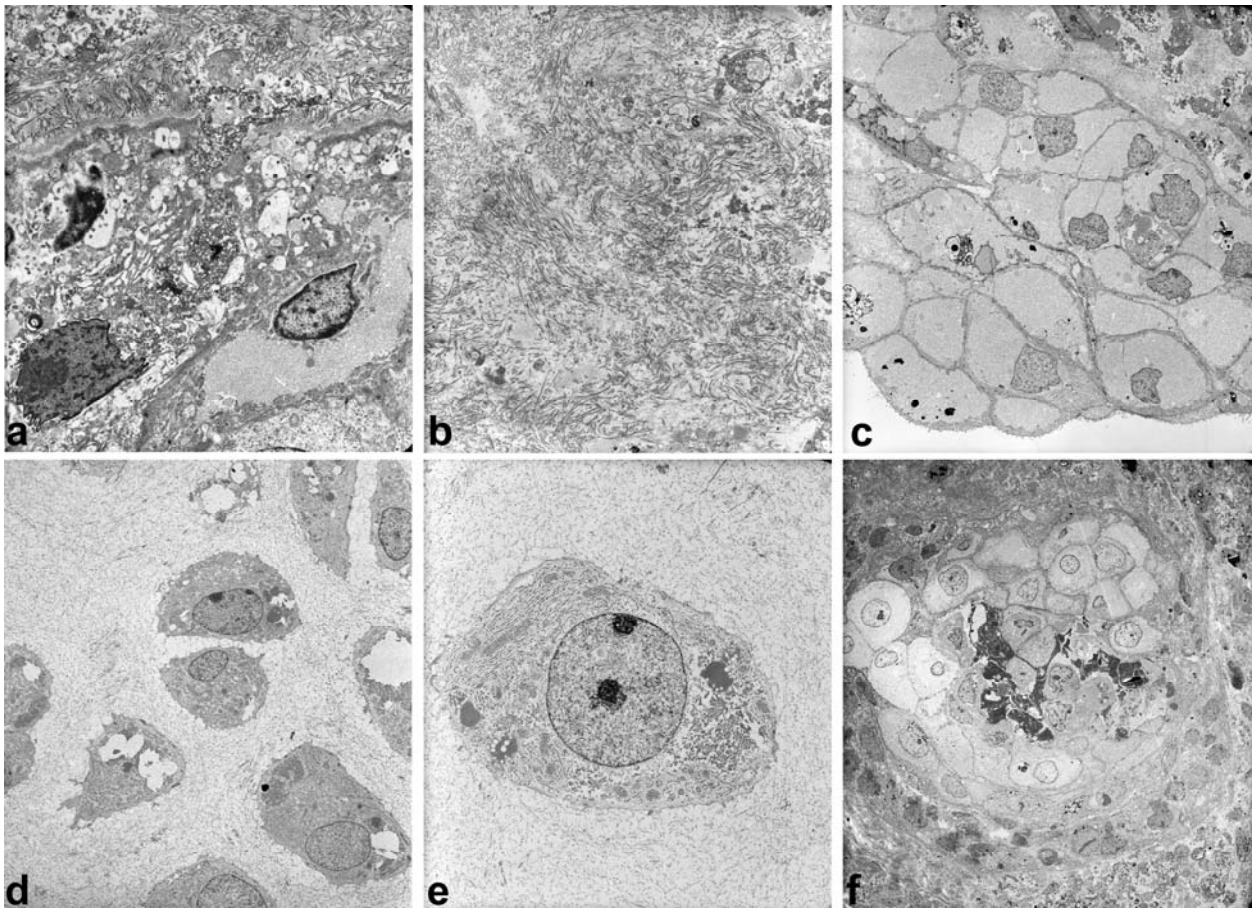

Figure 22: Electron microscopic analysis of tissue samples taken from the bioreactors. Connective tissue **(a)** containing extracellular matrix with collagen **(b)**. Hyaline cartilage composed of mature chondrocytes surrounded by a collagen rich extracellular matrix **(d, e).** Clusters of cells types with different morphologies **(c, f).**

In both epithelial cell types desmosomes and tight junctions at the cell-cell contacts could be identified (Figure 23c).

In addition to the structures that could be identified, clusters of cell types with many different morphologies could be observed in many places (Figure 22c, f) including few clusters of cells with low cytoplasm to nucleus ratio that resembled the morphology of undifferentiated hESC (Figure 23f).

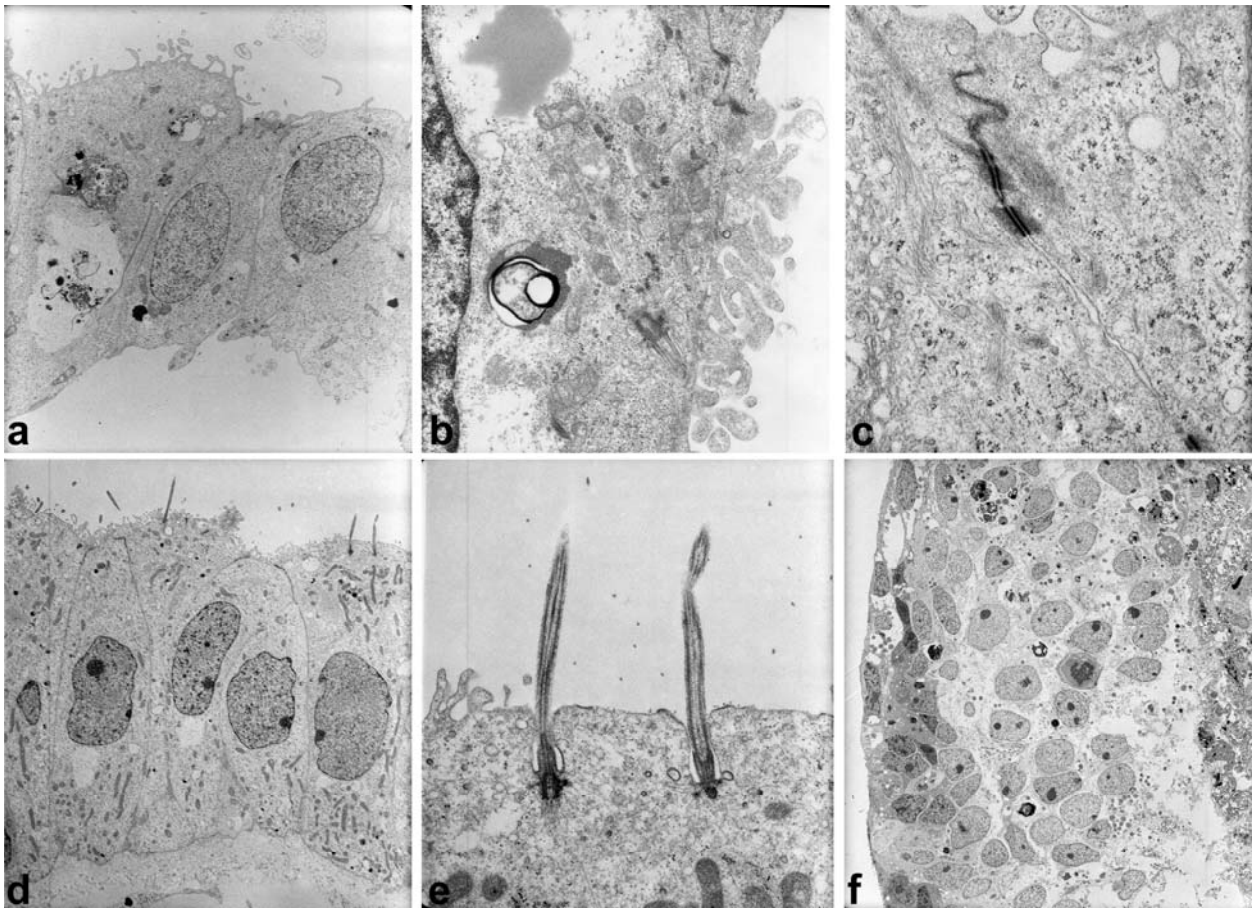

Figure 23: Electron microscopic analysis of tissue samples taken from the bioreactors. Epithelial cells with pseudopodia **(a, b)**, forming desmosomes and tight junctions at the cell-cell contacts **(c)**. Epithelial cells with kinocilia **(d, e)**. A few clusters of cells with low cytoplasm to nucleus ratio that resembled the morphology of undifferentiated hESC could be found **(f).**

3.3.4 Spontaneous differentiation of hESC in 2D cultures

To compare the spontaneous differentiation behavior of the hESC in the 3D bioreactor environment with their behavior in 2D cultures, hESC were cultured for 30 days without passaging in standard culture dishes using the same culture medium (VitroHES) as used in the bioreactor experiments that was supplemented with 10 ng/ml bFGF. During culture ß-hCG was measured in the culture medium and the cell morphology was regularly analyzed by microscopic observation. The cell morphology of the undifferentiated hESC started to change from day five on. Cells increased in size and many cells started to migrate away from the initial colonies. At the end of the observed time period many different cell types with discrete morphologies had been formed (Figure 24b, c). Here especially the appearance of a large number of cells exhibiting the typical morphology of neurons is noteworthy. ß-hCG production could first be detected

at about day 10 and continuously increased till the end of the experiment (Figure 24a), which resembled the time course of this factor in bioreactors hESC-1, -2 and -5.

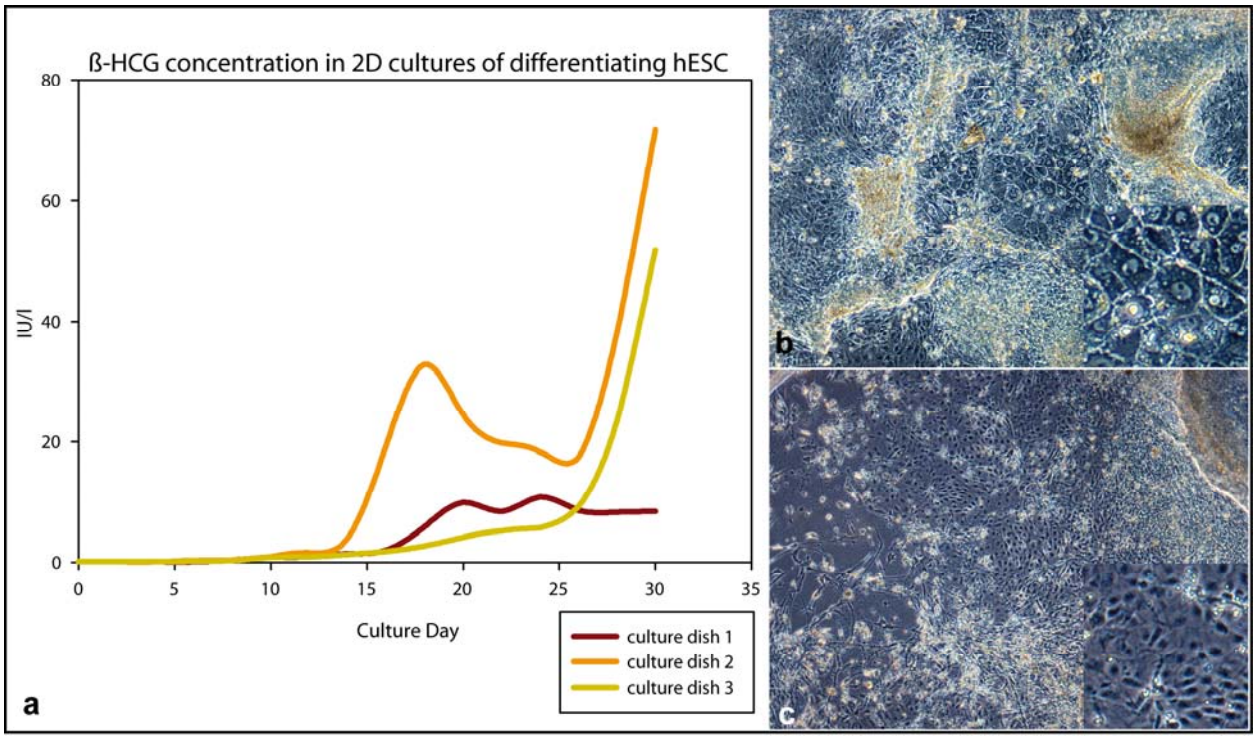

Figure 24: Spontaneous differentiation of hESC in 2D cultures. hESC were cultured for 30 days in 2D culture dishes in VitroHES containing bFGF **(a)**. The concentration of ß-hCG increased starting day 9. hESC differentiated into various cell types e.g. cells with epithelial-like **(b)** or endothelial-like morphology **(c)**. (mag. of both pictures 100x)

3.4 Culture of HFF in the investigated bioreactor

To analyze the behavior of active HFF in the bioreactor two experiments using different experimental conditions were carried out. In the first experiment (HFF-1) HFF were cultured in HFF growth medium containing serum. Initially no bFGF was added to the medium, then between culture day 19 and 23, 4 ng/ml bFGF and from day 23 on 10 ng/ml bFGF was added to the medium. Until day 19 glucose and lactate metabolism showed a slow increase and LDH release decreased. Upon addition of bFGF from day 19 onwards glucose consumption and lactate production showed a strong increase suggesting increased cell proliferation. Further increase of the bFGF concentration did not lead to enhanced increase of the metabolic activity. The release of LDH also increased following bFGF addition (Figure 25a). A low activin A production could be detected after cell inoculation that decreased until it could not be detected anymore at about day 10 of the experiment (Figure 26a). The addition of bFGF to the medium did not have any effect on the production of activin A.

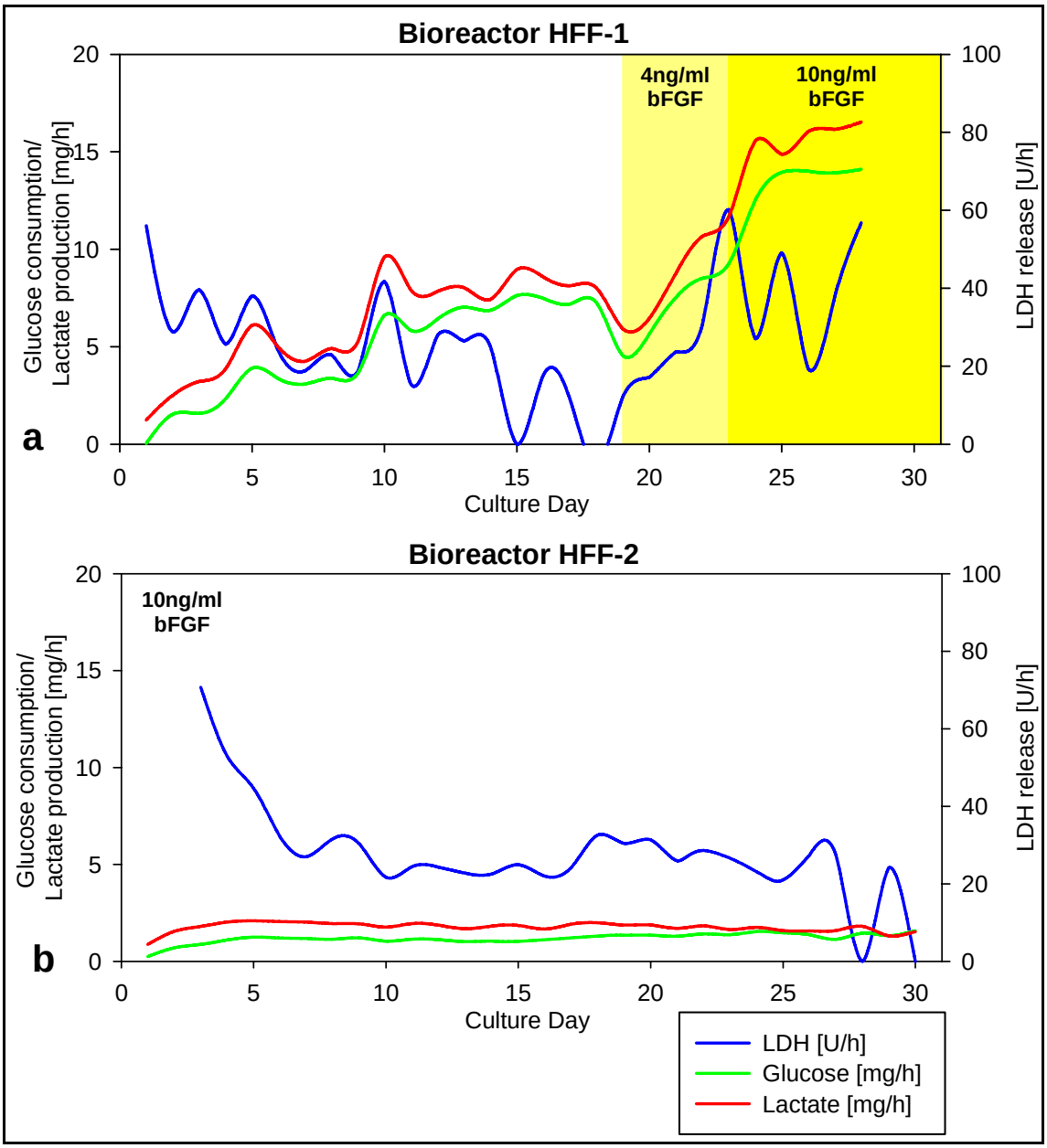

Figure 25: Time course of the metabolic parameters measured in the medium outflow of bioreactors HFF-1 and -2. Glucose consumption (green), lactate production (red) and LHD release (blue) of the cells in bioreactors HFF-1 in which medium containing serum was used **(a)** and HFF-2 in which medium containing serum replacement was used **(b)**

In the second experiment (HFF-2) initially the same medium as used in the bioreactor experiments on the spontaneous differentiation of hESC (VitroHES, which already contains serum replacement and was supplemented with 10ng/ml bFGF) and after day 13 a self made medium containing 20% serum replacer and 10ng/ml bFGF was used. Glucose and lactate metabolism showed a low but stable level. Similarly, LDH after an initial peak showed a stable level during the experiment. Activin A production showed an initial peak and a slowly increasing level until the end of the experiment. The change of the culture medium from day 13 on had no significant impact on the factors analyzed.

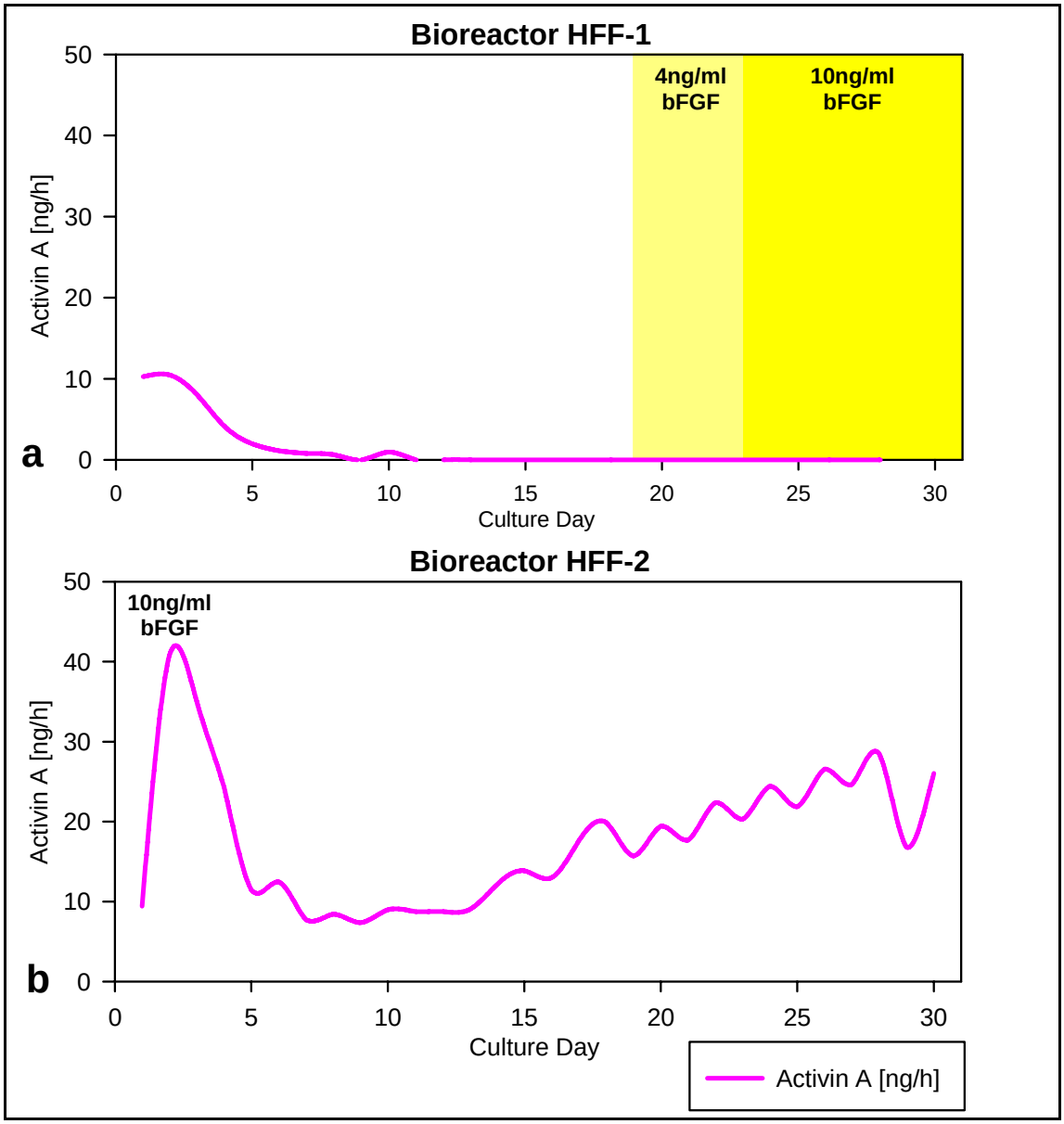

Figure 26: Time course of activin A production of the HFF measured in the medium outflow of bioreactors HFF-1 (a) and HFF-2 (b).

Histochemical staining of tissue samples taken at the end of the experiments from the HFF bioreactors showed that HFF had proliferated in both bioreactors and formed connective tissue like structures (Figure 27).

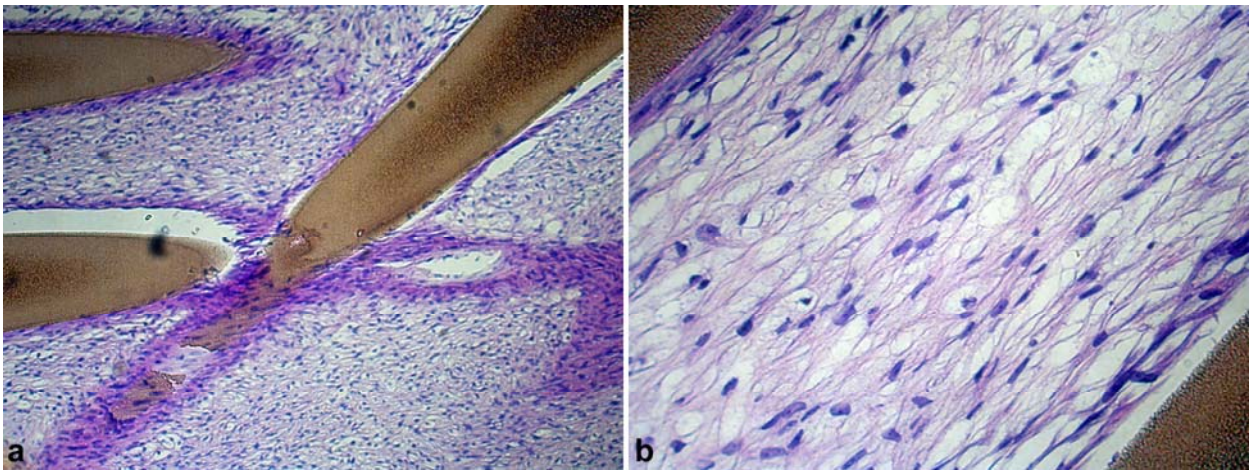

Figure 27: H&E staining of tissue samples taken from bioreactors HFF-1 (a) and HFF2 (b) (magn. a: 100x; b: 200x)

3.4.1 Stimulation of human foreskin fibroblasts with bFGF in 2D cultures

The influence of basic fibroblast growth factor (bFGF) and culture medium was further analyzed in 2D cultures of active or inactivated human foreskin fibroblasts (HFF) alone using HFF expansion medium containing fetal calf serum (FCS) and hESC culture medium containing serum replacement (VitroHES). Both media were tested without or with addition of 4 or 10 ng/ml bFGF.

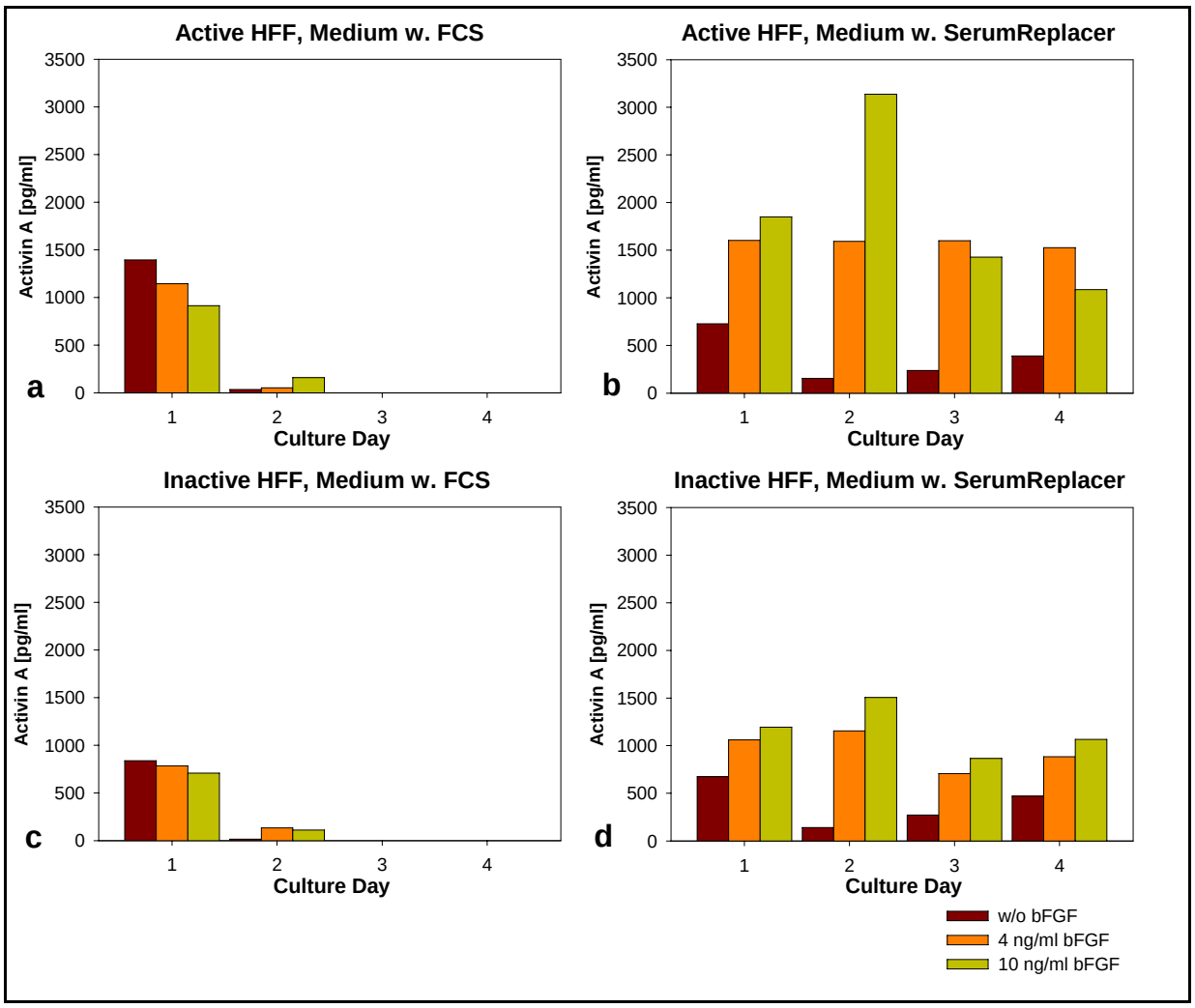

Figure 28: Effect of different culture media and bFGF on HFF. Active or inactivated HFF were cultured in different culture media supplemented with or without bFGF and their production of activin A was measured in the culture medium. **(a, b)** In general both active and inactivated HFF showed a similar behavior. In medium containing FCS, activin A production could only be detected until culture day 2. **(c, d)** In medium containing serum replacement, activin A could be detected on all examined days whereas the presence of bFGF induced six times higher activin A levels compared to HFF cultured without bFGF.

In the medium of all different cultures no AFP and no ß-hCG could be detected (not shown). In general activin A production of active and inactive HFF showed similar

responses to the different culture conditions tested. In the standard culture medium with or without bFGF, activin A production could be detected on the first day after cell seeding, decreased on day 2 to very low levels and could not be detected on day three and four (Figure 28a, c). When cultured in hESC culture medium a constant production of activin A could be measured during the examined period. The production of activin A in hESC culture medium supplemented with bFGF was six times higher than in medium without bFGF while no significant difference between cultures with 4 µg/ml to cultures with 10 µg/ml bFGF could be observed (Figure 28b, d).

3.5 Hepatic Differentiation

Based on the results of the previous experiments on the spontaneous differentiation behavior of the hESC in the bioreactor system and a hepatic differentiation protocol established by Cellartis for hESC cultured in 2D standard culture dishes, two pilot experiments on the directed hepatic differentiation of hESC in the 3D bioreactor system were designed and performed. The two bioreactor experiments differed only in the additional inoculation of inactivated MEF into one of the bioreactors (see Table 1 in the methods chapter).

3.5.1 Metabolic parameters in the perfusion medium

The comparison of the two bioreactors regarding the metabolic parameters measured in the medium shows that the bioreactor, in which additional feeder cells were inoculated (HepDiff-2) initially had a much higher cell activity in terms of glucose and lactate metabolism and regarding the production of differentiation markers. However, in bioreactor HepDiff-2 a steady decrease of glucose consumption and lactate production during the experiment was observed (Figure 29a). The peak of LDH on day 20 was presumably due to technical malfunction of the heating unit of the perfusion system. The peaks of LDH release after day 40 were presumably related to a pressure build up in the bioreactor. Since a precipitation of unidentified medium components was observed, which could lead to clotting of the capillary membranes this might have resulted in suboptimal supply of the cells with nutrients. AFP production in this bioreactor increased exponentially between day 17 and 24 and then decreased until the end of the experiment. The beginning of the down-regulation of AFP production correlates with the change to another differentiation medium (DiffMed-5; see Table 2 in the methods

chapter). The hepatic differentiation marker urea showed a small peak in its production between day 1 and 20 and albumin production stayed on a relative low level of about 0.4 µg/h during the whole experiment (Figure 30a).

In Bioreactor HepDiff-1, in which no additional MEF were inoculated, very low but stable glucose consumption and lactate production levels were measured (Figure 29b). Only the differentiation factor AFP showed a small peak between days 17-35 with a maximum at day 26, which resembles the time course but not the magnitude of AFP in bioreactor HepDiff-2 (Figure 30b).

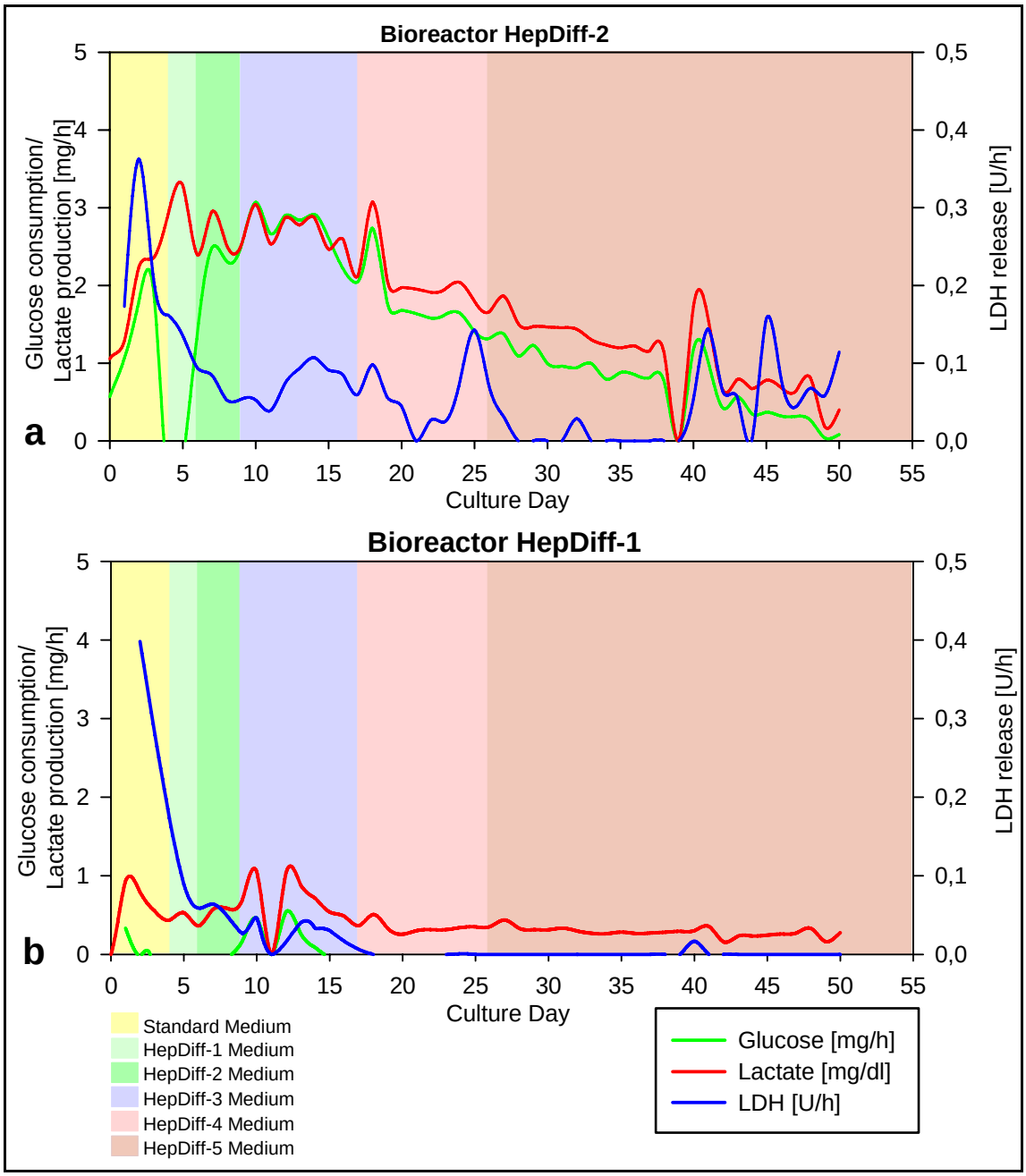

Figure 29: Time course of the metabolic parameters measured in the medium outflow of bioreactors hESC-1, -2 and -3. Glucose consumption (green), lactate production (red) and LHD release (blue) by the cells in bioreactors HepDiff-2 **(a)** and HepDiff-1 **(b).**

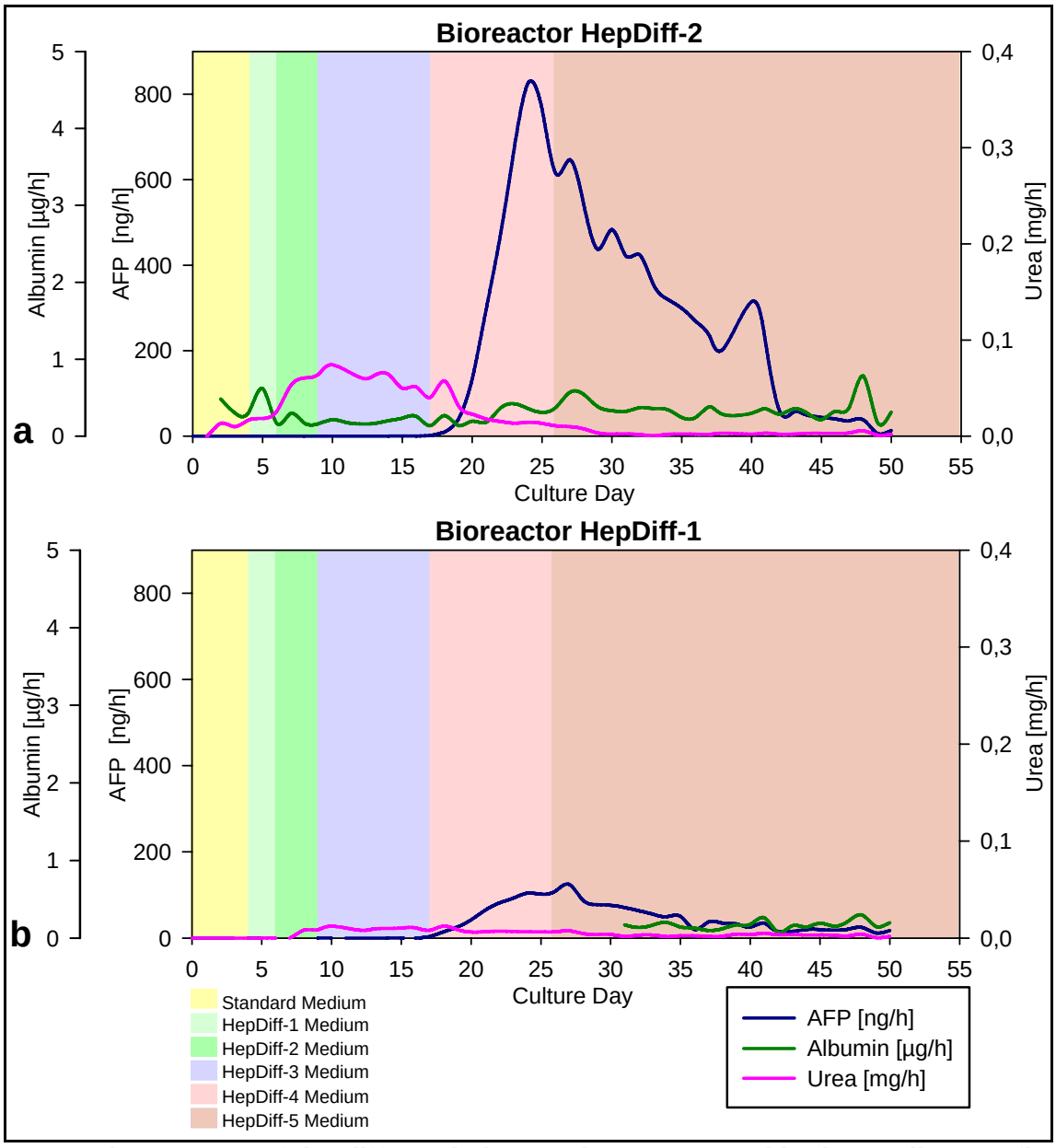

Figure 30: Time course of the differentiation markers measured in the medium outflow of bioreactors HepDiff-1 and -2. AFP production (dark blue), albumin production (dark green), and urea production (pink) by the cells in bioreactors HepDiff-1 **(a)** and HepDiff-2 **(b).**

In addition to the factors described above, the concentrations of activin A and insulin were measured in the culture medium to evaluate the used perfusion conditions with regard to the resulting exchange dynamics of the differentiation media (Figure 31a). Both factors play an important role in inducing differentiation towards definitive endoderm in undifferentiated hESC whereas insulin antagonises endoderm induction through high activin A concentrations. In both bioreactors activin A concentrations in the medium had a maximum of 26 ng/ml between day seven and eight. Insulin concentrations, only measured in bioreactor HepDiff-2 on days 0 to 22, showed a

maximum of 150 ng/ml at day 3 and decreased rapidly to 2 ng/ml until day 9 with an intermediate concentration of about 35 ng/ml between day seven and eight.

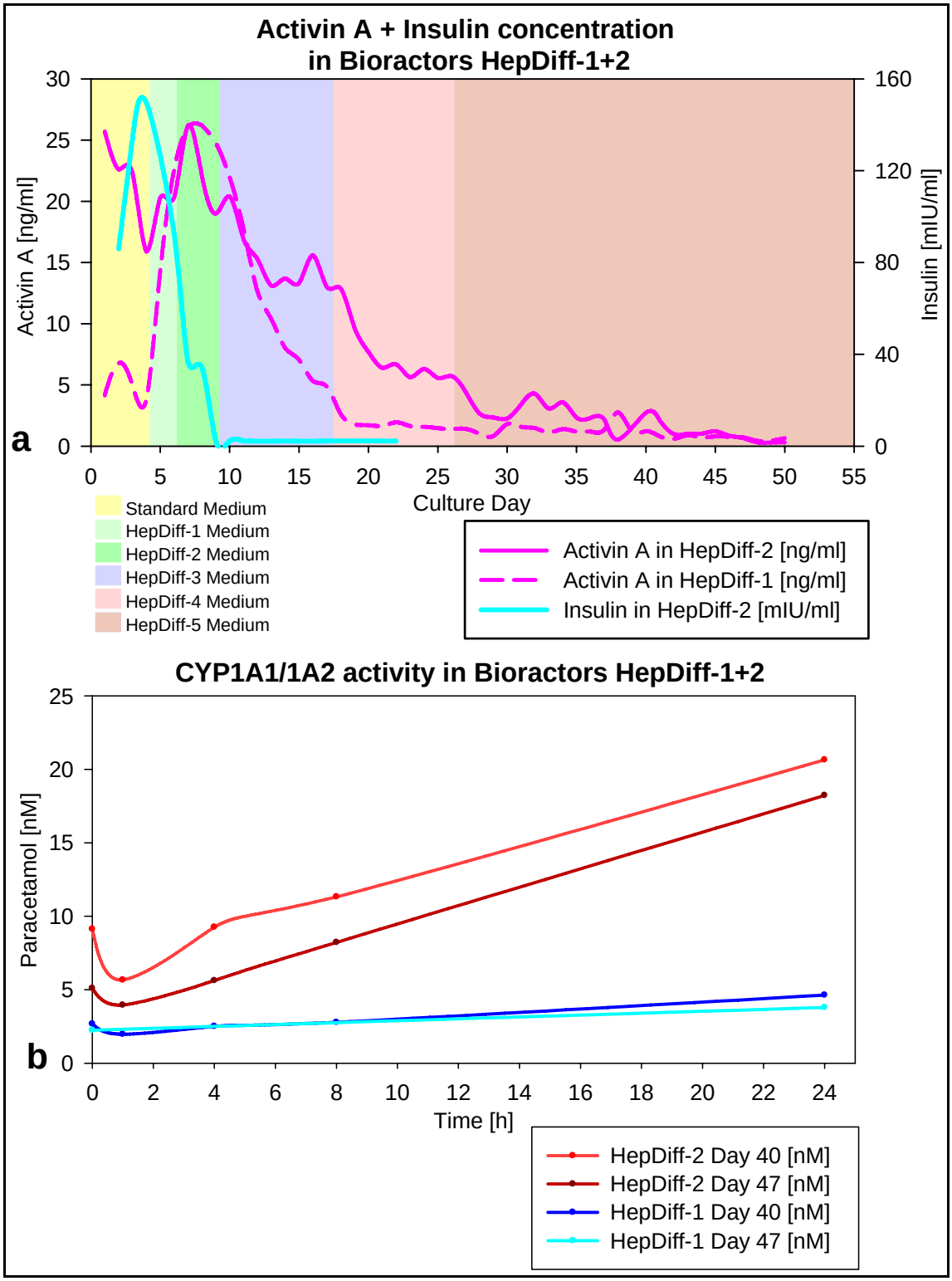

Figure 31: Time course of the activin A and insulin concentrations measured in the medium and cytochrome activity measurement in bioreactors HepDiff-1 and -2. (a) Activin A concentration (pink) insulin concentration (turquoise, only measured in bioreactor HepDiff-2). **(b)** Cytochrome P450 1A1/1A1 activity measured in the bioreactors HepDiff-1 (blue) and HepDiff-2 (red) at days 40 and 47.

3.5.2 CYP450 activity

To test for hepatocyte specific cell activity in the bioreactors the ability to metabolize phenacetin, diclophenac and midazolam via the phase I cytochrome P450 enzymes CYP1A2/1A2, CYP2C9 and CYP3A4, respectively was tested (see Figure 4 in the methods chapter).

The tests were performed at days 40 and 47 after hESC inoculation. In both bioreactors no metabolism of diclophenac and midazolam could be detected. Metabolism of phenacetin into paracetamol was higher in bioreactor HepDiff-2 compared to reactor HepDiff-1 and dropped only slightly on day 47 (Figure 31b).

3.5.3 Histology

As described above, both bioreactors exhibited a very low metabolic activity at the end of the experiment. This observation correlated with the fact that during histological analysis in bioreactor HepDiff-2 only very few areas containing tissue structures and in the samples of bioreactor HepDiff-1 no structures at all could be found.

In the tissue clusters observed in bioreactor HepDiff-2 many structures with different epithelial morphologies could be observed (Figure 32b, c, e, f) indicating a pronounced endodermal differentiation. In addition areas with loose connective tissue and a few cell aggregates comprised of cells with a low cytoplasm to nucleus ratio were found (Figure 32a, d).

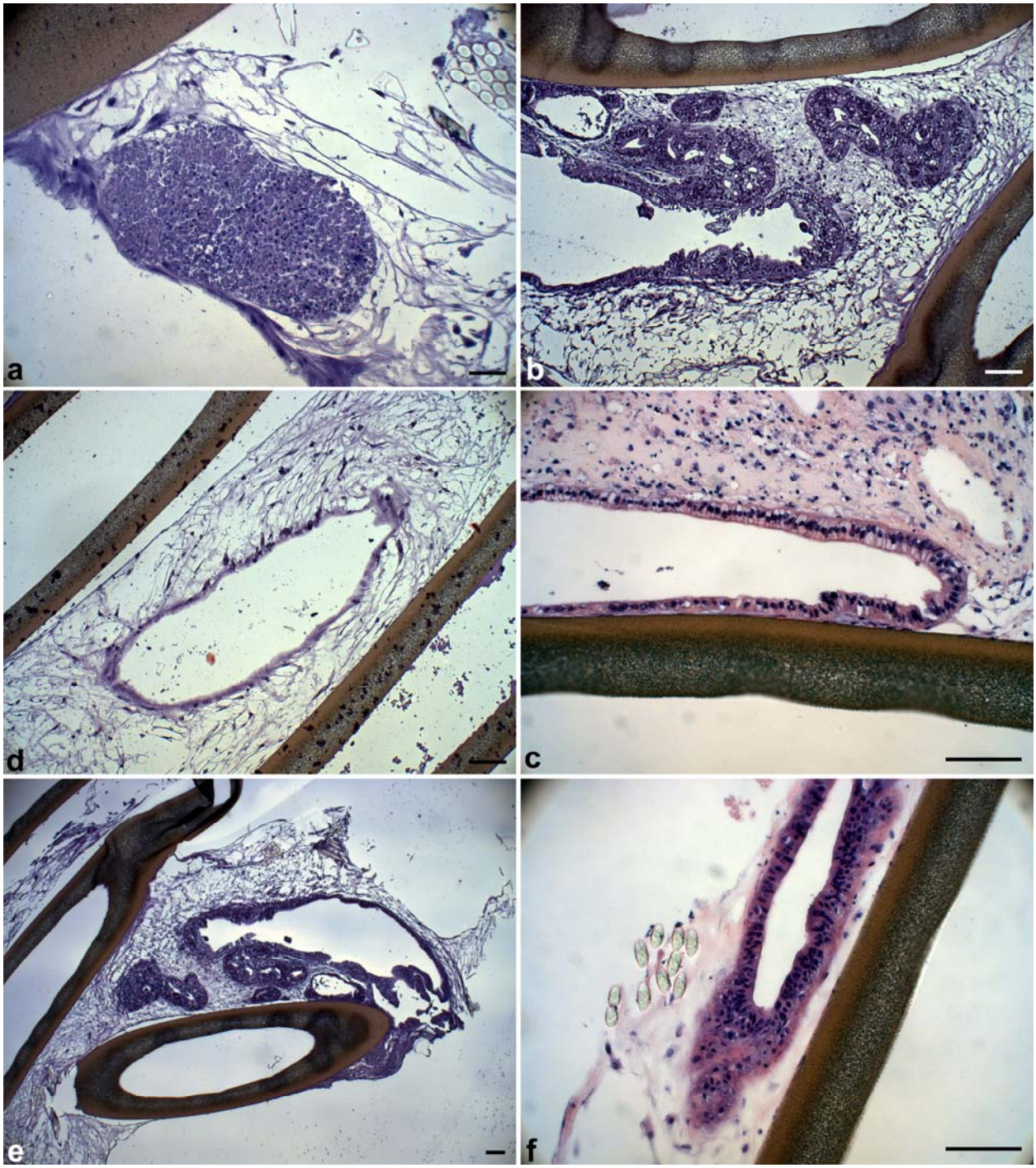

Figure 32: H&E staining of tissue samples taken from bioreactors HepDiff-2. Examination of the morphology of tissues formed in the bioreactor showed many epithelial-like structures **(b, c, e, f)** but also some areas of loose connective tissue **(d)** and aggregates of small cells with a low cytoplasm to nucleus ration **(a)**. (Bar = 50 µm)

4 Discussion

4.1 Human embryonic stem cells grow and differentiate in the investigated three compartment hollow fiber bioreactor

The performed bioreactor experiments on spontaneous differentiation can be grouped regarding their similarity by comparison of their metabolic, gene expression and histological profile (see Table 1 above and Table 5 below for details on the experimental conditions and results).

Table 5: Summary of the experimental conditions and analysis results of the bioreactor experiments on spontaneous hESC differentiation

Experiment Name	Inoculated Cell Types	Used Medium	Summary of the analysis results
hESC-1	hESC HFF (irradiated)	VitroHES +10ng/ml bFGF	Formation of tissues derived from the three germ layers Indications for differentiation into cells of extra embryonic tissues
hESC-2	hESC HFF (irradiated)		
hESC-5	hESC		
hESC-3	hESC HFF (irradiated)	VitroHES +10ng/ml bFGF	Differentiation towards fibroblast like cells
hESC-4	hESC	DMEM/F12 +20% FCS +Glutamax +NEAA	Little differentiation, presence of undifferentiated hESC

The bioreactors hESC-1, -2 and -5 fall into one group. In these three bioreactors the same medium was used and bioreactor hESC-5 differed from the other two only in that no additional feeder cells were inoculated. The observed increase of glucose and lactate metabolism over culture time in these bioreactors indicated that the 3D perfusion conditions supported cell expansion. The other factors measured in the medium of bioreactors hESC-1 and -2 display nearly the same time curves. Both reactors show an initial high production of activin A that decreased to a minimum between day 15 and 25. This is the expected time span the inactivated HFF feeder cells survive in the bioreactors. Further evidence that the measured activin A is produced by the HFF feeder cells is provided by the results from the 2D and 3D bioreactor experiments with HFF alone. These experiments show that activin A production of the HFF is stimulated by bFGF in combination with medium containing serum replacer.

Activin A, a peptide belonging to the transforming growth factor β (TGFβ) superfamily that is known to play roles in cell proliferation, differentiation and apoptosis (Hubner et

al. 1999; Chen et al. 2006), has a strong positive effect on the self-renewal of undifferentiated hESC by inducing the expression of OCT4, NANOG, NODAL, WNT3, bFGF, FGF8 and suppression of BMP signaling (Xiao et al. 2006). It has been shown that low concentrations of FGFs together with activin/TGFß signaling are essential for hESC self-renewal (Beattie et al. 2005; James et al. 2005; Vallier et al. 2005). Additional evidence suggests that bFGF up-regulates the expression of TGFß ligands in both feeder cells and hESC, which in turn promote hESC self-renewal (Greber et al. 2007). Another study has identified the requirement of insulin-like growth factor-1 (IGF1) receptor and ERBB2 receptor signaling for hESC proliferation and self-renewal (Wang et al. 2007), which demonstrates the importance of high insulin concentrations in media for undifferentiated hESC expansion.

In bioreactor hESC-5, in which no additional HFF feeder cells were inoculated initially only a low and then rapidly decreasing production of activin A was detected. This is also in line with the conclusion that the measured activin A was produced by the HFF. At the beginning of the experiment this bioreactor contains only the HFF that were present in the inoculated cell suspensions derived from the hESC/HFF co-cultures used for cell production.

The beginning of hESC differentiation in this group of bioreactors was marked by the onset of AFP and ß-hCG production and started as soon as activin A concentration in the medium reached a minimum.

In human embryonic development AFP is first expressed in the extraembryonic primitive endoderm (yolk sac), then in the hind- and midgut endoderm, and eventually in the foregut hepatic diverticulum at 26 days post ovulation. Later on AFP expression is found in the mesonephric duct and tubules and also transiently in the developing pancreas (Mizejewski 2004). Therefore the immediate onset of AFP production at the beginning of hESC differentiation most probably indicates differentiation towards primitive endoderm.

The other differentiation marker detected in the culture medium was ß-hCG, which represents a marker for the differentiation of hESC towards trophectoderm (Xu et al. 2002) and is also known as a clinical pregnancy test marker and a diagnostic marker for germ cell tumors (Stenman et al. 2006). In normal fetal development, ß-hCG is produced by the embryo soon after conception and later by the syncytiotrophoblast. Therefore the detection of ß-hCG indicates that next to differentiation towards primitive endoderm cells of the trophectodermal lineage are formed by spontaneous differentiation of the hESC. Quantitative comparison of the production levels of AFP and

ß-HCG in bioreactors hESC-1, -2 and -5 indicates that the addition of HFF feeder cells enhances differentiation towards primitive endoderm, while in their absence trophectodermal differentiation is increased.

On the histological level bioreactors hESC-1, -2 and -5 exhibited also a high degree of similarity. The morphology together with detected differentiation markers analyzed by immunofluorescence staining showed that hESC differentiated into cells of the three germ layers and formed differentiated tissue structures. Comparison of the average maturational degree of the tissue types between the three bioreactors showed that bioreactors hESC-1 and -2 exhibited a similar maturational degree that was lower than that observed in bioreactor hESC-5. This result was confirmed by data from the gene expression analysis that showed a higher correlation between bioreactors hESC-1 and hESC-2 than these had with bioreactor hESC-5. These results can be explained with the earlier onset of differentiation in bioreactor hESC-5 due to the low HFF feeder cell activity. Therefore the absolute time period the hESC could differentiate in this bioreactor was longer.

Results from bioreactors hESC-3 and -4 are different compared to the previously described and among each other. In bioreactor hESC-3 a continuously stable activin A production and no release of differentiation markers were observed. In histochemical analysis only cells with fibroblast morphology could be observed that had the same morphology as the HFF cultured without hESC in the bioreactors. Further prove for the fibroblast identity of these cells comes from the expression analysis that showed a high degree of similarity of these cells with HFF. This leads to the conclusion that in this bioreactor all inoculated hESC had differentiated into fibroblasts. Since a constant activin A expression was observed, the possibility that the hESC have died and the observed cells are the co-inoculated inactive HFF can be excluded. If the observed cells would have been the co-inoculated inactive HFF, production of activin A would display a similar time curve of decreasing levels as in bioreactors hESC-1 and -2. In general this bioreactor experiment can be seen as an outliner because of its dissimilar behavior despite using the same experimental conditions as bioreactors hESC-1 and -2. An explanation for this behavior could be the temperature fluctuations due to technical malfunction of the used perfusion monitor leading to increased temperatures during the bioreactor run that might have induced an early differentiation of the hESC into fibroblasts.

To examine the influence of the culture medium on hESC differentiation, a medium supplemented with a high concentration of fetal calf serum and no bFGF was used in bioreactor hESC-4, in which also no additional HFF feeder cells were inoculated. In this bioreactor the initially high activin A production decreased very slowly compared to all other reactors and reached a minimum after about twice the length of the time period observed in the bioreactors with feeder cells. Histological analysis revealed not only fibroblasts but also clusters of cells exhibiting a low cytoplasm to nucleus ratio, which is a typical feature of undifferentiated hESC. In addition many of these clusters co-expressed the pluripotency markers OCT4 and TRA-1-81, which suggests that these clusters represent undifferentiated hESC. These results together with the expression profile that showed a high correlation to hESC/HFF co-cultures leads to the interpretation that differentiation in this reactor was suppressed by a “feeder cell like” activity. A possible explanation for the origin of this “feeder cell like” activity is that under the influence of the used culture medium some of the hESC differentiated into cells exhibiting self-renewal supportive activity. This is in accordance with studies by other groups that showed that autologous hESC derived feeder cells are able to support the self-renewal of undifferentiated hESC (Xu et al. 2004; Stojkovic et al. 2005; Yoo et al. 2005; Gonzalez et al. 2008). In contrary to this are the results of the experiments on the influence of medium and bFGF on HFF that showed that activin A production was suppressed by serum containing medium. Therefore the activin A production in this bioreactor either originates from cells that differ from HFF or the production of activin A is not influenced by FCS but by other components of the used medium.

In summary these results show that hESC are able to differentiate into cells of the three germ layers as well as cells of the extraembryonic lineages in the bioreactor system. Differentiation is influenced by the presence of feeder cells, the used culture medium and physical culture parameters. Additionally activin A was identified as a soluble marker for the self-renewal supportive activity of the feeder cells.

4.2 Tissue structures formed by the hESC in the bioreactor closely resemble these of teratomas formed *in vivo*

One major topic addressed in this study was the comparison of the spontaneous hESC differentiation behavior under the *in vitro* conditions in the bioreactor to the *in vivo* conditions when the hESC are transplanted into a mouse.

This comparison showed that the differentiated tissue structures that were observed in the group of bioreactors hESC-1, -2 and -5 closely resemble the structures found in the teratomas formed *in vivo* on the histological, ultrastructural and RNA expression level.

In general, tissue structures and typical gene expression patterns showing differentiation into derivates of all three germ layers could be detected in both the bioreactors and teratomas but the overall proportions of the individual structures derived from the three germ layers differed between the two culture models. In the histological analysis less ectodermal structures in the teratomas compared to the bioreactors could be detected. These structures could be identified by their morphology, mostly in the form of embryonic neural rosettes and the expression of the characteristic markers nestin and ß-III-tubulin. Nestin, a class VI intermediate filament protein, is observed in cells in nervous tissue during the embryonic period of ontogenesis. It is absent from nearly all mature central nervous system cells and therefore is considered as a marker for neural progenitors (Gilyarov 2008). Expression of nestin has also been described in non-neural progenitor populations, such as pancreatic islet, hematopoietic as well as skeletal muscle progenitors (Sejersen et al. 1993; Shih et al. 2001; Zulewski et al. 2001). Besides in progenitor cells nestin is also expressed in mature cells of, for example, the retina, striated muscle, cardiac muscle, skin, teeth, kidneys, testicles or adrenals (Gilyarov 2008). This expression pattern shows that the detection of nestin alone is not sufficient for the identification of neural cells and therefore also the expression of ß-III-tubulin was examined. ß-III-tubulin is regarded as a neuron-specific marker. During fetal and postnatal development ß-III-tubulin is abundantly expressed in the central and peripheral nervous systems and has been suggested to be one of the earliest markers indicating neuronal commitment in primitive neuroepithelium (Katsetos et al. 2003). In adult tissues ß-III-tubulin is specifically expressed in neurons (Katsetos et al. 2003).

Mesodermal derived tissues were equally expressed in bioreactors and teratomas. These tissues were identified by their typical morphology and marker expression. In general a high percentage of connective tissue comprised of fibroblasts and collagen rich extracellular matrix and also numerous clusters of hyaline cartilage were detected in the examined samples. The presence of further mesodermal tissues was confirmed by examination of the markers α-smooth muscle actin, a marker of smooth muscle cells, the type III intermediate filament desmin, which is one of the earliest protein markers for

muscle tissue in embryogenesis (Bar et al. 2004) and vimentin as a general marker for mesenchymal cells.

Endodermal derived tissues were found at a low proportion in the examined samples and quantities did not differ between bioreactors and teratomas. These structures were identified by their typical morphology in the form of epithelial and glandular structures and also by ultra structural features like kinocilia. Furthermore expression of the transcription factor HNF-3ß (FOXA2) used as a marker for endodermal differentiation could be detected.

The pluripotency marker OCT4, indicating the presence of undifferentiated hESC, could only be detected in very few samples from the bioreactors but not in the teratomas, which is in accordance with observations of other studies (Gertow et al. 2004; Adewumi et al. 2007).

The detailed analysis and comparison of the expression profiles confirmed the observations made on the histological level. Functional analysis of the exclusively expressed genes within the bioreactors showed that many of these are involved in neural differentiation processes. Further statistical comparison of the transcriptomes of bioreactors and teratomas showed that only a very low number of genes are differentially expressed. Functional analysis of these differentially expressed genes also indicated that neural differentiation was pronounced in the bioreactors.

These differences between bioreactors and teratomas regarding their differentiation patterns can be explained by the various factors specific for the *in vitro* and the *in vivo* environments respectively. It has been reported that one of the default pathways of spontaneous differentiation of hESC in standard 2D culture conditions is neural differentiation that includes for example the development of neurons and glia (Reubinoff et al. 2001; Hornstein et al. 2004). Further evidence comes from the analysis of the 2D control cultures, in which the spontaneous differentiation behavior was examined. In these cultures next to other cell types many cells displaying neuron morphology developed. This behavior *in vitro* is also in accordance with normal embryonic development *in vivo* in which neurulation is the first step in organogenesis.

One major factor that influenced the pronounced neural differentiation in the bioreactor could be the used culture medium and in particular the contained bFGF. bFGF plays an important role in nervous system development by influencing proliferation, differentiation, migration and cell survival of neural cell types (Gremo et al. 2000; Dono 2003). It has been shown *in vitro* that bFGF has a strong mitogenic effect on neural

stem and precursor cells (Hsu et al. 2007) and it is also used as a differentiation factor in combination with other factors in many protocols for the neural differentiation of hESC (Schwartz et al. 2008). On the other hand, bFGF promotes the self-renewal of hESC both in co-cultures with MEF (Amit et al. 2000) and in feeder free cultures when used in high concentrations (Xu et al. 2005; Xu et al. 2005). Thus it can be hypothesized that after the feeder cell activity decreased the used bFGF concentration was too low to sustain pluripotency and hESC started to differentiate. The spontaneous differentiation of the hESC was influenced by the mitogenic and neurotophic activity of bFGF that resulted in an enrichment of neural cell types in the bioreactors.

The low percentage of ectodermal derived tissues observed in the teratomas is in contrast to the results of other studies on teratoma formation of hESC in mice. In these studies a predominance of ectodermal and mesodermal differentiation is described. Gertow et al. injected the hESC line HS181 into SCID/beige mice and observed predominantly differentiation along a neuronal lineage, the formation of bone/cartilage and epithelia (Gertow et al. 2004). In a further study of teratomas derived from 37 different hESC lines a predominance of ectodermal and mesodermal tissues has also been reported (Adewumi et al. 2007). One explanation for the different result in this study could be the influence of the specific mouse model and the graft site. For example it has been shown by analysis of teratomas derived by transplantation of hESC subcutaneously or into the liver of nude (nu/nu) mice that the graft site of teratomas has an influence on their growth and differentiation pattern (Cooke et al. 2006).

In summary the results of the comparison of the differentiation pattern of hESC in the bioreactors with teratomas in this study show that a 3D environment is essential for the development of a teratoma *in vivo* and teratoma like tissue structures *in vitro.* Furthermore the results indicate that direct cellular interaction with the host cells is not an important factor that influences teratoma formation *in vivo.* Instead soluble factors in the blood of the host or in the culture medium respectively seem to play a major role.

These results open several perspectives on applications of the bioreactor culture system in research: The bioreactor could provide an *in vitro* alternative for the teratoma formation assay applied to explore the developmental potential of pluripotent cell types (e.g. ES cells or induced pluripotent cells). It could also be applied for safety testing of remaining undifferentiated cells in cell preparations derived from pluripotent cells. In addition the development of embryotoxicity testing methods using the bioreactor could

be possible. Finally the system can be used as an *in vitro* system to examine certain aspects of tissue development.

The application of the bioreactor model has some advantages to the teratoma model because it allows defined and controllable growth conditions and upon replacement of the teratoma formation model in mice animal testing will be reduced.

4.3 Directed hepatic differentiation of hESC in the bioreactor

Based on the results of the experiments on the spontaneous differentiation behavior of the hESC in the bioreactor system two pilot experiments on the directed hepatic differentiation of hESC in the bioreactor were performed. The two bioreactor experiments differed only in the additional inoculation of inactivated MEF into one of the bioreactors.

The differentiation protocol used was developed by Cellartis in 2D cultures for hESC cultured on MEF. Considering the results of the previous bioreactor experiments this protocol was transferred to the 3D bioreactor system.

Following inoculation, the hESC were cultured during the first four days of the experiments in standard culture medium which is similar to the medium used in the previous bioreactor experiments and contains serum replacement (DiffMed-1). This initial step was chosen to allow the hESC to adapt to the new culture environment and to start differentiation when the HFF loose their differentiation inhibiting activity but before the onset of spontaneous differentiation. The step was chosen based on three observations: Firstly in all foregoing bioreactor experiments an increased rate of cell death, indicated by a peak of LDH, was observed after cell inoculation. This increased cell death might be due to the process of cell harvesting from the 2D cultures, the inoculation process itself and/or induced by the changed environment of bioreactor to that the cells have to adapt to. Secondly the differentiation conditions applied in the following step have a high selection pressure on the cells. Therefore applying these conditions directly after cell inoculation is another stress factor for the cells and could lead to increased cell death. Thirdly the culture length of four days before start of directed differentiation was chosen based on the observation that in neither of the previous experiments differentiation markers were detected in this time period and HFF activity, measured by their activin A production, constantly decreased.

The following initial step of the differentiation protocol is the induction of hESC differentiation towards definitive endoderm (DE) that is based on a protocol developed by D'Amour et al. (D'Amour et al. 2005). In this protocol a high ratio of differentiation of hESC into DE cells is archived by treatment with a high activin A concentration in low serum conditions. This step is crucial for successful further cell differentiation towards liver cells. After DE induction the next two differentiation steps should direct differentiation of the cells towards a hepatoblasts phenotype. And the final step should support cell maturation into fully differentiated hepatocytes.

Bioreactor HepDiff-2, in which additional inactive MEF were inoculated showed a much higher metabolism of glucose and lactate compared to HepDiff-1 without feeders. This indicates that the presence of MEF is cell protective for the hESC and results in a better cell survival after inoculation. A lower cell survival in the absence of feeders becomes also evident when comparing AFP production and CYP450 activity in the bioreactors. The levels of these parameters were about eight times lower in the bioreactor HepDiff-1 without feeders compared to bioreactor HepDiff-2 with feeder cells.

Time courses of the examined differentiation factors AFP, albumin and urea did not indicate successful hepatic differentiation. Upon ongoing hepatic differentiation interim production of AFP and increasing levels of albumin and urea production towards the end of the experiment would have been expected. Production of AFP was observed in both bioreactors and started at about experimental day 17. This can be interpreted as a sign of early hepatic differentiation presuming preceding successful DE differentiation of the hESC. AFP is a marker for differentiation of DE cells into hepatoblasts, the major cell type of the fetal liver, but can also indicate differentiation of the hESC into primitive endodermal cells.

In neither bioreactor a significant production of the hepatocytes specific markers urea and albumin was observed. However significant metabolism of phenacetin by CYP1A1/1A2 was detected in the bioreactors. CYP1A1 is expressed in fetal liver during the first and second trimester and also in other fetal tissues like lung and adrenal tissue and can not be detected anymore in adult liver whereas CYP1A2, CYP2C9 and CYP3A4 expression is absent in fetal liver and expressed in adult liver (Hines et al. 2002). CYP2C9 and CYP3A4 activities were not detected in the bioreactors.

The histology of the structures observed in the bioreactor revealed mostly structures with epithelial morphology but no cells displaying typical hepatocyte morphology (polygonal cells with round nuclei) were detected.

In summary these results suggest no significant hepatic maturation in the bioreactors. The time course of AFP rather suggests differentiation towards primitive endoderm. This assumption is also supported by a similar time course of AFP and the histology as found in bioreactor hESC-5.

To evaluate the applied differentiation conditions the levels of insulin and activin A were analyzed. This analysis revealed an overlap of high levels of insulin with high levels of activin A. The observed high level of insulin comes from the serum replacer contained in DiffMed-1 and, as reported by Wang et al., can support hESC proliferation and self-renewal by stimulation of insulin-like growth factor-1 receptor signaling together with ERBB2 receptor signaling (Wang et al. 2007). It has also been shown that signaling by activin/nodal family members in combination with reduced insulin/insulin-like growth factor signaling is critical for cell fate commitment into DE (McLean et al. 2007). This shows that the differentiation conditions of concurrent high insulin and activin A levels in the bioreactors were not optimal for induction of DE and that this is most likely the reason for absence of hepatic differentiation. Therefore, to achieve successful differentiation of hESC into definitive endodermal cells in the bioreactor, the standard culture medium has to be quickly and completely exchanged with the differentiation medium to remove all insulin from the system as a prerequisite for an efficient induction of DE by activin A.

4.4 Outlook

For the development and implementation of stem cell-based applications in regenerative medicine and applied research, like drug screening or toxicology testing, large numbers of cells with well defined characteristics are needed. Therefore culture systems are required that allow the expansion of undifferentiated human embryonic stem cells and/or a directed reproducible differentiation into mature cell types with a high yield and purity.

Current 3D suspension culture model approaches using aggregates or microcarriers are limited in central mass exchange. By offering perfusion-based dynamic culture conditions with continuous medium exchange and decentral oxygenation at controllable gas tensions in larger cell masses, the 3D perfusion four-compartment capillary membrane bioreactor technology enables using the advantages of both culture concepts. In addition, application of differentiation regimes in a closed system, suitable

for good manufacturing practice (GMP) conditions is possible. The technology allows varying but controllable medium- and system parameters including, e.g., oxygen tensions, gas factor application, medium factor gradients, or generating physical stimuli such as flow and pressure on the cells. A further aspect of dynamic perfusion technique is that a combination of “twin bioreactors” in one perfusion circuit can be easily performed, where factors or soluble mediators of a first bioreactor can stimulate the second bioreactor, while cells remain compartmentalized. This would be of interest if unknown soluble factors of a co-culture are to be used, but cell transfer between the cultures has to be avoided.

4.4.1 Production of conditioned medium with the bioreactor system for culture of undifferentiated hESC

The bioreactor experiments examining the spontaneous differentiation of hESC also show that the presence of inactive HFF delays the start of hESC differentiation until the HFF loose their activity. The pluripotency supporting activity of the HFF could be correlated with their production of activin A. To further examine the behavior of the HFF feeder cells several experiments only with HFF were carried out in 2D cultures and in two bioreactors. Results from 2D and 3D experiments show that activin A production is stimulated by bFGF in combination with medium containing serum replacer. In medium supplemented with serum, bFGF did not stimulate activin A production but exhibited a strong mitogenic effect on active HFF. This effect was also observed in bioreactor experiment HFF-1 characterized by increasing levels of glucose and lactate metabolism upon bFGF addition to the medium. This mitogenic effect was not observed in the bioreactor experiment HFF-2, in which medium supplemented with serum replacement was used. In this experiment glucose and lactate metabolism stayed on a constant level which shows that the cells did not proliferate.

These results show that a possible application of the bioreactor technology could be the production of conditioned medium that is needed for feeder free expansion of undifferentiated hESC.

The standard method for the production of conditioned medium (CM) is incubation of culture medium for 24 hours in standard culture vessels seeded with inactive MEF feeder cells at a high density. This method is labor intensive and space consuming, because large numbers of feeder cells have to be produced that can only be used for a

limited amount of time for medium conditioning until they loose their activity. Therefore the production of larger volumes of CM is limited by the poor scalability of this method.

An alternative approach to the use of CM for culture hESC is the use of defined culture media. Several defined medium formulations have been described for feeder independent culture of hESC (Li et al. 2005; Ludwig et al. 2006). While the use of defined medium has several advantages like the possibility to culture hESC under conditions completely free of animal derived substances, its major disadvantage is that these media formulations include significant amounts of expensive supplements like recombinant cytokines and growth factors.

Cultivation of HFF in a bioreactor to produce CM could be an alternative to these methods. It would enable high cell densities of human feeder cells in a scalable system that allows automatic control of the culture parameters and defined rates of medium in- and outflow. Therefore standardization of the conditioning process will be possible resulting in an increased quality of the produced CM compared to manual methods.

One further advantage when using the bioreactor could be the possibility to use active feeder cells because it has been shown that active feeder cells also support maintenance of pluripotency (Xie et al. 2005). This would decrease the number of active feeder cells that have to be produced in conventional 2D cultures for initial bioreactor inoculation.

Based on the results of the HFF bioreactor experiments the approach could be the following: Initially the bioreactor will be inoculated with active HFF that will be cultured in medium supplemented with serum and bFGF to stimulate HFF proliferation. An increase of the cell number can be monitored by the levels of glucose consumption and lactate production. When a sufficient cell number is reached culture medium is changed to hESC medium for conditioning. Optimal medium exchange rates have to be determined for example measuring activin A and glucose concentrations in the conditioned medium as quality control parameters. A low glucose level might indicate the demand for increasing the medium feed rate and a low activin A level might be a sign for insufficient conditioning unsuitable to promote hESC pluripotency.

4.4.2 Undifferentiated expansion of hESC in the bioreactor

Strategies for the expansion of hESC in the bioreactor can also be developed based on the results of the experiments on spontaneous differentiation that give indications regarding the utilization of feeder cells and medium composition.

Direct co-culture with inactive feeder cells is impracticable because of their limited activity. This limitation also would not be solved by increasing the initial seeding density of the feeder cells and/or addition of fresh feeder cells into the bioreactor at defined intervals due to space limitations. Direct co-culture of hESC with active feeder cells is also problematic because the feeder cells will tend to outgrow the hESC due to their much faster cell cycling (Xie et al. 2005). Therefore the most promising approaches to keep the hESC in their undifferentiated state can be seen in the use of conditioned medium in the bioreactor.

For bioreactor expansion using CM the needed medium could be produced in a separate bioreactor as described above. The disadvantage of this approach is that the produced medium has to be further processed and stored until usage, which can decrease its quality and increases the risk of contamination.

An indirect co-culture facilitated by interconnecting two bioreactors in a perfusion circuit could solve these problems. This way the cells are separated by the medium capillary membranes but bidirectional exchange of soluble substances between the cells in the individual bioreactors is possible. Such a setup would also allow the use of active feeder cells.

A possible disadvantage of using CM could be that additional surface coating of the cell-compartment of the bioreactor might be necessary. Because most of the currently described feeder free hESC culture models that use CM are dependent on the use of an extracellular matrix such as Matrigel to coat the surface of standard culture vessels (Xu et al. 2001) or, when using suspension cultures, the surface microcarriers (Nie et al. 2009). But coating can lead to clogging of the membranes of medium capillaries resulting in insufficient substance exchange in the cell compartment. An approach to circumvent this problem could be injection of pre-coated microcarriers into the cell compartment prior to cell inoculation to provide a suitable growth surface. Another possibility is the use of hESC that have been adopted to matrix free culture as described by Bigdeli et al. who has shown that hESC can be adopted to grow on plastic surfaces in CM without use of an extracellular matrix (Bigdeli et al. 2008).

Successfully expanded hESC could be either harvested form the system by enzymatic dissociation and flushing or differentiated inside the bioreactor toward a desired cell type.

4.4.3 Clinical perspective

The lack of causal liver therapies and the insufficient availability of donor organs for liver transplantation create a demand for the development of new cell-based liver therapies. Transplantation of stem cells capable of proliferation and differentiation to replace the injured tissue could replace whole-organ transplantation in some clinical indications.

The results of this study show that the 3D perfusion culture technology represents a promising tool for stem cell expansion and differentiation at high densities in a highly controlled environment. And could possibly be used to for the production of embryonic or pluripotent stem cell-derived cell preparations for transplantation in patients with hepatic insufficiency, e.g. in the case of certain genetic defects or acute to chronic liver failure. A further therapeutic option can be seen in the application of the bioreactor technology for extracorporeal liver support intended to bridge the liver function until transplantation or until organ regeneration by using hESC derived liver cells as a human cell source. Extracorporeal systems could also provide an interesting therapeutic option to bridge the liver function after stem cell transplantation until the applied cells show sufficient functional performances. Finally stem cells and stem cell derived differentiated cells expanded and maintained in the bioreactor system could also be used to produce regenerative substances that stimulate the endogenous regeneration process *in vivo*.

4.4.4 Other pluripotent cell types as alternative cell sources

A future clinical use of hESC derived cells is under an ongoing debate because of the ethical concerns regarding their derivation. The possibility of an insufficient histocompatibility of hESC derived cell and safety aspects regarding an inherent risk of tumor formation by contaminating undifferentiated hESC in transplanted cell preparations are also discussed. Therefore alternative cell sources are examined with the goal to derive histocompatible, pluripotent cells that could solve these problems. The bioreactor technology could be applied in the characterization and the comparison of the candidate cell types with hESC which at the moment represent the gold standard.

For example, recently the isolation of human adult germline stem cells from testis has been reported (Conrad et al. 2008; Kossack et al. 2008; Gallicano et al. 2009). These cell exhibit similar characteristics as hESC: They express the pluripotency markers OCT3/4, NANOG, SSEA-4, TRA1-81, and TRA1-60, showed high telomerase activity and could be cultured for more then 40 passages while maintaining a normal karyotype. *In vitro* they can be differentiated into various types of somatic cells of all three germ layers and form teratomas when transplanted in immunodeficient mice.

It has also recently demonstrated that by transduction of stemness factors somatic cells can be reprogrammed into pluripotent cells, so called induced pluripotent stem cells (iPSC). First, the induction of pluripotent capabilities in fibroblasts from mouse tail-tip employing retroviral-mediated transduction of OCT4, SOX2, KLF4 and C-MYC has been shown (Takahashi et al. 2006; Maherali et al. 2007; Okita et al. 2007; Wernig et al. 2007). Further reports demonstrated that the combined expression of four transcription factors, OCT4, SOX2, NANOG and LIN28 or OCT4, SOX2, KLF4 and C-MYC is sufficient to reprogram human fetal foreskin or adult human dermal fibroblasts into pluripotent cells (Takahashi et al. 2007; Yu et al. 2007; Lowry et al. 2008; Nakagawa et al. 2008; Park et al. 2008). These human iPSC resemble human embryonic stem cells by their morphologic and gene expression properties. iPSC have normal karyotypes, express telomerase activity, express cell surface makers and genes that characterize human ES cells, and maintain the developmental potential to differentiate into advanced derivatives of all three primary germ layers, including teratoma formation when transplanted into immunodeficient mice.

5 Abstract

Embryonic stem cells are pluripotent cells capable of unlimited self-renewal and differentiation into cells representative of all three embryonic germ layers. Because of their unique characteristics human embryonic stem cells (hESC) hold great potential as a cell source for applications in basic science, pharmacological drug screening, toxicity testing and cell based therapies in regenerative medicine. For these, methods for the efficient generation of highly enriched specific cell preparations are key prerequisites.

The goal of the project was to investigate growth and differentiation of hESC in a specific multicompartment bioreactor system for 3D cell perfusion with decentral mass exchange and integrated oxygenation. Emphasis was on spontaneous and hepatic differentiation. This target was based on the hypothesis that the 3D environment of the bioreactor constitutes a more *in vivo*–like environment than standard 2D culture systems and therefore better supports growth and differentiation of hESC.

One aim of this study was to analyze the capacity of the bioreactor system to support spontaneous multilineage differentiation and tissue formation of hESC and to compare it to teratoma formation of hESC in mice. Furthermore the influence of serum added to the culture medium and the presence of feeder cells on hESC differentiation were examined. To better understand the role of feeder cells experiments with feeder cells were carried out in the bioreactor and in 2D cultures. Another aim of this study was the evaluation of the directed differentiation of hESC towards the hepatic lineage. For this purpose a method of directed hepatic differentiation that was originally developed for 2D cultures of hESC was translated to the 3D system and two pilot experiments were performed. The growth and differentiation behavior of the cells in the different experiments of this study was examined by the analysis of metabolic parameters in the culture medium, RNA expression profiling using microarrays, expression of differentiation markers, histology and the ultra structure of the cells.

Results of the experiments on the spontaneous differentiation of hESC showed that hESC differentiated into cells of the three germ layers as well as cells of the extraembryonic lineages and formed differentiated tissue-like structures in the bioreactor system. Comparison of these tissue structures with those formed in teratomas showed a high degree of similarity on the RNA, protein and histological levels.

The presence of feeder cells in the bioreactor resulted in suppression of hESC differentiation as long as the feeder cells were active. The presence of serum in the culture medium also inhibited differentiation. Activin A was identified as a soluble marker for the self-renewal supporting activity of the feeder cells.

The results of the two pilot experiments on hepatic differentiation in the bioreactor system suggested no significant hepatic maturation but rather spontaneous differentiation. Therefore the concentrations of factors that influence hepatic differentiation used in the applied differentiation protocol have to be further optimized in future studies.

The results of this study suggest that 3D perfusion bioreactors provide a technology supporting spontaneous hESC differentiation, similar to an *in vivo* environment. Therefore the bioreactor system could be used as an *in vitro* alternative for the *in vivo* teratoma formation assay that is commonly used to explore the developmental potential of pluripotent cell types and this way can help to reduce animal testing. Furthermore the defined and controllable culture conditions render the system suitable for applications such as the safety testing of remaining undifferentiated cells in cell preparations derived from pluripotent cells, the development of embryotoxicity testing methods and its use as an *in vitro* system to examine certain aspects of tissue development. The results also indicate possible applications of the bioreactor system for production of undifferentiated hESC for example by using feeder cell cultures in the bioreactor to produce conditioned medium needed for hESC expansion.

6 Zusammenfassung

Embryonale Stammzellen sind pluripotente Zellen. Sie haben die Fähigkeit, sich unbegrenzt selbst zu erneuern und in Zellen aller drei Keimblätter zu differenzieren.

Wegen dieser einzigartigen Eigenschaften haben humane embryonale Stammzellen (hESC) ein großes Potential als Zellquelle für Anwendungen in der Grundlagenforschung, bei der pharmakologischen Wirkstoffsuche, in der Toxizitätstestung und in zellbasierten Therapien in der regenerativen Medizin. Eine Grundvoraussetzung für solche Anwendungen ist die Verfügbarkeit von Methoden, mit denen sich Zellpräparationen von hoher Reinheit und ausreichender Zellzahl generieren lassen.

Das Ziel des Projektes war die Untersuchung des Wachstums und der Differenzierung von hESC in einem speziellen Mehrkompartimentbioreaktorsystem für die 3D Zellperfusion mit dezentralem Massenaustausch und integrierter Oxygenation. Der Schwerpunkt lag dabei auf der Untersuchung der spontanen und hepatischen Differenzierung dieser Zellen. Dieses Ziel basierte auf der Hypothese, dass die 3D Umgebung des Bioreaktors eine *in vivo* ähnlichere Umgebung darstellt als gewöhnliche 2D Kultursysteme und deshalb das Wachstum und die Differenzierung von hESC besser unterstützt.

Ein spezifisches Ziel dieser Studie bestand in der Untersuchung, inwieweit das Bioreaktorsystem die spontane Differenzierung von hESC in verschiedene Zelllinien und die Gewebebildung unterstützt sowie in dem Vergleich dieser Differenzierung mit der Teratombildung aus hESC in Mäusen. Weiterhin wurde der Einfluss von Serum im Kulturmedium und die Anwesenheit von Feeder-Zellen auf die Differenzierung der hESC untersucht. Um die Rolle der Feeder-Zellen besser zu verstehen, wurden Experimente mit Feeder-Zellen sowohl in Bioreaktoren als auch in 2D Kulturen durchgeführt. Ein weiteres spezifisches Ziel dieser Studie war die Untersuchung der gerichteten Differenzierung von hESC in die hepatische Zelllinie. Hierzu wurde eine Methode, die ursprünglich zur gerichteten hepatischen Differenzierung von hESC in 2D Kulturen entwickelt worden ist, auf das 3D System übertragen und zwei Pilotexperimente durchgeführt.

Das Wachstums- und Differenzierungsverhalten der Zellen in den verschiedenen Experimenten dieser Studie wurde durch die Analyse von metabolischen Parametern im

Kulturmedium, des RNA Expressionsprofils mithilfe von Microarrays, der Expression von Differenzierungsmarkern, der Histologie und der Ultrastruktur der Zellen untersucht.
Die Ergebnisse der Experimente zur spontanen Differenzierung von hESC zeigten, dass die hESC sowohl in Zellen der drei Keimblätter als auch in Zellen der extraembryonalen Linien differenzierten und im Bioreaktor gewebeähnliche Strukturen bildeten. Der Vergleich dieser Gewebestrukturen auf RNA, Protein und histologischer Ebene mit den in Teratomen gebildeten Geweben zeigte eine sehr hohe Ähnlichkeit.
Ferner konnte beobachtet werden, dass die Differenzierung der hESC im Bioreaktor so lange unterdrückt blieb, wie anwesende Feeder-Zellen aktiv waren. Auch der Zusatz von Serum zum Kulturmedium verzögerte die Differenzierung. Activin A wurde als ein löslicher Marker für die die Selbsterneuerung erhaltende Aktivität der Feeder-Zellen identifiziert.
In den beiden Pilotexperimenten zur hepatischen Differenzierung im Biorektorsystem ergaben sich keine signifikanten Anzeichen für eine hepatische Reifung, sondern eher für eine spontane Zelldifferenzierung. In zukünftigen Studien müssten deshalb die Konzentrationen der die hepatische Differenzierung beeinflussenden Faktoren in dem benutzten Differenzierungsprotokoll weiter optimiert werden.
Die Studie ergab insgesamt, dass 3D Perfusionsbioreaktoren eine Technologie darstellen, welche die spontane hESC Differenzierung ähnlich wie eine *in vivo* Umgebung unterstützt. Diese Bioreaktorsysteme könnten daher als eine *in vitro* Alternative zur *in vivo* Testung der Teratombildung, welche häufig angewandt wird um das Entwicklungspotential von pluripotenten Zellarten zu untersuchen, dienen. Die Anzahl von Tierversuchen ließe sich so reduzieren. Die definierten und kontrollierbaren Kulturbedingungen in 3D Perfusionsbioreaktoren könnten auch genutzt werden, um verbleibende undifferenzierte Zellen in aus pluripotenten Zellen gewonnenen Zellpräparationen aufzuspüren, für die Entwicklung von Methoden zur Testung von Embryotoxizität und als ein *in vitro* System zur Untersuchung bestimmter Aspekte der Gewebeentwicklung. Die Ergebnisse zeigen schließlich auch Möglichkeiten auf, das Bioreaktorsystem zur Produktion von undifferenzierten hESC einzusetzen wie zum Beispiel im Rahmen von Feeder-Zellkulturen zur Herstellung von konditionierten Medium, benötigt für die Expansion von hESC.

7 List of own publications

Stachelscheid H, Urbaniak T, Ring A, Spengler B, Gerlach JC, Zeilinger K. Isolation and characterization of adult human liver progenitors from ischemic liver tissue derived from therapeutic hepatectomies. Tissue Eng Part A. 2008, Dec 24. [Epub ahead of print]

Wohlers I*, Stachelscheid H*, Borstlap J, Zeilinger K and Gerlach JC. The Characterization Tool: A Knowledge-Based Stem Cell, Differentiated Cell and Tissue Database with a Web-Based Analysis Front-End. Stem Cell Res. 2009 [in press] DOI: 10.1016/j.scr.2009.05.001
*equal contribution

Gerlach JC, Hout M, Edsbagge J, Björquist P, Lübberstedt M, Miki T, Stachelscheid H, Schmelzer E, Schatten G, Zeilinger K. Dynamic 3D culture promotes spontaneous embryonic stem cell differentiation in vitro. Tissue Eng 2009 [in press]

Stachelscheid H, Bussmann P, Wulf-Goldenberg A,Eckert K, Heider W, Jensen J, Edsbagge J, Björquist P, Jozefczuk J, Adjaye J, Zeilinger K and Gerlach JC. In vitro teratoma formation of human embryonic stem cells in 3D perfusion culture bioreactors [in preparation]

Jozefczuk J*, Stachelscheid H*, Chavez L*, Herwig R, Lehrach H, Zeilinger K, Gerlach J and Adjaye J. Molecular characterization of cultured adult human liver progenitor cells. [in preparation]
*equal contribution

7.1 Poster presentations

Stachelscheid H, Bussmann P, Ring A, Wulf-Goldenberg A, Eckert K, Fichtner I, Zeilinger K, Gerlach JC. Spontaneous Differentiation of Human Embryonic Stem Cells in 3D Perfusion Bioreactors. 2nd International Congress on Stem Cells and Tissue Formation Dresden July 2008

Urbaniak T, Stachelscheid H, Knöspel F, Gerlach J, Zeilinger K. Enhanced Proliferation of human adult liver progenitor cells under culture conditions supporting human embryonic stem cell propagartion. 2nd International Congress on Stem Cells and Tissue Formation Dresden July 2008

Keil M, Siegert A, Wulf-Goldenberg A, Heider W, Stachelscheid H, Zeilinger K, Eckert K, Fichtner I. In vitro/ in vivo differentiation potential of human embryonic H1 and SA002 stem cells. 2nd International Congress on Stem Cells and Tissue Formation Dresden July 2008

Urbaniak T, Stachelscheid H, Gerlach JC, Zeilinger K. Proliferation of hepatic progenitors isolated from adult human liver in coculture with mouse embryonic fibroblasts. 2nd Biennial Leopoldina Conference and Final Meeting of the Stem Cell Priority Program 1109 of the German Research Foundation (DFG) Dresden Sep 2006

Stachelscheid H, Urbaniak T, Gerlach JC, Zeilinger K. Characterization of two distinct proliferating liver epithelial cells isolated from liver tissue after ischemic treatment. 3rd International Meeting of the Stem Cell Network North Rhine Westphalia, Münster May 2005

Stachelscheid H, Zeilinger K, Katenz E, Gast B, Neuhaus P, Gerlach JC. Effect of Ischemic Treatment of Human Liver Tissue on the Subsequent Isolation of Adult Liver Stem Cells. Z Gastroenterol 43; 2005: 96.

Stachelscheid H, Zeilinger K, Katenz E, Neuhaus P, Gerlach JC. Development of a new method for the isolation of adult human liver stem cells. Int J Artif Organs 2005; 28: 414 - 415

Efimova E, Zeilinger K, Sauer IM, Pless G, Mieder T, Kehr D, Roth S, Stachelscheid H, Schwartlander R, Becker C, Rossberg I, Gerlach JC, Neuhaus P. Collagenase P versus Liberase perfusion for large-scale isolation of primary liver cells from discarded human grafts. Z Gastroenterol 42; 2004: 85.

Stachelscheid H, Gast B, Zeilinger K, Gerlach JC, Neuhaus P. Entwicklung einer Zeitraffer¬mikroskopiemethode zur Untersuchung des Wachstumsverhaltens humaner adulter Leberstammzellen in vitro. Z Gastroenterol 41; 2003: 110.

Efimova E, Zeilinger K, Sauer IM, Pless G, Mieder T, Kehr D, Roth S, Stachelscheid H, Hwang YJ, Becker C, Neuhaus P, Gerlach JC. Large-scale isolation of priming human liver cells originating from discarded grafts. Int J Artif Organs 2003; 26(7): 656.

8 References

Abranches, E., E. Bekman, D. Henrique and J. M. S. Cabral (2007). "Expansion of mouse embryonic stem cells on microcarriers." Biotechnology and Bioengineering **96**(6): 1211-21.

Adewumi, O., B. Aflatoonian, L. Ahrlund-Richter, M. Amit, P. W. Andrews, G. Beighton, P. A. Bello, N. Benvenisty, L. S. Berry, S. Bevan, B. Blum, J. Brooking, K. G. Chen, A. B. H. Choo, G. A. Churchill, M. Corbel, I. Damjanov, J. S. Draper, P. Dvorak, K. Emanuelsson, R. A. Fleck, A. Ford, K. Gertow, M. Gertsenstein, P. J. Gokhale, R. S. Hamilton, A. Hampl, L. E. Healy, O. Hovatta, J. Hyllner, M. P. Imreh, J. Itskovitz-Eldor, J. Jackson, J. L. Johnson, M. Jones, K. Kee, B. L. King, B. B. Knowles, M. Lako, F. Lebrin, B. S. Mallon, D. Manning, Y. Mayshar, R. D. G. McKay, A. E. Michalska, M. Mikkola, M. Mileikovsky, S. L. Minger, H. D. Moore, C. L. Mummery, A. Nagy, N. Nakatsuji, C. M. O'Brien, S. K. W. Oh, C. Olsson, T. Otonkoski, K.-Y. Park, R. Passier, H. Patel, M. Patel, R. Pedersen, M. F. Pera, M. S. Piekarczyk, R. A. R. Pera, B. E. Reubinoff, A. J. Robins, J. Rossant, P. Rugg-Gunn, T. C. Schulz, H. Semb, E. S. Sherrer, H. Siemen, G. N. Stacey, M. Stojkovic, H. Suemori, J. Szatkiewicz, T. Turetsky, T. Tuuri, S. van den Brink, K. Vintersten, S. Vuoristo, D. Ward, T. A. Weaver, L. A. Young and W. Zhang (2007). "Characterization of human embryonic stem cell lines by the International Stem Cell Initiative." Nature Biotechnology **25**(7): 803-16.

Agarwal, S., K. L. Holton and R. Lanza (2008). "Efficient differentiation of functional hepatocytes from human embryonic stem cells." Stem Cells **26**(5): 1117-27.

Aleckovic, M. and C. Simon (2008). "Is teratoma formation in stem cell research a characterization tool or a window to developmental biology?" Reprod Biomed Online **17**(2): 270-80.

Amit, M., M. K. Carpenter, M. S. Inokuma, C. P. Chiu, C. P. Harris, M. A. Waknitz, J. Itskovitz-Eldor and J. A. Thomson (2000). "Clonally derived human embryonic stem cell lines maintain pluripotency and proliferative potential for prolonged periods of culture." Dev Biol **227**(2): 271 - 278.

Amit, M., V. Margulets, H. Segev, K. Shariki, I. Laevsky, R. Coleman and J. Itskovitz-Eldor (2003). "Human feeder layers for human embryonic stem cells." Biol Reprod **68**(6): 2150 - 2156.

Arias, I. M. and J. L. Boyer (2001). The liver : biology and pathobiology. Philadelphia ; London, Lippincott Williams & Wilkins.

Asahina, K., K. Teramoto and H. Teraoka (2006). "Embryonic stem cells: hepatic differentiation and regenerative medicine for the treatment of liver disease." Curr Stem Cell Res Ther **1**(2): 139-56.

Baharvand, H., S. M. Hashemi, S. Kazemi Ashtiani and A. Farrokhi (2006). "Differentiation of human embryonic stem cells into hepatocytes in 2D and 3D culture systems in vitro." Int J Dev Biol **50**(7): 645-52.

Bar, H., S. V. Strelkov, G. Sjoberg, U. Aebi and H. Herrmann (2004). "The biology of desmin filaments: how do mutations affect their structure, assembly, and organisation?" J Struct Biol **148**(2): 137-52.

Basma, H., A. S.-G. rrez, G. R. Yannam, L. Liu, R. Ito, T. Yamamoto, E. Ellis, S. D. Carson, S. Sato, Y. Chen, D. Muirhead, N. N.-. lvarez, R. J. Wong, J. Roy-Chowdhury, J. L. Platt, D. F. Mercer, J. D. Miller, S. C. Strom, N. Kobayashi and I. J. Fox (2008). "Differentiation and Transplantation of Human Embryonic Stem Cell-Derived Hepatocytes." Gastroenterology.

Beattie, G. M., A. D. Lopez, N. Bucay, A. Hinton, M. T. Firpo, C. C. King and A. Hayek (2005). "Activin A maintains pluripotency of human embryonic stem cells in the absence of feeder layers." Stem Cells **23**(4): 489-95.

Ben-Shushan, E., J. R. Thompson, L. J. Gudas and Y. Bergman (1998). "Rex-1, a gene encoding a transcription factor expressed in the early embryo, is regulated via Oct-3/4 and Oct-6 binding to an octamer site and a novel protein, Rox-1, binding to an adjacent site." Mol Cell Biol **18**(4): 1866-78.

Bigdeli, N., M. Andersson, R. Strehl, K. Emanuelsson, E. Kilmare, J. Hyllner and A. Lindahl (2008). "Adaptation of human embryonic stem cells to feeder-free and matrix-free culture conditions directly on plastic surfaces." J Biotechnol **133**(1): 146-53.

Blum, B. and N. Benvenisty (2008). "The tumorigenicity of human embryonic stem cells." Adv Cancer Res **100**: 133-58.

Braam, S. R., C. Denning, E. Matsa, L. E. Young, R. Passier and C. L. Mummery (2008). "Feeder-free culture of human embryonic stem cells in conditioned medium for efficient genetic modification." Nat Protoc **3**(9): 1435-43.

Bradley, A., M. Evans, M. H. Kaufman and E. Robertson (1984). "Formation of germ-line chimaeras from embryo-derived teratocarcinoma cell lines." Nature **309**(5965): 255-6.

Buitrago, W. and D. R. Roop (2007). "Oct-4: the almighty POUripotent regulator?" J Invest Dermatol **127**(2): 260-2.

Cai, J., Y. Zhao, Y. Liu, F. Ye, Z. Song, H. Qin, S. Meng, Y. Chen, R. Zhou, X. Song, Y. Guo, M. Ding and H. Deng (2007). "Directed differentiation of human embryonic stem cells into functional hepatic cells." Hepatology **45**(5): 1229-39.

Catalina, P., R. Montes, G. Ligero, L. Sanchez, T. de la Cueva, C. Bueno, P. E. Leone and P. Menendez (2008). "Human ESCs predisposition to karyotypic instability: Is a matter of culture adaptation or differential vulnerability among hESC lines due to inherent properties?" Mol Cancer **7**: 76.

Chen, Y. G., Q. Wang, S. L. Lin, C. D. Chang, J. Chuang and S. Y. Ying (2006). "Activin signaling and its role in regulation of cell proliferation, apoptosis, and carcinogenesis." Exp Biol Med (Maywood) **231**(5): 534-44.

Cheng, L., H. Hammond, Z. Ye, X. Zhan and G. Dravid (2003). "Human adult marrow cells support prolonged expansion of human embryonic stem cells in culture." Stem Cells **21**(2): 131 - 142.

Choo, A., A. S. Ngo, V. Ding, S. Oh and L. S. Kiang (2008). "Autogeneic feeders for the culture of undifferentiated human embryonic stem cells in feeder and feeder-free conditions." Methods in Cell Biology **86**: 15-28.

Come, J., X. Nissan, L. Aubry, J. Tournois, M. Girard, A. L. Perrier, M. Peschanski and M. Cailleret (2008). "Improvement of Culture Conditions of Human Embryoid Bodies Using

a Controlled Perfused and Dialyzed Bioreactor System." Tissue Engineering. Part C, Methods.

Conrad, S., M. Renninger, J. Hennenlotter, T. Wiesner, L. Just, M. Bonin, W. Aicher, H. J. Buhring, U. Mattheus, A. Mack, H. J. Wagner, S. Minger, M. Matzkies, M. Reppel, J. Hescheler, K. D. Sievert, A. Stenzl and T. Skutella (2008). "Generation of pluripotent stem cells from adult human testis." Nature **456**(7220): 344-9.

Cooke, M. J., M. Stojkovic and S. A. Przyborski (2006). "Growth of teratomas derived from human pluripotent stem cells is influenced by the graft site." Stem Cells Dev **15**(2): 254-9.

D'Amour, K. A., A. D. Agulnick, S. Eliazer, O. G. Kelly, E. Kroon and E. E. Baetge (2005). "Efficient differentiation of human embryonic stem cells to definitive endoderm." Nat Biotechnol **23**(12): 1534-41.

Daheron, L., S. L. Opitz, H. Zaehres, M. W. Lensch, P. W. Andrews, J. Itskovitz-Eldor and G. Q. Daley (2004). "LIF/STAT3 signaling fails to maintain self-renewal of human embryonic stem cells." Stem Cells **22**(5): 770-8.

Dang, S. M., S. Gerecht-Nir, J. Chen, J. Itskovitz-Eldor and P. W. Zandstra (2004). "Controlled, scalable embryonic stem cell differentiation culture." Stem Cells **22**(3): 275-82.

Dang, S. M., M. Kyba, R. Perlingeiro, G. Q. Daley and P. W. Zandstra (2002). "Efficiency of embryoid body formation and hematopoietic development from embryonic stem cells in different culture systems." Biotechnol Bioeng **78**(4): 442-53.

Davie, J. R. (2003). "Inhibition of Histone Deacetylase Activity by Butyrate." J. Nutr. **133**(7): 2485S-2493-2485S-2493.

Dennis, G., Jr., B. T. Sherman, D. A. Hosack, J. Yang, W. Gao, H. C. Lane and R. A. Lempicki (2003). "DAVID: Database for Annotation, Visualization, and Integrated Discovery." Genome Biol **4**(5): P3.

Dono, R. (2003). "Fibroblast growth factors as regulators of central nervous system development and function." Am J Physiol Regul Integr Comp Physiol **284**(4): R867-81.

Dvash, T., D. Ben-Yosef and R. Eiges (2006). "Human embryonic stem cells as a powerful tool for studying human embryogenesis." Pediatr Res **60**(2): 111-7.

Ellerstrom, C., R. Strehl, K. Noaksson, J. Hyllner and H. Semb (2007). "Facilitated Expansion of Human Embryonic Stem Cells by Single-Cell Enzymatic Dissociation." Stem Cells **25**(7): 1690-1696.

Evans, M. J. and M. H. Kaufman (1981). "Establishment in culture of pluripotential cells from mouse embryos." Nature **292**(5819): 154-6.

Fernandes, A. M., T. G. Fernandes, M. M. Diogo, C. L. da Silva, D. Henrique and J. M. S. Cabral (2007). "Mouse embryonic stem cell expansion in a microcarrier-based stirred culture system." Journal of Biotechnology **132**(2): 227-36.

Fok, E. Y. L. and P. W. Zandstra (2005). "Shear-Controlled Single-Step Mouse Embryonic Stem Cell Expansion and Embryoid Body-Based Differentiation." Stem Cells **23**(9): 1333-1342.

Fong, W. J., H. L. Tan, A. Choo and S. K. Oh (2005). "Perfusion cultures of human embryonic stem cells." Bioprocess Biosyst Eng **27**(6): 381-7.

Gallicano, G. I., N. Golestaneh, M. Kokkinaki, D. Pant, J. Jiang, D. Destefano, C. Fernandez-Bueno, J. D. Rome, B. R. Haddad and M. Dym (2009). "Pluripotent Stem Cells Derived from Adult Human Testes." Stem Cells Dev.

Genbacev, O., A. Krtolica, T. Zdravkovic, E. Brunette, S. Powell, A. Nath, E. Caceres, M. McMaster, S. McDonagh, Y. Li, R. Mandalam, J. Lebkowski and S. J. Fisher (2005). "Serum-free derivation of human embryonic stem cell lines on human placental fibroblast feeders." Fertil Steril **83**(5): 1517 - 1529.

Gentleman, R. C., V. J. Carey, D. M. Bates, B. Bolstad, M. Dettling, S. Dudoit, B. Ellis, L. Gautier, Y. Ge, J. Gentry, K. Hornik, T. Hothorn, W. Huber, S. Iacus, R. Irizarry, F. Leisch, C. Li, M. Maechler, A. J. Rossini, G. Sawitzki, C. Smith, G. Smyth, L. Tierney, J. Y. H. Yang and J. Zhang (2004). "Bioconductor: open software development for computational biology and bioinformatics." Genome Biology **5**(10): R80-R80.

Gerecht-Nir, S., S. Cohen and J. Itskovitz-Eldor (2004). "Bioreactor cultivation enhances the efficiency of human embryoid body (hEB) formation and differentiation." Biotechnol Bioeng **86**(5): 493-502.

Gerlach, J. C., J. Encke, O. Hole, C. M ller, C. J. Ryan and P. Neuhaus (1994). "Bioreactor for a larger scale hepatocyte in vitro perfusion." Transplantation **58**(9): 984-8.

Gerlach, J. C., K. Mutig, I. M. Sauer, P. Schrade, E. Efimova, T. Mieder, G. Naumann, A. Grunwald, G. Pless, A. Mas, S. Bachmann, P. Neuhaus and K. Zeilinger (2003). "Use of primary human liver cells originating from discarded grafts in a bioreactor for liver support therapy and the prospects of culturing adult liver stem cells in bioreactors: a morphologic study." Transplantation **76**(5): 781-6.

Gerlach, J. C., N. Schnoy, J. Encke, M. D. Smith, C. Müller and P. Neuhaus (1995). "Improved hepatocyte in vitro maintenance in a culture model with woven multicompartment capillary systems: electron microscopy studies." Hepatology **22**(2): 546-52.

Gertow, K., S. Wolbank, B. r. Rozell, R. Sugars, M. AndÃ¤ng, C. L. Parish, M. P. Imreh, M. Wendel and L. Ahrlund-Richter (2004). "Organized development from human embryonic stem cells after injection into immunodeficient mice." Stem Cells and Development **13**: 421-35.

Gilyarov, A. V. (2008). "Nestin in central nervous system cells." Neurosci Behav Physiol **38**(2): 165-9.

Ginis, I., Y. Luo, T. Miura, S. Thies, R. Brandenberger, S. Gerecht-Nir, M. Amit, A. Hoke, M. K. Carpenter, J. Itskovitz-Eldor and M. S. Rao (2004). "Differences between human and mouse embryonic stem cells." Dev Biol **269**(2): 360-80.

Gonzalez, R., J. F. Loring and E. Y. Snyder (2008). "Preparation of autogenic human feeder cells for growth of human embryonic stem cells." Curr Protoc Stem Cell Biol **Chapter 1**: Unit 1C 5 1-1C 5 15.

Greber, B., H. Lehrach and J. Adjaye (2007). "Fibroblast growth factor 2 modulates transforming growth factor beta signaling in mouse embryonic fibroblasts and human ESCs (hESCs) to support hESC self-renewal." Stem Cells **25**(2): 455-64.

Gremo, F. and M. Presta (2000). "Role of fibroblast growth factor-2 in human brain: a focus on development." Int J Dev Neurosci **18**(2-3): 271-9.

Hanson, C. and G. Caisander (2005). "Human embryonic stem cells and chromosome stability." APMIS **113**(11-12): 751-5.

Hay, D. C., D. Zhao, J. Fletcher, Z. A. Hewitt, D. McLean, A. Urruticoechea-Uriguen, J. R. Black, C. Elcombe, J. A. Ross, R. Wolf and W. Cui (2008). "Efficient differentiation of hepatocytes from human embryonic stem cells exhibiting markers recapitulating liver development in vivo." Stem Cells **26**(4): 894-902.

Hay, D. C., D. Zhao, A. Ross, R. Mandalam, J. Lebkowski and W. Cui (2007). "Direct differentiation of human embryonic stem cells to hepatocyte-like cells exhibiting functional activities." Cloning Stem Cells **9**(1): 51-62.

Heins, N., M. C. O. Englund, C. Sjoblom, U. Dahl, A. Tonning, C. Bergh, A. Lindahl, C. Hanson and H. Semb (2004). "Derivation, Characterization, and Differentiation of Human Embryonic Stem Cells." Stem Cells **22**(3): 367-376.

Heng, B. C., H. Yu, Y. Yin, S. G. Lim and T. Cao (2005). "Factors influencing stem cell differentiation into the hepatic lineage in vitro." J Gastroenterol Hepatol **20**(7): 975-87.

Hines, R. N. and D. G. McCarver (2002). "The ontogeny of human drug-metabolizing enzymes: phase I oxidative enzymes." J Pharmacol Exp Ther **300**(2): 355-60.

Hornstein, E. and N. Benvenisty (2004). "The "brainy side" of human embryonic stem cells." J Neurosci Res **76**(2): 169-73.

Hsu, Y. C., D. C. Lee and I. M. Chiu (2007). "Neural stem cells, neural progenitors, and neurotrophic factors." Cell Transplant **16**(2): 133-50.

Hubner, G., C. Alzheimer and S. Werner (1999). "Activin: a novel player in tissue repair processes." Histol Histopathol **14**(1): 295-304.

Humphrey, R. K., G. M. Beattie, A. D. Lopez, N. Bucay, C. C. King, M. T. Firpo, S. Rose-John and A. Hayek (2004). "Maintenance of pluripotency in human embryonic stem cells is STAT3 independent." Stem Cells **22**(4): 522-30.

Hwang, Y.-S., J. Cho, F. Tay, J. Y. Y. Heng, R. Ho, S. G. Kazarian, D. R. Williams, A. R. Boccaccini, J. M. Polak and A. Mantalaris (2009). "The use of murine embryonic stem cells, alginate encapsulation, and rotary microgravity bioreactor in bone tissue engineering." Biomaterials **30**(4): 499-507.

Inanc, B., A. E. Elcin and Y. M. Elcin (2008). "Human Embryonic Stem Cell Differentiation on Tissue Engineering Scaffolds: Effects of NGF and Retinoic Acid Induction." Tissue Eng Part A.

Ito, M., H. Nagata, S. Miyakawa and I. J. Fox (2009). "Review of hepatocyte transplantation." J Hepatobiliary Pancreat Surg **16**(2): 97-100.

Itskovitz-Eldor, J., M. Schuldiner, D. Karsenti, A. Eden, O. Yanuka, M. Amit, H. Soreq and N. Benvenisty (2000). "Differentiation of human embryonic stem cells into embryoid bodies compromising the three embryonic germ layers." Molecular Medicine **6**(2): 88?95-88?95.

James, D., A. J. Levine, D. Besser and A. Hemmati-Brivanlou (2005). "TGFbeta/activin/nodal signaling is necessary for the maintenance of pluripotency in human embryonic stem cells." Development **132**(6): 1273-82.

Jensen, J., J. Hyllner and P. Bjorquist (2009). "Human embryonic stem cell technologies and drug discovery." J Cell Physiol **219**(3): 513-9.

Joannides, A., C. Fiore-Heriche, K. Westmore, M. Caldwell, A. Compston, N. Allen and S. Chandran (2006). "Automated Mechanical Passaging: A Novel and Efficient Method for Human Embryonic Stem Cell Expansion." Stem Cells **24**(2): 230-235.

Kamiya, A., T. Kinoshita and A. Miyajima (2001). "Oncostatin M and hepatocyte growth factor induce hepatic maturation via distinct signaling pathways." FEBS Letters **492**(1-2): 90-4.

Katsetos, C. D., M. M. Herman and S. J. Mork (2003). "Class III beta-tubulin in human development and cancer." Cell Motil Cytoskeleton **55**(2): 77-96.

Katsetos, C. D., A. Legido, E. Perentes and S. J. Mork (2003). "Class III beta-tubulin isotype: a key cytoskeletal protein at the crossroads of developmental neurobiology and tumor neuropathology." J Child Neurol **18**(12): 851-66; discussion 867.

Kim, B. G., D. H. Hwang, S. I. Lee, E. J. Kim and S. U. Kim (2007). "Stem cell-based cell therapy for spinal cord injury." Cell Transplant **16**(4): 355-64.

Kinoshita, T. and A. Miyajima (2002). "Cytokine regulation of liver development." Biochimica Et Biophysica Acta **1592**(3): 303-12.

Koestenbauer, S., N. H. Zech, H. Juch, P. Vanderzwalmen, L. Schoonjans and G. Dohr (2006). "Embryonic stem cells: similarities and differences between human and murine embryonic stem cells." Am J Reprod Immunol **55**(3): 169-80.

Kossack, N., J. Meneses, S. Shefi, H. N. Nguyen, S. Chavez, C. Nicholas, J. Gromoll, P. J. Turek and R. A. Reijo-Pera (2008). "Isolation and Characterization of Pluripotent Human Spermatogonial Stem Cell-Derived Cells." Stem Cells.

Kubo, A., K. Shinozaki, J. M. Shannon, V. Kouskoff, M. Kennedy, S. Woo, H. J. Fehling and G. Keller (2004). "Development of definitive endoderm from embryonic stem cells in culture." Development **131**(7): 1651-1662.

Kuhn, K., S. C. Baker, E. Chudin, M. H. Lieu, S. Oeser, H. Bennett, P. Rigault, D. Barker, T. K. McDaniel and M. S. Chee (2004). "A novel, high-performance random array platform for quantitative gene expression profiling." Genome Res **14**(11): 2347-56.

Lavon, N., O. Yanuka and N. Benvenisty (2004). "Differentiation and isolation of hepatic-like cells from human embryonic stem cells." Differentiation **72**(5): 230-8.

Lees, J. G., S. A. Lim, T. Croll, G. Williams, S. Lui, J. Cooper-White, L. R. McQuade, B. Mathiyalagan and B. E. Tuch (2007). "Transplantation of 3D scaffolds seeded with human embryonic stem cells: biological features of surrogate tissue and teratoma-forming potential." Regenerative Medicine **2**(3): 289-300.

Lemaigre, F. and K. S. Zaret (2004). "Liver development update: new embryo models, cell lineage control, and morphogenesis." Curr Opin Genet Dev **14**(5): 582-90.

Levenberg, S., N. F. Huang, E. Lavik, A. B. Rogers, J. Itskovitz-Eldor and R. Langer (2003). "Differentiation of human embryonic stem cells on three-dimensional polymer scaffolds." Proceedings of the National Academy of Sciences of the United States of America **100**(22): 12741-6.

Li, Y., D. A. Kniss, L. C. Lasky and S.-T. Yang (2003). "Culturing and differentiation of murine embryonic stem cells in a three-dimensional fibrous matrix." Cytotechnology **41**(1): 23-35.

Li, Y., S. Powell, E. Brunette, J. Lebkowski and R. Mandalam (2005). "Expansion of human embryonic stem cells in defined serum-free medium devoid of animal-derived products." Biotechnol. Bioeng. **91**(6): 688 - 698.

Lo, C. M., C. R. Keese and I. Giaever (1994). "pH changes in pulsed CO2 incubators cause periodic changes in cell morphology." Experimental Cell Research **213**(2): 391-7.

Lowry, W. E., L. Richter, R. Yachechko, A. D. Pyle, J. Tchieu, R. Sridharan, A. T. Clark and K. Plath (2008). "Generation of human induced pluripotent stem cells from dermal fibroblasts." Proc Natl Acad Sci U S A **105**(8): 2883-8.

Ludwig, T. E., M. E. Levenstein, J. M. Jones, W. T. Berggren, E. R. Mitchen, J. L. Frane, L. J. Crandall, C. A. Daigh, K. R. Conard, M. S. Piekarczyk, R. A. Llanas and J. A. Thomson (2006). "Derivation of human embryonic stem cells in defined conditions." Nat. Biotechnol. **24**(2): 185 - 187.

Maherali, N., R. Sridharan, W. Xie, J. Utikal, S. Eminli, K. Arnold, M. Stadtfeld, R. Yachechko, J. Tchieu, R. Jaenisch, K. Plath and K. Hochedlinger (2007). "Directly reprogrammed fibroblasts show global epigenetic remodeling and widespread tissue contribution." Cell Stem Cell **1**(1): 55-70.

Maitra, A., D. E. Arking, N. Shivapurkar, M. Ikeda, V. Stastny, K. Kassauei, G. Sui, D. J. Cutler, Y. Liu, S. N. Brimble, K. Noaksson, J. Hyllner, T. C. Schulz, X. Zeng, W. J. Freed, J. Crook, S. Abraham, A. Colman, P. Sartipy, S. Matsui, M. Carpenter, A. F. Gazdar, M. Rao and A. Chakravarti (2005). "Genomic alterations in cultured human embryonic stem cells." Nat Genet **37**(10): 1099-103.

Martin, G. R. (1981). "Isolation of a pluripotent cell line from early mouse embryos cultured in medium conditioned by teratocarcinoma stem cells." Proc Natl Acad Sci U S A **78**(12): 7634-8.

Martin, M. J., A. Muotri, F. Gage and A. Varki (2005). "Human embryonic stem cells express an immunogenic nonhuman sialic acid." Nat Med **11**(2): 228-32.

Matsumoto, K., H. Mizumoto, K. Nakazawa, H. Ijima, K. Funatsu and T. Kajiwara (2008). "Hepatic Differentiation of Mouse Embryonic Stem Cells in a Bioreactor Using Polyurethane/Spheroid Culture." Transplantation Proceedings **40**(2): 614-616.

Matsumoto, K., H. Yoshitomi, J. Rossant and K. S. Zaret (2001). "Liver organogenesis promoted by endothelial cells prior to vascular function." Science **294**(5542): 559-63.

McLean, A. B., K. A. D'Amour, K. L. Jones, M. Krishnamoorthy, M. J. Kulik, D. M. Reynolds, A. M. Sheppard, H. Liu, Y. Xu, E. E. Baetge and S. Dalton (2007). "Activin A Efficiently Specifies Definitive Endoderm from Human Embryonic Stem Cells Only When Phosphatidylinositol 3-Kinase Signaling Is Suppressed." Stem Cells **25**(1): 29-38.

McLin, V. A., S. A. Rankin and A. M. Zorn (2007). "Repression of Wnt/{beta}-catenin signaling in the anterior endoderm is essential for liver and pancreas development." Development **134**(12): 2207-2217.

Mizejewski, G. J. (2004). "Biological roles of alpha-fetoprotein during pregnancy and perinatal development." Exp Biol Med (Maywood) **229**(6): 439-63.

Nakagawa, M., M. Koyanagi, K. Tanabe, K. Takahashi, T. Ichisaka, T. Aoi, K. Okita, Y. Mochiduki, N. Takizawa and S. Yamanaka (2008). "Generation of induced pluripotent stem cells without Myc from mouse and human fibroblasts." Nat Biotechnol **26**(1): 101-6.

Narkilahti, S., K. Rajala, H. Pihlajamaki, R. Suuronen, O. Hovatta and H. Skottman (2007). "Monitoring and analysis of dynamic growth of human embryonic stem cells: comparison of automated instrumentation and conventional culturing methods." BioMedical Engineering OnLine **6**(1): 11-11.

Nie, Y., V. Bergendahl, D. J. Hei, J. M. Jones and S. P. Palecek (2009). "Scalable culture and cryopreservation of human embryonic stem cells on microcarriers." Biotechnol Prog **25**(1): 20-31.

Niebruegge, S., A. Nehring, H. B„r, M. Schroeder, R. Zweigerdt and J. Lehmann (2008). "Cardiomyocyte production in mass suspension culture: embryonic stem cells as a source for great amounts of functional cardiomyocytes." Tissue Engineering. Part A **14**(10): 1591-601.

Odorico, J. S., D. S. Kaufman and J. A. Thomson (2001). "Multilineage differentiation from human embryonic stem cell lines." Stem Cells **19**(3): 193-204.

Okita, K., T. Ichisaka and S. Yamanaka (2007). "Generation of germline-competent induced pluripotent stem cells." Nature **448**(7151): 313-7.

Ouyang, A. and S.-T. Yang (2008). "A two-stage perfusion fibrous bed bioreactor system for mass production of embryonic stem cells." Expert Opinion on Biological Therapy **8**(7): 895-909.

Pan, G. and J. A. Thomson (2007). "Nanog and transcriptional networks in embryonic stem cell pluripotency." Cell Res **17**(1): 42-9.

Park, I. H., R. Zhao, J. A. West, A. Yabuuchi, H. Huo, T. A. Ince, P. H. Lerou, M. W. Lensch and G. Q. Daley (2008). "Reprogramming of human somatic cells to pluripotency with defined factors." Nature **451**(7175): 141-6.

Pellizzer, C., S. Bremer and T. Hartung (2005). "Developmental toxicity testing from animal towards embryonic stem cells." ALTEX **22**(2): 47-57.

Pera, M. F. and A. O. Trounson (2004). "Human embryonic stem cells: prospects for development." Development **131**(22): 5515-25.

Phillips, B. W., R. Horne, T. S. Lay, W. L. Rust, T. T. Teck and J. M. Crook (2008). "Attachment and growth of human embryonic stem cells on microcarriers." Journal of Biotechnology **138**(1-2): 24-32.

Przyborski, S. A. (2005). "Differentiation of human embryonic stem cells after transplantation in immune-deficient mice." Stem Cells **23**(9): 1242-50.

Rambhatla, L., C. P. Chiu, P. Kundu, Y. Peng and M. K. Carpenter (2003). "Generation of hepatocyte-like cells from human embryonic stem cells." Cell Transplant **12**(1): 1-11.

Rao, M. (2004). "Conserved and divergent paths that regulate self-renewal in mouse and human embryonic stem cells." Dev Biol **275**(2): 269-86.

Reubinoff, B. E., P. Itsykson, T. Turetsky, M. F. Pera, E. Reinhartz, A. Itzik and T. Ben-Hur (2001). "Neural progenitors from human embryonic stem cells." Nat Biotechnol **19**(12): 1134-40.

Richards, M., S. Tan, C.-Y. Fong, A. Biswas, W.-K. Chan and A. Bongso (2003). "Comparative evaluation of various human feeders for prolonged undifferentiated growth of human embryonic stem cells." Stem Cells **21**(5): 546 - 556.

Saeed, A. I., V. Sharov, J. White, J. Li, W. Liang, N. Bhagabati, J. Braisted, M. Klapa, T. Currier, M. Thiagarajan, A. Sturn, M. Snuffin, A. Rezantsev, D. Popov, A. Ryltsov, E. Kostukovich, I. Borisovsky, Z. Liu, A. Vinsavich, V. Trush and J. Quackenbush (2003). "TM4: a free, open-source system for microarray data management and analysis." BioTechniques **34**(2): 374-8.

Sartipy, P., P. Bjorquist, R. Strehl and J. Hyllner (2007). "The application of human embryonic stem cell technologies to drug discovery." Drug Discov Today **12**(17-18): 688-99.

Sauer, I. M., K. Zeilinger, G. Pless, D. Kardassis, T. Theruvath, A. Pascher, M. Goetz, P. Neuhaus and J. C. Gerlach (2003). "Extracorporeal liver support based on primary human liver cells and albumin dialysis--treatment of a patient with primary graft non-function." J Hepatol **39**(4): 649-53.

Schmelzer, E., K. Mutig, P. Schrade, S. Bachmann, J. C. Gerlach and K. Zeilinger (2009). "Effect of human patient plasma ex vivo treatment on gene expression and progenitor cell activation of primary human liver cells in multi-compartment 3D perfusion bioreactors for extra-corporeal liver support." Biotechnol Bioeng.

Schroeder, M., S. Niebruegge, A. Werner, E. Willbold, M. Burg, M. Ruediger, L. J. Field, J. Lehmann and R. Zweigerdt (2005). "Differentiation and lineage selection of mouse embryonic stem cells in a stirred bench scale bioreactor with automated process control." Biotechnol Bioeng **92**(7): 920-33.

Schuldiner, M., O. Yanuka, J. Itskovitz-Eldor, D. A. Melton and N. Benvenisty (2000). "Effects of eight growth factors on the differentiation of cells derived from human embryonic stem cells." Proc. Natl. Acad. Sci. USA **97**(21): 11307 - 11312.

Schwartz, P. H., D. J. Brick, A. E. Stover, J. F. Loring and F.-J. Müller (2008). "Differentiation of neural lineage cells from human pluripotent stem cells." Methods **45**(2): 142-158.

Schwartz, R. E., J. L. Linehan, M. S. Painschab, W.-S. Hu, C. M. Verfaillie and D. S. Kaufman (2005). "Defined conditions for development of functional hepatic cells from human embryonic stem cells." Stem Cells and Development **14**(6): 643-55.

Schwartz, R. E., J. L. Linehan, M. S. Painschab, W. S. Hu, C. M. Verfaillie and D. S. Kaufman (2005). "Defined conditions for development of functional hepatic cells from human embryonic stem cells." Stem Cells Dev **14**(6): 643-55.

Sejersen, T. and U. Lendahl (1993). "Transient expression of the intermediate filament nestin during skeletal muscle development." J Cell Sci **106 (Pt 4)**: 1291-300.

Shih, C. C., Y. Weng, A. Mamelak, T. LeBon, M. C. Hu and S. J. Forman (2001). "Identification of a candidate human neurohematopoietic stem-cell population." Blood **98**(8): 2412-22.

Shirahashi, H., J. Wu, N. Yamamoto, A. Catana, H. Wege, B. Wager, K. Okita and M. A. Zern (2004). "Differentiation of human and mouse embryonic stem cells along a hepatocyte lineage." Cell Transplant **13**(3): 197-211.

Shiraki, N., K. Umeda, N. Sakashita, M. Takeya, K. Kume and S. Kume (2008). "Differentiation of mouse and human embryonic stem cells into hepatic lineages." Genes to Cells: Devoted to Molecular & Cellular Mechanisms **13**(7): 731-46.

Snykers, S., J. De Kock, V. Rogiers and T. Vanhaecke (2008). "In vitro differentiation of embryonic and adult stem cells into hepatocytes: state of the art." Stem Cells: stemcells.2008-0963-stemcells.2008-0963.

Soto-Gutierrez, A., N. Navarro-Alvarez, J. D. Rivas-Carrillo, Y. Chen, T. Yamatsuji, N. Tanaka and N. Kobayashi (2006). "Differentiation of human embryonic stem cells to hepatocytes using deleted variant of HGF and poly-amino-urethane-coated nonwoven polytetrafluoroethylene fabric." Cell Transplant **15**(4): 335-41.

Stenman, U. H., A. Tiitinen, H. Alfthan and L. Valmu (2006). "The classification, functions and clinical use of different isoforms of HCG." Hum Reprod Update **12**(6): 769-84.

Stojkovic, P., M. Lako, R. Stewart, S. Przyborski, L. Armstrong, J. Evans, A. Murdoch, T. Strachan and M. Stojkovic (2005). "An autogeneic feeder cell system that efficiently supports growth of undifferentiated human embryonic stem cells." Stem Cells **23**(3): 306-14.

Takahashi, K., K. Tanabe, M. Ohnuki, M. Narita, T. Ichisaka, K. Tomoda and S. Yamanaka (2007). "Induction of pluripotent stem cells from adult human fibroblasts by defined factors." Cell **131**(5): 861-72.

Takahashi, K. and S. Yamanaka (2006). "Induction of pluripotent stem cells from mouse embryonic and adult fibroblast cultures by defined factors." Cell **126**(4): 663-76.

Terstegge, S., I. Laufenberg, J. Pochert, S. Schenk, J. Itskovitz-Eldor, E. Endl and O. Brüstle (2007). "Automated maintenance of embryonic stem cell cultures." Biotechnology and Bioengineering **96**(1): 195-201.

Thomson, J. A., J. Itskovitz-Eldor, S. S. Shapiro, M. A. Waknitz, J. J. Swiergiel, V. S. Marshall and J. M. Jones (1998). "Embryonic stem cell lines derived from human blastocysts." Science **282**(5391): 1145-7.

Thomson, J. A., J. Kalishman, T. G. Golos, M. Durning, C. P. Harris, R. A. Becker and J. P. Hearn (1995). "Isolation of a primate embryonic stem cell line." Proceedings of the National Academy of Sciences of the United States of America **92**(17): 7844-8.

Valbuena, D., A. Galán, E. Sánchez, M. E. Poo, E. Gómez, S. Sánchez-Luengo, D. Melguizo, A. García, V. Ruiz, R. Moreno, A. Pellicer and C. Simón (2006). "Derivation and characterization of three new Spanish human embryonic stem cell lines (VAL -3 -4 -5) on human feeder and in serum-free conditions." Reproductive Biomedicine Online **13**(6): 875-86.

Vallier, L., M. Alexander and R. A. Pedersen (2005). "Activin/Nodal and FGF pathways cooperate to maintain pluripotency of human embryonic stem cells." J. Cell Sci. **118**(Pt - 19): 4495 - 4509.

Veraitch, F. S., R. Scott, J.-W. Wong, G. J. Lye and C. Mason (2008). "The impact of manual processing on the expansion and directed differentiation of embryonic stem cells." Biotechnology and Bioengineering **99**(5): 1216-1229.

Wang, L., T. C. Schulz, E. S. Sherrer, D. S. Dauphin, S. Shin, A. M. Nelson, C. B. Ware, M. Zhan, C. Z. Song, X. Chen, S. N. Brimble, A. McLean, M. J. Galeano, E. W. Uhl, K. A.

D'Amour, J. D. Chesnut, M. S. Rao, C. A. Blau and A. J. Robins (2007). "Self-renewal of human embryonic stem cells requires insulin-like growth factor-1 receptor and ERBB2 receptor signaling." Blood **110**(12): 4111-9.

Wernig, M., A. Meissner, R. Foreman, T. Brambrink, M. Ku, K. Hochedlinger, B. E. Bernstein and R. Jaenisch (2007). "In vitro reprogramming of fibroblasts into a pluripotent ES-cell-like state." Nature **448**(7151): 318-24.

Xiao, L., X. Yuan and S. J. Sharkis (2006). "Activin A maintains self-renewal and regulates fibroblast growth factor, Wnt, and bone morphogenic protein pathways in human embryonic stem cells." Stem Cells **24**(6): 1476-86.

Xie, C. Q., G. Lin, D. Yuan, J. Wang, T. C. Liu and G. X. Lu (2005). "Proliferative feeder cells support prolonged expansion of human embryonic stem cells." Cell Biol Int **29**(8): 623-8.

Xie, J., S. M. Willerth, X. Li, M. R. Macewan, A. Rader, S. E. Sakiyama-Elbert and Y. Xia (2009). "The differentiation of embryonic stem cells seeded on electrospun nanofibers into neural lineages." Biomaterials **30**(3): 354-362.

Xu, C., M. S. Inokuma, J. Denham, K. Golds, P. Kundu, J. D. Gold and M. K. Carpenter (2001). "Feeder-free growth of undifferentiated human embryonic stem cells." Nat Biotechnol **19**(10): 971-4.

Xu, C., J. Jiang, V. Sottile, J. McWhir, J. Lebkowski and M. K. Carpenter (2004). "Immortalized fibroblast-like cells derived from human embryonic stem cells support undifferentiated cell growth." Stem Cells **22**(6): 972-80.

Xu, C., E. Rosler, J. Jiang, J. S. Lebkowski, J. D. Gold, C. O'Sullivan, K. Delavan-Boorsma, M. Mok, A. Bronstein and M. K. Carpenter (2005). "Basic fibroblast growth factor supports undifferentiated human embryonic stem cell growth without conditioned medium." Stem Cells **23**(3): 315 - 323.

Xu, R.-H., R. M. Peck, D. S. Li, X. Feng, T. Ludwig and J. A. Thomson (2005). "Basic FGF and suppression of BMP signaling sustain undifferentiated proliferation of human ES cells." Nat Methods **2**(3): 185 - 190.

Xu, R. H., X. Chen, D. S. Li, R. Li, G. C. Addicks, C. Glennon, T. P. Zwaka and J. A. Thomson (2002). "BMP4 initiates human embryonic stem cell differentiation to trophoblast." Nat Biotechnol **20**(12): 1261-4.

Yin, C.-H., W. Chen, C.-C. Hsiao, C.-Y. Kuo, C.-L. Chen and W.-T. Wu (2007). "Production of mouse embryoid bodies with hepatic differentiation potential by stirred tank bioreactor." Bioscience, Biotechnology, and Biochemistry **71**(3): 728-34.

Ying, Q. L., J. Nichols, I. Chambers and A. Smith (2003). "BMP induction of Id proteins suppresses differentiation and sustains embryonic stem cell self-renewal in collaboration with STAT3." Cell **115**(3): 281-92.

Yoo, S. J., B. S. Yoon, J. M. Kim, J. M. Song, S. Roh, S. You and H. S. Yoon (2005). "Efficient culture system for human embryonic stem cells using autologous human embryonic stem cell-derived feeder cells." Exp Mol Med **37**(5): 399-407.

Yu, J., M. A. Vodyanik, K. Smuga-Otto, J. Antosiewicz-Bourget, J. L. Frane, S. Tian, J. Nie, G. A. Jonsdottir, V. Ruotti, R. Stewart, Slukvin, II and J. A. Thomson (2007). "Induced pluripotent stem cell lines derived from human somatic cells." Science **318**(5858): 1917-20.

Zaret, K. S. and M. Grompe (2008). "Generation and Regeneration of Cells of the Liver and Pancreas." Science **322**(5907): 1490-1494.

Zeilinger, K., I. M. Sauer, G. Pless, C. Strobel, J. Rudzitis, A. Wang, A. K. Nussler, A. Grebe, L. Mao, S. H. Auth, J. Unger, P. Neuhaus and J. C. Gerlach (2002). "Three-dimensional co-culture of primary human liver cells in bioreactors for in vitro drug studies: effects of the initial cell quality on the long-term maintenance of hepatocyte-specific functions." Altern Lab Anim **30**(5): 525-38.

Zhang, F. and K. B. Pasumarthi (2008). "Embryonic stem cell transplantation: promise and progress in the treatment of heart disease." BioDrugs **22**(6): 361-74.

Zhang, L., N. Theise, M. Chua and L. M. Reid (2008). "The stem cell niche of human livers: symmetry between development and regeneration." Hepatology **48**(5): 1598-607.

Zulewski, H., E. J. Abraham, M. J. Gerlach, P. B. Daniel, W. Moritz, B. Muller, M. Vallejo, M. K. Thomas and J. F. Habener (2001). "Multipotential nestin-positive stem cells isolated from adult pancreatic islets differentiate ex vivo into pancreatic endocrine, exocrine, and hepatic phenotypes." Diabetes **50**(3): 521-33.

zur Nieden, N. I., J. T. Cormier, D. E. Rancourt and M. S. Kallos (2007). "Embryonic stem cells remain highly pluripotent following long term expansion as aggregates in suspension bioreactors." Journal of Biotechnology **129**(3): 421-32.

9 Appendix

9.1 Overview of published protocols for hepatic differentiation of human embryonic stem cells

Table 6: Overview of published protocols for hepatic differentiation of hESC

(Used abbreviations: D: Culture Day, HCM: hepatocyte culture medium, DEX: dexametasone, DMSO: dimethyl sulfoxide, ICG: Indocyanine green, IHC: immunhistochemistry, ITS: insulin-transferring-selenium, KO-DMEM: KnockOut Dulbecco's Modified Eagle Medium, L-Glu: l-glutamine, ß-ME: beta-mercaptoethanol, NaB: sodium butyrate, NEAA: non essential amino acids, SQ: Single Quots [Ascorbic Acid, BSA-FAF, Transferrin, Insulin, hEGF, GA-1000, Hydrocortisone], SR: SerumReplacer)

Differentiation Protocol (Media, Growth Factors, Cytokines)		Matrix/ Feeder	Examined Markers	Described Cell Functions	Refs
H1 + H9 Feeder free culture ***a)*** KO-DMEM 20% FBS 1% NEAA 1 mM L-Glu 0.1 mM ß-ME **D-4-0:** EB formation **D0-5:** 5mM NaB or 1% DMSO	***b)*** KO-DMEM 20% FBS 1% NEAA 1 mM glutamine 0,1 mM ß-mercatoethanol **D0-4:** 1% DMSO **D4-10:** 2,5mM NaB **D10-14:** HCM 2,5mM NaB 2,5 ng/ml HGF	Matrigel	IHC, RT-PCR: **+:** ALB, AAT, AGRP, HNF-4, TTR, C/EBPa, C/EBPß, CK18, CK8 **-:** AFP	Glycogen storage (PAS) ALB synthesis CYP1A2 activity (EROD assay)	(Rambhatla et al. 2003)
RPMI 1640 **D1-3:** 0.5 mg/ml albumin fraction V 100 ng/ml Activin A **D2-3:** 0.5 mg/ml albumin fraction V 100 ng/ml Activin A 0.1% or 1% ITS **D3-8:** HCM+SQ 30 ng/ml FGF4 20 ng/ml BMP2	**D8-13:** HCM+SQ 20 ng/ml HGF **D13-18:** HCM+SQ 10 ng/ml OSM 0.1 µM Dexametason *EGF was omitted from HCM!!*	MEF	IHC, RT-PCR: **+:** AFP, ALB, CK8 CK18, G6P, AAT, HNF-4α, PEPCK, TDO2, TAT, CYP7A1, CYP3A4, CYP2B6	LDL uptake ICG uptake Glycogen storage (PAS) CYP450 activity (PROD) ALB secretion	(Cai et al. 2007)
KO-DMEM 20% FCS 2 mM L-Glu 1%NEAA 0.1 mM ß-ME **D0-5:** EB formation	***a)*** **D9-12:** 100ng/ml aFGF **D12-20:** 20ng/ml HGF **D15-20:** 10^{-7}M DEX 10ng/ml OSM 5mg/ml insulin 5mg/ml transferrin 5µg/ml selenium ***b)*** No growth factors	3D collagen scaffold Or 2D collagen	RT-PCR: ***a)*** CK19, CK18, CK8, TTR, ALB, α1AT, TO, TAT, G6P, CYP7A1 ***b)*** **+:** AFP, CK19, TTR, α1AT, CK8, CK18, ALB **-:** G6P, TAT	1) AFP, ALB and Urea production, ICG uptake Glycogen storage (PAS) 2) Low AFP, ALB, urea production	(Baharvand et al. 2006)
D0-4: conditioned medium (feeder free) 8 ng/ml bFGF -> grown to 70% confluence **D4-11:** unconditioned medium 1% DMSO	**D11-20:** HCM +SQ 2.5 or 10 ng/ml HGF **D20-24:** HCM+SQ 10 ng/ml HGF 10 ng/ml Oncostatin M	Matrigel	IHC+RT-PCR: **+:** AFP, ALB, AAT, TODO2, HNF4α, C/EBPα, TTR, SOX 17, c-met, E-Cad, Hepar1 **-:** Oct4, hTERT, SOX7	ICG uptake glycogen storage (PAS) CYP3A4 activity (testosterone metabolism) Alb + AFP secretion	(Hay et al. 2007)

Differentiation Protocol (Media, Growth Factors, Cytokines)		Matrix/ Feeder	Examined Markers	Described Cell Functions	Refs
hESC lines H1, H7 feeder free ~70% confluent **D1-2:** RPMI1640 1x B27 Supplement 1 mM NaB 100ng/ml activin A **D2-3:** RPMI1640 1x B27 0.5 mM NaB 100ng/ml activin A **D3-10:** KO-DMEM 20% SR 1mM L-Glu 1% NEAA 0.1mM β-ME 1% DMSO	**D10-17:** CL15 medium L15 medium supplemented 8.3% FCS 8.3% tryptose phosphate broth 10 µM Hydrocortisone 21-hemisuccinate 1 µM insulin 2 mM L-Glu 10 ng/ml HGF 20 ng/ml Oncostatin M	Matrigel	IHC, RT-PCR: **+:** HNF3β, HNF1/4α, AFP, ALB, TAT, TTR, CAR, ApoF, CK7, CK18, CK19, c-Met, E-Cad, CYP3A4/7, CYP2C9/19 **-:** Nanog, hTERT, Brachy, GSC, SOX17, PAX6, CXCR4, HNF6,	Glycogen storage ALB/ fibrinogen/ fibronectin/ A2M secretion inducible CYP activity	(Hay et al. 2008)
DMEM **D0-7:** EB formation **D7-21:** serumfree basal medium FGF4 HGF		Collagen I	IHC, RT-PCR: HNF3β, GATA4, HNF1, CK18	Urea, ALB production, phenobarbital-induced CYP450 activity ICG uptake	(Schwartz et al. 2005)
RPMI1640+ **D0-D3:** 0.5%FBS 100 ng/ml Activin A **D3-D5:** 1% SR 100 ng/ml Activin A **D5-D8:** 2%SR 10 ng/ml FGF4 10 ng/ml HGF	**D8-D11:** MDBK-MM medium 0.5 mg/ml BSA 10 ng/ml FGF4 10 ng/ml HGF **D11-D20:** HCM medium 10 ng/ml FGF4 10 ng/ml HGF, 10 ng/ml OSM 7-11 M DEX	**>D5:** Collagen I	IHC+PT-PCR **D11-D20:** +: GATA4, HNF4, AFP, ALB DPPIV,α1AT **D20:** +: CYP7A1, CYP3A4	Glycogen storage (PAS) ICG uptake ALB secretion	(Agarwal et al. 2008)
D-5-0: *EB formation* DMEM/F12 10%FCS **D0-3:** 100 ng/ml bFGF **D3-11:** 100 ng/ml HGF 1% DMSO **D11-14:** 10^{-7} M DEX		PAU-coated nonwoven PTFE	RT-PCR: ALB	Lidocaine metabolism ALB + Urea production Ammonia uptake	(Soto-Gutierrez et al. 2006)
hESC line KhES-1 DMEM w. 4.5g/lglucose 10% KSR, NEAA, L-Glu, ß-ME **D0-D10:** 20ng/ml activin A 10µM LY294002 (PI3 kinase inhibitor)	**D10-D50:** 10ng/ml HGF, DEX	inactive meso-nephric cells (line M15)	ICC+RT-PCR: **D18:** +: Sox17, 80% AFP, ALB, CK7/18/19, CYP7A1 **D18-50:** ↑ALB, ↓AFP, CYP3A4, OATP1B1	Glycogen storage (PAS)	(Shiraki et al. 2008)
DMEM 20%FBS 100nM DEX, ITS **D0-6:** EB formation **D6-43:** maturation		Collagen I	RT-PCR: AAT, ALB	ALB secretion	(Shirahashi et al. 2004)

Differentiation Protocol (Media, Growth Factors, Cytokines)		Matrix/ Feeder	Examined Markers	Described Cell Functions	Refs
KO-DMEM 20% SR 1 mM L-Glu 0.1 mM ß-ME 1% NEAA **D0-20:** EB formation 1.	**D20-30:** EBs separately added: 2. 100ng/ml aFGF 3. 5ng/ml bFGF 4. HGF (20ng/ml) 5. BMP4 (50ng/ml) Hep conditioned medium		IHC, RT-PCR: **+:** AFP, APOA4, FGA, APOB, FGB, FGG, ALB, APOH **-:** APOF, ADH1C Alb-eGFP transfection ->only aFGF improved hepatic differentiation		(Lavon et al. 2004)
DMEM/F12 **D0-2:** Embryonic bodies (EBs) 15% SR, 1 mM NEAA L-Glu **D2-5:** 100 ng/ml Activin A 100 ng/m bFGF D3: 0.2% FCS D4: 2% FCS	**D5-13:** 10% FCS or SR 1 mM NEAA L-Glu 1% DMSO 100 ng/mL HGF **D13-16:** 10%FCS or SR 1 mM NEAA L-Glu 10^{-7}M DEX	Matrigel	IHC, RT-PCR: **+:** AFP, ALB, ASGPR 1, CF VII, CYP1A1,1A2, 3A4, 2B6 and 7A1 **-:** OCT4,Nanog	ALB, Urea, A1A production CYP1A2 activity (EROD assay) CYP3A activity (testosterone metabolism) Engraftment and functional activity after transplantation into mice	(Basma et al. 2008)

9.2 Compositions media used in the hepatic differentiation experiments

Table 7: Medium compositions used in the hepatic differentiation experiments

Concentration		Component	Manufacturer
hESC culture medium			
		Knockout DMEM	Invitrogen
1	%	Glutamax-I	Invitrogen
1	%	NEAA	Biochrom
20	%	Knockout SerumReplacer	Invitrogen
50	µg/ml	Gentamycin	Biochrom
0.1	mM	ß Mercaptoethanol	Sigma Aldrich
10	ng/ml	bFGF	PeproTec
HepDiff-1			
		RPMI Advanced medium	Invitrogen
1	%	Glutamax-I	Invitrogen
4	ng/ml	bFGF	PeproTec
100	ng/ml	Activin A	PeproTec
50	µg/ml	Gentamycin	Biochrom
HepDiff-2			
		RPMI Advanced medium	Invitrogen
1	%	Glutamax-I	Invitrogen
0.20	%	FCS (Heat-Inactivated)	Invitrogen
4	ng/ml	bFGF	PeproTec
100	ng/ml	Activin A	PeproTec
50	µg/ml	Gentamycin	Biochrom
HepDiff-3			
		RPMI Advanced Medium	Biochrom
1	%	Glutamax-I	Invitrogen
100	ng/ml	aFGF	PeproTec
5	ng/ml	bFGF	PeproTec
50	ng/ml	BMP2	PeproTec
200	ng/ml	BMP4	PeproTec
0.2	%	FCS (Heat-Inactivated)	Invitrogen
50	µg/ml	Gentamycin	Biochrom
HepDiff-4			
		Williams E (Phenol red free)	Biochrom
1x	/500ml	SingleQuots	Lonza, Basel, Switzerland
1	%	Glutamax	Invitrogen
1000	mg/l	D-Galactose	Sigma Aldrich
1000	mg/l	D-Sorbitol	Sigma Aldrich
20	ng/ml	HGF	PeproTec
2	ng/ml	bFGF	PeproTec
50	µg/ml	Gentamycin	Biochrom
HepDiff-5			
		Williams E (Phenol red free)	Biochrom
1x	/500ml	SingleQuots	Lonza
1	%	Glutamax	Invitrogen
1000	mg/l	D-Galactose	Sigma Aldrich
1000	mg/l	D-Sorbitol	Sigma Aldrich
10	ng/ml	Oncostatin M	PeproTec
2	ng/ml	HGF	PeproTec
2	ng/ml	bFGF	PeproTec
0.1	µM	Dexametasone	Sigma Aldrich
50	µg/ml	Gentamycin	Biochrom

(**SingleQuots** consist of hEGF, Transferrin, Hydrocortisone, BSA, Ascorbic Acid, Insulin with proprietary concentrations)

Table 8: Details of the measurement methods of soluble factors measured in the medium

Factor	Measurement Kit (+manufacturer if different to instrument manufacturer)	Instrument	Instrument manufacturer	Detection range (min-max)	Test principle
α-fetoprotein (AFP)	AFP	ARCHITECT	Abbott Diagnostics Division, Sligo, Ireland	0,4-350 ng/ml	Chemiluminescent Microparticle Immunoassay (CMIA)
alkaline phosphatase (ALP)	ALP	MODULAR	Roche Diagnostics GmbH, Mannheim, Germany	2-12000 U/l	colorimetric assay in accordiance with a standardized method
alanine transaminase (ALT)	ALT (ALAT/GPT)	MODULAR PPP	Roche Diagnostics GmbH, Mannheim, Germany	4-6600 U/l	UV test according to a standardized method
ammonia	NH3L	COBAS e601	Roche Diagnostics GmbH, Mannheim, Germany	10-700 µmol/l	enzymatical in vitro test
aspartate transaminase (AST)	AST (ASAT/GOT)	MODULAR PPP	Roche Diagnostics GmbH, Mannheim, Germany	4-8800 U/l	UV test according to a standardized method
beta-human chorionic gonadotropin (ß-hCG)	HCG+ß	COBAS e601	Roche Diagnostics GmbH, Mannheim, Germany	0,100-10000 mIU/ml	Sandwich principle
c-peptide	C-Peptide	IMMULITE	Siemens Medical Solutions Diagostics, Llanberis, United Kingdom	0,1-20 ng/ml	solid-phase, two-site chemiluminescent immunometric assay
carcinoembryonic antigen (CEA)	CEA	ARCHITECT	Abbott Diagnostics Division, Sligo, Ireland	0-1,500 ng/ml	Chemiluminescent Microparticle Immunoassay (CMIA)
cytokeratin fragment 19 (Cyfra 21-1)	CYFRA 21-1	ELECSYS 2010	Roche Diagnostics GmbH, Mannheim, Germany	0,100-500 ng/ml	electrochemi-luminescence immunoassay "ECLIA"
erythropoetin	EPO	IMMULITE	Siemens Medical Solutions Diagostics, Llanberis, United Kingdom	1-200 mIU/ml	solid-phase, two-site chemiluminescent immunometric assay
estradiol	ESTRADIOL II	COBAS e601	Roche Diagnostics GmbH, Mannheim, Germany	18,4-15781 pmol/l	Competition principle
follicle stimulating hormone (FSH)	FSH	COBAS e601	Roche Diagnostics GmbH, Mannheim, Germany	0,100-200 IU/l	Sandwich principle
Factor XIII	F XIII; Dade Behring GmbH, Marburg, Germany	KONELAB	Thermo Fisher Scientific, Dreieich, Germany	70-140 %	F XIII contained in the sample is converted by the action of thrombin into F XIIIa
Factor X	STA Factor X	STA evolution	Roche Diagnostics GmbH, Mannheim, Germany	1-200%	The assay consists of the maesurement of the clotting time, in the presence of the STA Neoplastin Plus reagent, of a system in which all the coagulation factors are present, constant and in excess (supplied by STA Factor X) except factor X which is derived from the sample being tested.

Factor	Measurement Kit (+manufacturer if different to instrument manufacturer)	Instrument	Instrument manufacturer	Detection range (min-max)	Test principle
Factor V	STA Factor V	STA evolution	Roche Diagnostics GmbH, Mannheim, Germany	3,5-200%	The assay consist of the measurement of the clotting time, in the presence of the STA Neoplastin Plus reagent, of a system in which all the factors are present, constant and in excess (supplied by STA Factor V) except factor V which is derived from the sample being tested.
Factor II	STA Factor II	STA evolution	Roche Diagnostics GmbH, Mannheim, Germany	2-150%	The assay consist of the measurement of the clotting time, in the presence of the STA Neoplastin Plus reagent, of a system in which all the factors are present, constant and in excess (supplied by STA Factor II) except factor II which is derived from the sample being tested
fibrinogen	STA Fibrinogen	STA evolution	Roche Diagnostics GmbH, Mannheim, Germany	1,5-9,0 g/l	In the presence of excess thrombin, the coagulation time of a diluted plasma sample is inversely proportional to the fibrinogen concentration.
gamma-glutamyltransferase (GGT)	GGT	MODULAR PPP	Roche Diagnostics GmbH, Mannheim, Germany	4-13200 U/l	Enzymatic colorimetric assay
galactose	Lactose/D-Galactose ; Boehringer Mannheim/R-Biopharm AD, Darmstadt, Germany	COBAS MIRA	Roche Diagnostics GmbH, Mannheim, Germany	0-250 mg/dl	UV-method
glucose	GLU	MODULAR PPP	Roche Diagnostics GmbH, Mannheim, Germany	2-1650 mg/dl	UV test
glutamate dehydrogenase (GLDH)	GLDH	MODULAR PPP	Roche Diagnostics GmbH, Mannheim, Germany	1-400 U/l	UV test according to a standardized method
insulin	Insulin	IMMULITE	Siemens Medical Solutions Diagostics, Llanberis, United Kingdom	2-300 µlU/ml	solid-phase, two-site chemiluminescent immunometric assay
lactate	Lactate	MODULAR PPP	Roche Diagnostics GmbH, Mannheim, Germany	0-210 mg/dl	L-lactate is oxidized to pyruvate by the specific enzyme lactate oxidase (LCD)
lactate dehydrogenase (LDH)	LDH	MODULAR PPP	Roche Diagnostics GmbH, Mannheim, Germany	10-4000 U/l	UV-assay
luteinizing hormone (LH)	LH	COBAS e601	Roche Diagnostics GmbH, Mannheim, Germany	0,100-200 mIU/ml	Sandwich principle

Factor	Measurement Kit (+manufacturer if different to instrument manufacturer)	Instrument	Instrument manufacturer	Detection range (min-max)	Test principle
neuron-specific enolase (NSE)	NSE	ELECSYS 2010	Roche Diagnostics GmbH, Mannheim, Germany	0,050-370 ng/ml	Sandwich principle
osmolality	hand-operated or handmade	Osmomat 030	Gonotec, Berlin, Germany	0-3000 mOsmol/kg	The total osmolality of an aqueous solution is determined by comparing the freezing point of pure water and the freezing point of the sample.
osteocalcin	Osteocalcin	IMMULITE	Siemens Medical Solutions Diagostics, Llanberis, United Kingdom	2-100 ng/ml	solid-phase, two-site chemiluminescent immunometric assay
pseudocholinesterase (PCHE or cholinesterase II)	CHE2	MODULAR PPP	Roche Diagnostics GmbH, Mannheim, Germany	0,05-70000 U/l	Colorimetric assay
prealbumin	Prealbumin (Transthyretin); DakoCytomation, Glostrup, Denmark	KONELAB	Thermo Fisher Scientific, Bonn, Germany	0,06-1,4 g/L	The resulting immune complexes are measured by turbidimetry or nephelometry
progesterone	Progesterone II	COBAS e601	Roche Diagnostics GmbH, Mannheim, Germany	0,030-60,00 ng/ml	Competition principle
prolactin	Prolactin II	COBAS e601	Roche Diagnostics GmbH, Mannheim, Germany	1-10000 µU/ml	Sandwich principle
S-100	S100	LIAISON	DiaSorin, Dietzenbach, Germany	0,02-30 µg/l	Sandwich principle
sorbitol	D-Sorbit / Xylit ; Boehringer Mannheim/R-Biopharm AD, Darmstadt, Germany	COBAS MIRA	Roche Diagnostics GmbH, Mannheim, Germany	0-200 mg/dl	Colorimetric method
thyroid-stimulating hormone (TSH)	TSH	COBAS e601	Roche Diagnostics GmbH, Mannheim, Germany	0,005-100,0 µIU/ml	Sandwich principle
tissue polypeptide antigen (TPA)	TPA	LIAISON	DiaSorin, Dietzenbach, Germany	2-4000 U/l	two-site chemiluminescent immunometric assay
transferrin	Transferrin ver.2	MODULAR PPP	Roche Diagnostics GmbH, Mannheim, Germany	25-1040 mg/dl	Immunoturbidimetric assay
urea	UREA/BUN	MODULAR PPP	Roche Diagnostics GmbH, Mannheim, Germany	5-600 mg/dl	Kinatic UV assay

9.3 Additional analysis results of the microarray data

9.3.1 Correlogram

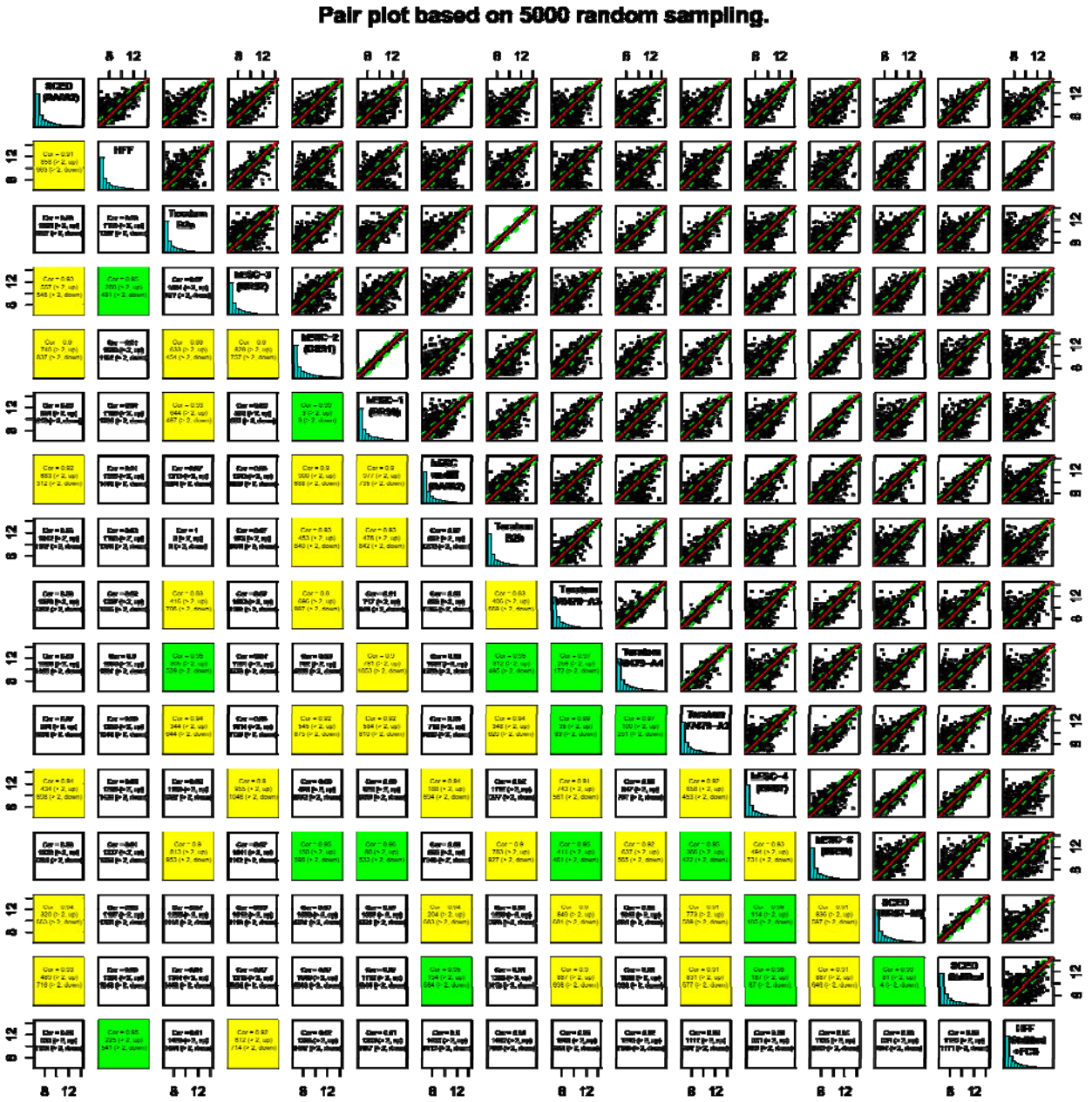

Figure 33: Pair wise scatter plot of the analyzed samples. Sample correlation coefficients ≥0.95 are marked in green and correlation coefficients ≥0.90 are marked in yellow.

9.3.2 Additional results of functional annotation clustering analysis

Table 9: Functional annotation clustering of genes expressed in the group of bioreactors hESC-1, -2 and -5 (terms describing neuronal differentiation are highlighted in yellow)

Category	Term	Count	PValue	Fold Enrichment
Functional Group 1				
GOTERM_BP_ALL	GO:0007275~multicellular organismal development	102	4.98E-08	1.6885397
GOTERM_BP_ALL	GO:0032502~developmental process	130	5.14E-08	1.54972099
GOTERM_BP_ALL	GO:0048856~anatomical structure development	94	1.65E-07	1.69776644
GOTERM_BP_ALL	GO:0048731~system development	81	2.01E-07	1.78964327
GOTERM_BP_ALL	GO:0007399~nervous system development	46	3.00E-07	2.2932814
GOTERM_BP_ALL	GO:0032501~multicellular organismal process	136	6.31E-06	1.40689181
GOTERM_BP_ALL	GO:0048869~cellular developmental process	76	2.57E-05	1.61054048
GOTERM_BP_ALL	GO:0030154~cell differentiation	76	2.57E-05	1.61054048
GOTERM_BP_ALL	GO:0048513~organ development	56	1.05E-04	1.69861174
Functional Group 2				
SP_PIR_KEYWORDS	Homeobox	20	7.88E-06	3.38650708
INTERPRO	IPR001356:Homeobox	18	4.07E-05	3.26622129
INTERPRO	IPR012287:Homeodomain-related	18	8.22E-05	3.08630232
GOTERM_MF_ALL	GO:0003700~transcription factor activity	46	1.01E-04	1.83219094
UP_SEQ_FEATURE	DNA-binding region:Homeobox	15	1.15E-04	3.44194899
SMART	SM00389:HOX	18	4.52E-04	2.64576961
GOTERM_MF_ALL	GO:0043565~sequence-specific DNA binding	26	0.00305713	1.88520443
INTERPRO	IPR000047:Helix-turn-helix motif, lambda-like repressor	7	0.00806517	3.98949251
Functional Group 3				
GOTERM_BP_ALL	GO:0007399~nervous system development	46	3.00E-07	2.2932814
GOTERM_BP_ALL	GO:0048699~generation of neurons	23	5.72E-06	3.09473961
GOTERM_BP_ALL	GO:0030182~neuron differentiation	21	7.30E-06	3.26643038
GOTERM_BP_ALL	GO:0022008~neurogenesis	23	1.91E-05	2.86660175
GOTERM_BP_ALL	GO:0007417~central nervous system development	19	1.37E-04	2.84167478
GOTERM_BP_ALL	GO:0007420~brain development	14	2.49E-04	3.40253165
GOTERM_BP_ALL	GO:0000904~cellular morphogenesis during differentiation	13	7.81E-04	3.19948726
GOTERM_BP_ALL	GO:0001764~neuron migration	7	0.00135359	5.67088608
GOTERM_BP_ALL	GO:0048667~neuron morphogenesis during differentiation	12	0.00144201	3.17437355
GOTERM_BP_ALL	GO:0048812~neurite morphogenesis	12	0.00144201	3.17437355
GOTERM_BP_ALL	GO:0007409~axonogenesis	11	0.00311839	3.07731536
GOTERM_BP_ALL	GO:0031175~neurite development	12	0.00391061	2.79420905
GOTERM_BP_ALL	GO:0016477~cell migration	16	0.00442613	2.29585688
GOTERM_BP_ALL	GO:0000902~cell morphogenesis	24	0.00501725	1.87027219
GOTERM_BP_ALL	GO:0032989~cellular structure morphogenesis	24	0.00501725	1.87027219
GOTERM_BP_ALL	GO:0032990~cell part morphogenesis	14	0.00782453	2.31661729
GOTERM_BP_ALL	GO:0030030~cell projection organization and biogenesis	14	0.00782453	2.31661729
GOTERM_BP_ALL	GO:0048858~cell projection morphogenesis	14	0.00782453	2.31661729
GOTERM_BP_ALL	GO:0007411~axon guidance	7	0.00787345	4.00297841
GOTERM_BP_ALL	GO:0048666~neuron development	12	0.01125044	2.41778711
GOTERM_BP_ALL	GO:0051674~localization of cell	18	0.04408981	1.66258757
GOTERM_BP_ALL	GO:0006928~cell motility	18	0.04408981	1.66258757
Functional Group 4				
GOTERM_BP_ALL	GO:0007267~cell-cell signaling	35	9.37E-05	2.05902066
GOTERM_BP_ALL	GO:0019226~transmission of nerve impulse	23	9.83E-05	2.57005674
GOTERM_BP_ALL	GO:0007268~synaptic transmission	19	8.98E-04	2.43037975
GOTERM_BP_ALL	GO:0003008~system process	47	0.08516785	1.25095522
GOTERM_BP_ALL	GO:0050877~neurological system process	37	0.16379567	1.2141644
Functional Group 5				
GOTERM_BP_ALL	GO:0045664~regulation of neuron differentiation	7	5.14E-05	10.0815752
GOTERM_BP_ALL	GO:0045595~regulation of cell differentiation	13	8.26E-04	3.1793647
GOTERM_BP_ALL	GO:0050793~regulation of developmental process	17	0.00109749	2.55236792
GOTERM_BP_ALL	GO:0045665~negative regulation of neuron differentiation	4	0.00310122	12.9620253
GOTERM_BP_ALL	GO:0051093~negative regulation of developmental process	8	0.00835563	3.45654008
GOTERM_BP_ALL	GO:0045596~negative regulation of cell differentiation	7	0.01173272	3.67841259
GOTERM_BP_ALL	GO:0045597~positive regulation of cell differentiation	5	0.0342138	4.05063291
GOTERM_BP_ALL	GO:0051094~positive regulation of developmental process	6	0.03738362	3.24050633

Table 10: Functional annotation clustering of genes commonly expressed in the group of bioreactors hESC-1, -2 and -5 and teratomas (terms describing neuronal differentiation are highlighted in yellow)

Category	Term	Count	PValue	Fold Enrichment
Functional Group 1				
GOTERM_BP_ALL	GO:0007399~nervous system development	90	5.59E-19	2.79985417
GOTERM_BP_ALL	GO:0007275~multicellular organismal development	168	1.17E-13	1.73545665
GOTERM_BP_ALL	GO:0048731~system development	136	2.38E-13	1.87505386
GOTERM_BP_ALL	GO:0048856~anatomical structure development	153	4.02E-12	1.72438766
GOTERM_BP_ALL	GO:0032502~developmental process	205	2.77E-11	1.52495634
GOTERM_BP_ALL	GO:0032501~multicellular organismal process	210	4.10E-07	1.3556091
GOTERM_BP_ALL	GO:0009653~anatomical structure morphogenesis	76	2.61E-05	1.6276881
GOTERM_BP_ALL	GO:0048513~organ development	79	2.87E-04	1.49529393
GOTERM_BP_ALL	GO:0030154~cell differentiation	102	0.00128151	1.34881258
GOTERM_BP_ALL	GO:0048869~cellular developmental process	102	0.00128151	1.34881258
Functional Group 2				
GOTERM_BP_ALL	GO:0000904~cellular morphogenesis during differentiation	24	1.30E-07	3.68588398
GOTERM_BP_ALL	GO:0048812~neurite morphogenesis	23	1.48E-07	3.79662766
GOTERM_BP_ALL	GO:0048667~neuron morphogenesis during differentiation	23	1.48E-07	3.79662766
GOTERM_BP_ALL	GO:0007409~axonogenesis	22	2.41E-07	3.84056736
GOTERM_BP_ALL	GO:0048699~generation of neurons	33	3.56E-07	2.77078994
GOTERM_BP_ALL	GO:0031175~neurite development	24	3.61E-07	3.48724352
GOTERM_BP_ALL	GO:0048666~neuron development	26	3.72E-07	3.26891437
GOTERM_BP_ALL	GO:0030030~cell projection organization and biogenesis	29	4.35E-07	2.99445397
GOTERM_BP_ALL	GO:0032990~cell part morphogenesis	29	4.35E-07	2.99445397
GOTERM_BP_ALL	GO:0048858~cell projection morphogenesis	29	4.35E-07	2.99445397
GOTERM_BP_ALL	GO:0030182~neuron differentiation	29	1.53E-06	2.81478673
GOTERM_BP_ALL	GO:0022008~neurogenesis	33	1.94E-06	2.56653299
GOTERM_BP_ALL	GO:0009653~anatomical structure morphogenesis	76	2.61E-05	1.6276881
GOTERM_BP_ALL	GO:0007411~axon guidance	12	9.50E-05	4.28212991
GOTERM_BP_ALL	GO:0000902~cell morphogenesis	40	9.63E-05	1.94512247
GOTERM_BP_ALL	GO:0032989~cellular structure morphogenesis	40	9.63E-05	1.94512247
GOTERM_BP_ALL	GO:0016477~cell migration	23	0.00192318	2.05942533
GOTERM_BP_ALL	GO:0051674~localization of cell	30	0.00473785	1.72912609
GOTERM_BP_ALL	GO:0006928~cell motility	30	0.00473785	1.72912609
GOTERM_BP_ALL	GO:0048468~cell development	69	0.00949469	1.34482956
Functional Group 3				
INTERPRO	IPR001356:Homeobox	26	3.44E-06	2.90990624
INTERPRO	IPR012287:Homeodomain-related	26	9.40E-06	2.74961479
SP_PIR_KEYWORDS	Homeobox	26	1.23E-05	2.70548933
SMART	SM00389:HOX	26	5.70E-05	2.44521927
UP_SEQ_FEATURE	DNA-binding region:Homeobox	19	1.08E-04	2.86086826
GOTERM_MF_ALL	GO:0043565~sequence-specific DNA binding	37	0.00522602	1.60889354
GOTERM_MF_ALL	GO:0003700~transcription factor activity	56	0.02283621	1.33764665
Functional Group 4				
GOTERM_MF_ALL	GO:0043167~ion binding	224	5.00E-05	1.25824575
GOTERM_MF_ALL	GO:0043169~cation binding	205	9.80E-05	1.26391199
GOTERM_MF_ALL	GO:0046872~metal ion binding	214	4.04E-04	1.22576986
INTERPRO	IPR007087:Zinc finger, C2H2-type	51	0.00129857	1.58513093
SP_PIR_KEYWORDS	zinc-finger	88	0.00764316	1.3041335
SP_PIR_KEYWORDS	zinc	100	0.0356543	1.20285448
GOTERM_MF_ALL	GO:0008270~zinc ion binding	113	0.05585337	1.16289665
SP_PIR_KEYWORDS	metal-binding	125	0.0704334	1.13916994
GOTERM_MF_ALL	GO:0046914~transition metal ion binding	132	0.09197855	1.12112348
Functional Group 5				
INTERPRO	IPR001849:Pleckstrin-like	24	7.55E-04	2.17026452
INTERPRO	IPR011993:Pleckstrin homology-type	24	0.00303537	1.95111729
SMART	SM00233:PH	24	0.00633323	1.82369197
UP_SEQ_FEATURE	domain:PH	13	0.02102132	2.09927938

Table 11: Functional annotation clustering of genes expressed in the group of teratomas

Category	Term	Count	PValue	Fold Enrichment
Functional Group 1				
GOTERM_CC_ALL	GO:0005576~extracellular region	62	4.40E-05	1.6975464
GOTERM_CC_ALL	GO:0005615~extracellular space	27	0.0019794	1.9155336
GOTERM_CC_ALL	GO:0044421~extracellular region part	36	0.00500321	1.62473424
Functional Group 2				
GOTERM_BP_ALL	GO:0032501~multicellular organismal process	138	3.04E-06	1.42038955
GOTERM_BP_ALL	GO:0007275~multicellular organismal development	89	1.40E-04	1.46591132
GOTERM_BP_ALL	GO:0032502~developmental process	114	3.08E-04	1.35213982
GOTERM_BP_ALL	GO:0048856~anatomical structure development	80	6.28E-04	1.43762847
GOTERM_BP_ALL	GO:0009653~anatomical structure morphogenesis	45	0.00417059	1.53667955
GOTERM_BP_ALL	GO:0048731~system development	62	0.00997805	1.36294939
GOTERM_BP_ALL	GO:0048513~organ development	46	0.02055166	1.38825906
GOTERM_BP_ALL	GO:0030154~cell differentiation	62	0.02204574	1.30724301
GOTERM_BP_ALL	GO:0048869~cellular developmental process	62	0.02204574	1.30724301
Functional Group 3				
INTERPRO	IPR000566:Lipocalin-related protein and Bos/Can/Equ allergen	8	6.90E-05	7.65879828
INTERPRO	IPR012674:Calycin	8	6.90E-05	7.65879828
PIR_SUPERFAMILY	PIRSF002390:lipid binding protein, FABP type	4	0.00534285	10.7437888
GOTERM_MF_ALL	GO:0005501~retinoid binding	4	0.00636539	10.190991
GOTERM_MF_ALL	GO:0019840~isoprenoid binding	4	0.00636539	10.190991
INTERPRO	IPR000463:Cytosolic fatty-acid binding	4	0.0091067	9.01035092
INTERPRO	IPR002345:Lipocalin	5	0.01024176	5.80211991
PIR_SUPERFAMILY	PIRSF500199:intracellular lipid-binding protein	3	0.04481523	8.67767559
Functional Group 4				
SP_PIR_KEYWORDS	signal	127	3.26E-08	1.59520455
SP_PIR_KEYWORDS	Secreted	74	1.52E-07	1.8841522
UP_SEQ_FEATURE	signal peptide	108	6.88E-06	1.48631205
GOTERM_CC_ALL	GO:0044459~plasma membrane part	78	0.00126697	1.41536127
SP_PIR_KEYWORDS	glycoprotein	132	0.00153341	1.27127003
GOTERM_CC_ALL	GO:0005886~plasma membrane	112	0.0065046	1.24919217
SP_PIR_KEYWORDS	membrane	167	0.01379799	1.16141605
GOTERM_CC_ALL	GO:0016020~membrane	219	0.01741069	1.11468358
UP_SEQ_FEATURE	disulfide bond	81	0.04275009	1.20857518
GOTERM_CC_ALL	GO:0044425~membrane part	182	0.0457554	1.10918584
GOTERM_CC_ALL	GO:0031226~intrinsic to plasma membrane	45	0.04749993	1.3180045
UP_SEQ_FEATURE	topological domain:Extracellular	75	0.05295624	1.20731277
GOTERM_CC_ALL	GO:0005887~integral to plasma membrane	44	0.05613094	1.30526402
UP_SEQ_FEATURE	glycosylation site:N-linked (GlcNAc...)	105	0.06877375	1.146184
UP_SEQ_FEATURE	topological domain:Cytoplasmic	87	0.09842627	1.14714568
SP_PIR_KEYWORDS	transmembrane	132	0.1600526	1.08709007
UP_SEQ_FEATURE	transmembrane region	104	0.18322912	1.09071992
GOTERM_CC_ALL	GO:0031224~intrinsic to membrane	155	0.19360493	1.06530664
GOTERM_CC_ALL	GO:0016021~integral to membrane	154	0.20581619	1.06258287
Functional Group 5				
GOTERM_CC_ALL	GO:0030054~cell junction	23	0.00117539	2.14682372
GOTERM_CC_ALL	GO:0005911~intercellular junction	11	0.00943832	2.62315964
SP_PIR_KEYWORDS	cell junction	16	0.02031475	1.92338798

10 Acknowledgement

An dieser Stelle möchte ich mich bei all jenen bedanken, die mich bei der Anfertigung dieser Dissertation unterstützt haben.

Ich möchte Prof. Jörg Gerlach und Dr. Katrin Zeilinger für die Möglichkeit danken, dass ich diese Doktorarbeit auf einem so spannenden Gebiet durchführen konnte. Danke für Unterstützung, Kritik und für die Freiheit, zu eigenen Entscheidungen.

Prof. Roland Lauster danke ich für die Übernahme der externen Betreuung und Begutachtung dieser Arbeit.

Mein besonderer Dank geht an Patricia Bussmann für die großartige Unterstützung während der gesamten Durchführung dieser Arbeit. Inken Wohlers für die gemeinsame und erfolgreiche Entwicklung des Characterisation Tools und der Bioreaktordatenbank. Zudem danke ich allen übrigen Mitarbeitern der AG Experimentelle Chirurgie/ Bioreactor Group für die Zusammenarbeit.

Annika Wulf-Goldenberg aus der Experimentellen Pharmakologie am Max Delbrück Centrum für Molekulare Medizin Berlin-Buch danke ich für die gemeinsame Etablierung hESC Kultur in unseren Arbeitsgruppen und der Durchführung der Teratomstudien.

Tack så mycket allen Mitarbeitern von Cellartis AB in Göteburg insbesondere Josefina Edsbagge, Janne Jensen, Mariela Rivero und Petter Björquist ohne die diese Arbeit so nicht möglich gewesen wäre.

Justyna Jozefczuk, Lukas Chavez und Dr. James Adjaye vom Max Planck Institut für Molekulargenetik für die Unterstützung bei der Durchführung der Microarray Analysen.

Petra Schrade aus der Arbeitsgruppe von Prof. Dr. Sebastian Bachmann am Institut für Vegetative Anatomie der Charité für die Zusammenarbeit bei der elektronen-mikroskopischen Analyse.

Meinen Eltern und Geschwistern danke ich für ihre stetige Unterstützung und ihr Vertrauen in mich. Zuletzt möchte ich Nicole danken, dass sie immer für mich da war und für die schönen Momente der Ablenkung.